

Pattern and Process in Crop Species Diversity
and Lime Requirements Models

By

FERNANDO ARAMBURU MERLOS
DISSERTATION

Submitted in partial satisfaction of the requirements for the degree of

DOCTOR OF PHILOSOPHY

in

Horticulture and Agronomy

in the

OFFICE OF GRADUATE STUDIES

of the

UNIVERSITY OF CALIFORNIA

DAVIS

Approved:

Robert J. Hijmans, Chair

Amélie C.M. Gaudin

Andrew M. Latimer

Committee in Charge

2022

TABLE OF CONTENTS

Title page	iii
Table of contents	iii
Acknowledgements	iii
Abstract	iv
Introduction	1
Chapter 1	9
The scale dependency of spatial crop species diversity and its relation to temporal diversity <i>Proceedings of the National Academy of Sciences, 117(42), 26176-26182.</i>	
Chapter 2	26
Potential, attainable, and current levels of global crop diversity <i>Environmental Research Letters, 17(4) 044071.</i>	
Chapter 3	73
Estimating lime requirements for tropical soils: model comparison and development <i>To be submitted for publication</i>	
Summary	120

ACKNOWLEDGEMENTS

I am grateful to Robert for sharing his wisdom and being a spectacular advisor, for his guidance and understanding, and for prioritizing our well-being above everything.

I want to thank the UC Davis staff, particularly Lisa and my Dissertation and QE Committee Members, for their time and willingness to help whenever I needed it.

I am also very grateful for all my friends in Davis, especially those with whom I shared the Ph.D. path and from whom I learned a lot.

And above all, I will be eternally grateful to my wife, Jimena, and my kids, Eliseo and Eva, for their unconditional support and love and for being my source of inspiration.

This dissertation is dedicated to my mom, who will always be with me wherever I go.

ABSTRACT

Changes in crop species diversity can affect agroecosystem function. However, most crop diversity studies insufficiently account for the influence of scale on spatial crop diversity, and its relation to temporal diversity has not been explored. Moreover, crop diversity might be limited by environmental constraints and market demand for specific crops, which needs to be considered when assessing opportunities for diversification. This dissertation developed and applied new approaches to gaining a quantitative understanding of diversity patterns and processes, allowing for improved comparison between regions and countries. It includes an analysis of the scale dependency of crop species diversity and its relation with temporal diversity using high-resolution crop-specific land-cover data for the conterminous US. It also shows the magnitude of environmental and demand-side constraints to crop diversity globally. For that purpose, a theoretical framework of hierarchical levels of crop species diversity is presented, in which potential, attainable, and current diversity levels are compared to compute diversity gaps.

We found that spatial diversity monotonically increases with the size of the observational unit, and the strongest association between spatial and temporal diversity is observed when measured in areas comparable to farm sizes. In larger areas, the association weakens because of the increasing diversity among farms. At the national level, the diversity among farms is usually higher than the diversity within them, which needs to be considered when inferring diversity effects with national-level data.

Environmental limits to crop diversity are higher in temperate and continental areas than in tropical and coastal regions. Crop diversity is also constrained by a high demand for a few crop species, which results in an attainable diversity that is much lower than the potential.

Nevertheless, there are large gaps between current and attainable diversity levels in most croplands. These gaps are particularly large in the Americas, where croplands are dominated by a few major annual crops (maize, soybean, wheat) mostly grown on fields with a very low temporal diversity. In contrast, diversity gaps are relatively small in Europe and East Asia.

Changes in food demand favoring minor crops could positively impact spatial and temporal crop species diversity by increasing the attainable diversity. But given current consumption patterns, the most effective strategy to increase crop diversity in areas with high diversity gaps might be to expand the area of a major crop adapted to that specific environment, but that is not widely planted.

Securing adequate soil fertility is also critical for diversification, especially in the tropics, where low soil pH is one of the main limiting factors of potential crop diversity, and soil acidity remains a key management challenge for smallholder farmers. Liming can boost the productivity of acid soils, but the lime rate required to achieve this is unknown for many tropical regions where food production increases are urgently needed. Therefore, lime requirement models based on readily available soil data could be very useful in these places. However, the great variety of lime requirement models available in the literature introduces much uncertainty. We evaluated current lime requirement models for acid tropical soils and introduced a new model based on acidity saturation using data from four soil incubation studies and 31 soil types. Foundational models based on acidity or base saturation are reasonably accurate ($r \geq 0.9$), but later attempts to

improve these models were unsuccessful. The new model, in contrast, has more precision than all earlier models across a wide range of acid tropical soils from different regions. Moreover, lime requirement estimates largely depend on the target soil chemical property of the model. For instance, many more African soils would require liming based on base saturation models than acidity saturation models, regardless of the accuracy. The new acidity saturation model can effectively estimate the lime rate required to address aluminum toxicity. This model could be incorporated into more comprehensive models once lime rates needed for other acidity problems are well established.

INTRODUCTION

There is a growing interest in better understanding factors affecting agroecosystem functions and services. One key property of agroecosystems that has received much attention in recent years is the diversity of crop species. National crop species diversity has been associated with the stability of food production (Renard and Tilman, 2019) and used as a proxy for pollination services (Aizen et al., 2019) partly because local crop diversity enhances associated biodiversity (Sirami et al., 2019). However, it is unclear how national crop diversity is related to local-scale diversity, and assuming that inferences made at one scale are maintained at other scales can be misleading. Crop species diversity also has a temporal dimension of great importance resulting from farmers' crop rotations. These crop rotations can reduce pressure from pathogens, pests, and weeds (Curl, 1963; Liebman et al., 2016) and improve soil quality (Tiemann et al., 2015) and yield stability (Gaudin et al., 2015). Yet, the temporal dimension of crop diversity is frequently ignored in most diversity assessments, mainly because it is hard to measure (Aguilar et al., 2015), and it is not clear how diversity in space and time relates. Therefore, a better understanding and treatment of the scale dependency of spatial crop species diversity and its relation with temporal diversity is needed to develop comprehensive theories of crop diversity effects on agroecosystem function.

The scope and potential for crop diversity increases are also uncertain. Most calls for more diverse farming systems do not consider regional differences that might limit farmers' diversification opportunities or demand-side constraints (Jones et al., 2021; Kremen and Miles, 2012; Renard and Tilman, 2021). Moreover, most studies on crop species diversity used

variation in diversity to explain other phenomena but there has been less progress in understanding factors that shape crop diversity (Roesch-McNally et al., 2018; Socolar et al., 2021). Thus, to gain a quantitative understanding of diversity patterns and processes and improve comparisons between regions and countries, environmental and crop demand constraints to crop diversity must be identified.

The first two chapters of this dissertation deal with some fundamental aspects of crop species diversity. The first chapter (Aramburu Merlos and Hijmans, 2020) explores how crop diversity can be measured, depending on the dimension (spatial or temporal) and scale considered and how these relate, using data for the conterminous United States. The second chapter (Aramburu Merlos and Hijmans, 2022) examines which factors define and limit crop diversity. It outlines a framework for quantifying potential and attainable levels of crop species diversity, which is then applied at the global level.

Crop species diversity in the USA increased during the first half of the 20th century, but it has gradually declined over the past 50 years in most of the country (Aguilar et al., 2015; Hijmans et al., 2016). This specialization, together with increasing use of inputs, allowed substantial yield gains, but it was also associated with important negative environmental impacts (Crossley et al., 2021; Foley et al., 2005). Consequently, there is an interest in developing more diverse and sustainable cropping systems (Kremen and Merenlender, 2018; Pretty, 2018). Most studies on diversified cropping systems consider crop rotation diversification a key management practice to be developed and (re)implemented (Davis et al., 2012; Gaudin et al., 2015; Olmstead and Brummer, 2008; Spiegel et al., 2018). However, there have been no comprehensive efforts to

analyze crop rotation diversity (or temporal diversity) across the US, probably because it needs to be observed at a very high spatial resolution (field level). The first chapter analyzes temporal and spatial crop species diversity patterns in the conterminous US and how they relate. It shows that crop rotation diversity is tightly associated with local diversity at a spatial resolution close to typical US farm size. It also shows that this diversity is lower for rotations that include major crops.

The observable patterns in the spatial distribution of crop species and their subsequent diversity are realizations of underlying processes that need to be elucidated (Mercer et al., 2019; O’Sullivan and Unwin, 2003). While drivers of current crop genetic diversity patterns have been studied (Thomas et al., 2012; Van Etten and Hijmans, 2010), there is very little knowledge on processes shaping the diversity of crop species. However, some concepts from macroecology and biogeography might be applicable (Metzger et al., 2013; Rosenzweig, 1995). For instance, one of the most established patterns in Ecology, latitudinal biodiversity gradients (Hawkins, 2001), can also be expected to regulate crop species diversity. But crop diversity depends on both natural and human-mediated processes. Thus, while some tropical regions might be suitable for many crop species (high potential diversity), current diversity patterns are also affected by individual and structural factors shaping farming decisions and resulting in different specialization levels (Esquivel et al., 2021). The second chapter sets a theoretical framework of hierarchical levels of crop diversity that considers crop-specific environmental requirements and the demand for agricultural products. This framework is then used to analyze the environmental drivers of potential and attainable crop diversity and quantify diversity gaps. The results show that potential and attainable crop diversity are lower in temperate and continental areas than in tropical and

coastal regions. Although current diversity follows these patterns to some extent, other processes also affect it, resulting in high spatial variability in diversity gaps.

The third chapter of this dissertation is on a different topic. It contributes to a project to better understand the opportunities for improved management of acid soils in Africa. One of the initial steps of the project is developing a spatially-explicit analysis of the costs and benefits of liming in Africa. This analysis is founded on models for lime requirement estimation. However, the literature on lime requirement estimation methods is sparse and inconsistent, particularly for acid tropical soils. Thus, the third chapter focused on a comparison of lime requirement models.

Acid tropical soils can have several problems affecting crop growth, such as aluminum and manganese toxicity and calcium and magnesium deficiencies (Kamprath, 1980). These issues can be addressed by applying liming materials (Coleman et al., 1959). The amount of agricultural lime required is often estimated with locally calibrated soil tests (Shoemaker et al., 1961). Both soil testing and liming might be relatively cheap and easy to access for intensive commercial farmers, but that is not the case for most smallholder farmers in tropical developing countries (Crawford et al., 2008). Lime application is relatively expensive in many tropical regions, and the experimental evidence on lime response is also limited. Furthermore, soil tests that work elsewhere cannot be assumed to work for these places and must be re-calibrated.

Therefore, general models to estimate lime requirements from generally available soil data could be useful as a starting point in developing locally optimal liming recommendations and for strategic research on future lime use. The third chapter compares and evaluates different models

for lime requirement estimation that can be used in acid tropical soils with readily available soil data and introduces an outperforming model developed based on past experiences and clear principles. It shows that there are important differences in model accuracy and prediction values and that liming estimates largely depend on the target soil chemical property of the model. Therefore, the most important soil acidity problems affecting crop yields must be identified to formulate liming recommendations in acid tropical soils. However, models for other acidity problems than aluminum toxicity still need to be developed.

References

- Aguilar, J., Gramig, G.G., Hendrickson, J.R., Archer, D.W., Forcella, F., Liebig, M.A., 2015. Crop species diversity changes in the United States: 1978–2012. *PloS One* 10, e0136580.
- Aizen, M.A., Aguiar, S., Biesmeijer, J.C., Garibaldi, L.A., Inouye, D.W., Jung, C., Martins, D.J., Medel, R., Morales, C.L., Ngo, H., Pauw, A., Paxton, R.J., Sáez, A., Seymour, C.L., 2019. Global agricultural productivity is threatened by increasing pollinator dependence without a parallel increase in crop diversification. *Glob. Change Biol.* 25, 3516–3527. <https://doi.org/10.1111/gcb.14736>
- Aramburu Merlos, F., Hijmans, R.J., 2022. Potential, attainable, and current levels of global crop diversity. *Environ. Res. Lett.* 17, 044071. <https://doi.org/10.1088/1748-9326/ac62ab>
- Aramburu Merlos, F., Hijmans, R.J., 2020. The scale dependency of spatial crop species diversity and its relation to temporal diversity. *Proc. Natl. Acad. Sci.* 117, 26176–26182. <https://doi.org/10.1073/pnas.2011702117>
- Coleman, N.T., Kamprath, E.J., Weed, S.B., 1959. Liming, in: Normax, A.G. (Ed.), *Advances in Agronomy*. Academic Press, pp. 475–522. [https://doi.org/10.1016/S0065-2113\(08\)60073-5](https://doi.org/10.1016/S0065-2113(08)60073-5)
- Crawford, T.W., Singh, U., Breman, H., 2008. Solving Agricultural Problems Related to Soil Acidity in Central Africa’s Great Lakes Region CATALIST Project Report. International Center for Soil Fertility and Agricultural Development (IFDC), Kigali, Rwanda.
- Crossley, M.S., Burke, K.D., Schoville, S.D., Radeloff, V.C., 2021. Recent collapse of crop belts and declining diversity of US agriculture since 1840. *Glob. Change Biol.* 27, 151–164. <https://doi.org/10.1111/gcb.15396>
- Curl, E.A., 1963. Control of plant diseases by crop rotation. *Bot. Rev.* 29, 413–479.
- Davis, A.S., Hill, J.D., Chase, C.A., Johanns, A.M., Liebman, M., 2012. Increasing cropping system diversity balances productivity, profitability and environmental health. *PloS One* 7, e47149.
- Esquivel, K.E., Carlisle, L., Ke, A., Olimpi, E.M., Baur, P., Ory, J., Waterhouse, H., Iles, A., Karp, D.S., Kremen, C., Bowles, T.M., 2021. The “Sweet Spot” in the Middle: Why Do Mid-Scale Farms Adopt Diversification Practices at Higher Rates? *Front. Sustain. Food Syst.* 5.
- Foley, J.A., DeFries, R., Asner, G.P., Barford, C., Bonan, G., Carpenter, S.R., Chapin, F.S., Coe, M.T., Daily, G.C., Gibbs, H.K., Helkowski, J.H., Holloway, T., Howard, E.A., Kucharik, C.J., Monfreda, C., Patz, J.A., Prentice, I.C., Ramankutty, N., Snyder, P.K., 2005. Global Consequences of Land Use. *Science* 309, 570–574. <https://doi.org/10.1126/science.1111772>
- Gaudin, A.C., Tolhurst, T.N., Ker, A.P., Janovicek, K., Tortora, C., Martin, R.C., Deen, W., 2015. Increasing crop diversity mitigates weather variations and improves yield stability. *PLoS One* 10, e0113261.
- Hawkins, B.A., 2001. Ecology’s oldest pattern? *Trends Ecol. Evol.* 16, 470. [https://doi.org/10.1016/S0169-5347\(01\)02197-8](https://doi.org/10.1016/S0169-5347(01)02197-8)
- Hijmans, R.J., Choe, H., Perlman, J., 2016. Spatiotemporal patterns of field crop diversity in the United States, 1870–2012. *Agric. Environ. Lett.* 1.
- Jones, S.K., Estrada-Carmona, N., Juventia, S.D., Dulloo, M.E., Laporte, M.-A., Villani, C., Remans, R., 2021. Agrobiodiversity Index scores show agrobiodiversity is underutilized

- in national food systems. *Nat. Food* 2, 712–723. <https://doi.org/10.1038/s43016-021-00344-3>
- Kamprath, E., 1980. Soil acidity in well-drained soils of the tropics as a constraint to food production. *Priorities Alleviating Soil-Relat. Constraints Food Prod. Trop.* 171–187.
- Kremen, C., Merenlender, A.M., 2018. Landscapes that work for biodiversity and people. *Science* 362, eaau6020.
- Kremen, C., Miles, A., 2012. Ecosystem Services in Biologically Diversified versus Conventional Farming Systems: Benefits, Externalities, and Trade-Offs. *Ecol. Soc.* 17. <https://doi.org/10.5751/ES-05035-170440>
- Liebman, M., Baraibar, B., Buckley, Y., Childs, D., Christensen, S., Cousens, R., Eizenberg, H., Heijting, S., Loddo, D., Merotto Jr, A., 2016. Ecologically sustainable weed management: How do we get from proof-of-concept to adoption? *Ecol. Appl.* 26, 1352–1369.
- Mercer, K.L., Vigouroux, Y., Castañeda-Álvarez, N.P., de Haan, S., Hijmans, Robert J., Leclerc, C., McKey, D., Vanek, S.J., 2019. Crop Evolutionary Agroecology: Genetic and Functional Dimensions of Agrobiodiversity and Associated Knowledge, in: *Agrobiodiversity: Integrating Knowledge for a Sustainable Future*, Strüngmann Forum Reports. The MIT Press, Cambridge, MA, pp. 20–62.
- Metzger, M.J., Bunce, R.G.H., Jongman, R.H.G., Sayre, R., Trabucco, A., Zomer, R., 2013. A high-resolution bioclimate map of the world: a unifying framework for global biodiversity research and monitoring. *Glob. Ecol. Biogeogr.* 22, 630–638. <https://doi.org/10.1111/geb.12022>
- Olmstead, J., Brummer, E.C., 2008. Benefits and barriers to perennial forage crops in Iowa corn and soybean rotations. *Renew. Agric. Food Syst.* 23, 97–107.
- O’Sullivan, D., Unwin, D., 2003. *Geographic information analysis*. John Wiley & Sons, Hoboken, NJ.
- Pretty, J., 2018. Intensification for redesigned and sustainable agricultural systems. *Science* 362, eaav0294.
- Renard, D., Tilman, D., 2021. Cultivate biodiversity to harvest food security and sustainability. *Curr. Biol.* 31, R1154–R1158. <https://doi.org/10.1016/j.cub.2021.06.082>
- Renard, D., Tilman, D., 2019. National food production stabilized by crop diversity. *Nature* 571, 257.
- Roesch-McNally, G.E., Arbuckle, J.G., Tyndall, J.C., 2018. Barriers to implementing climate resilient agricultural strategies: The case of crop diversification in the US Corn Belt. *Glob. Environ. Change* 48, 206–215.
- Rosenzweig, M.L., 1995. *Species diversity in space and time*. Cambridge University Press.
- Shoemaker, H.E., McLean, E.O., Pratt, P.F., 1961. Buffer Methods for Determining Lime Requirement of Soils With Appreciable Amounts of Extractable Aluminum. *Soil Sci. Soc. Am. J.* 25, 274–277. <https://doi.org/10.2136/sssaj1961.03615995002500040014x>
- Sirami, C., Gross, N., Baillod, A.B., Bertrand, C., Carrié, R., Hass, A., Henckel, L., Miguet, P., Vuillot, C., Alignier, A., 2019. Increasing crop heterogeneity enhances multitrophic diversity across agricultural regions. *Proc. Natl. Acad. Sci.* 116, 16442–16447.
- Socolar, Y., Goldstein, B.R., Valpine, P. de, Bowles, T.M., 2021. Biophysical and policy factors predict simplified crop rotations in the US Midwest. *Environ. Res. Lett.* 16, 054045. <https://doi.org/10.1088/1748-9326/abf9ca>

- Spiegel, S., Bestelmeyer, B.T., Archer, D.W., Augustine, D.J., Boughton, E.H., Boughton, R.K., Cavigelli, M.A., Clark, P.E., Derner, J.D., Duncan, E.W., 2018. Evaluating strategies for sustainable intensification of US agriculture through the Long-Term Agroecosystem Research network. *Environ. Res. Lett.* 13, 034031.
- Thomas, E., Zonneveld, M. van, Loo, J., Hodgkin, T., Galluzzi, G., Etten, J. van, 2012. Present Spatial Diversity Patterns of *Theobroma cacao* L. in the Neotropics Reflect Genetic Differentiation in Pleistocene Refugia Followed by Human-Influenced Dispersal. *PLOS ONE* 7, e47676. <https://doi.org/10.1371/journal.pone.0047676>
- Tiemann, L.K., Grandy, A.S., Atkinson, E.E., Marin-Spiotta, E., McDaniel, M.D., 2015. Crop rotational diversity enhances belowground communities and functions in an agroecosystem. *Ecol. Lett.* 18, 761–771.
- Van Etten, J., Hijmans, R.J., 2010. A geospatial modelling approach integrating archaeobotany and genetics to trace the origin and dispersal of domesticated plants. *PLoS One* 5, e12060.

CHAPTER 1

The scale dependency of spatial crop species diversity and its relation to temporal diversity

Proceedings of the National Academy of Sciences, 117(42), 26176-26182.



The scale dependency of spatial crop species diversity and its relation to temporal diversity

Fernando Aramburu Merlos^{a,b,1} and Robert J. Hijmans^a

^aDepartment of Environmental Science and Policy, University of California, Davis, CA 95616; and ^bInstituto Nacional de Tecnología Agropecuaria, Unidad Integrada Balcarce, 7620 Balcarce, Buenos Aires, Argentina

Edited by Colin K. Khoury, International Center for Tropical Agriculture, Cali, Colombia, and accepted by Editorial Board Member Ruth DeFries August 21, 2020 (received for review June 7, 2020)

Increasing crop species diversity can enhance agricultural sustainability, but the scale dependency of the processes that shape diversity and of the effects of diversity on agroecosystems is insufficiently understood. We used 30 m spatial resolution crop classification data for the conterminous United States to analyze spatial and temporal crop species diversity and their relationship. We found that the US average temporal (crop rotation) diversity is 2.1 effective number of species and that a crop's average temporal diversity is lowest for common crops. Spatial diversity monotonically increases with the size of the unit of observation, and it is most strongly associated with temporal diversity when measured for areas of 100 to 400 ha, which is the typical US farm size. The association between diversity in space and time weakens as data are aggregated over larger areas because of the increasing diversity among farms, but at intermediate aggregation levels (counties) it is possible to estimate temporal diversity and farm-scale spatial diversity from aggregated spatial crop diversity data if the effect of beta diversity is considered. For larger areas, the diversity among farms is usually much greater than the diversity within them, and this needs to be considered when analyzing large-area crop diversity data. US agriculture is dominated by a few major annual crops (maize, soybean, wheat) that are mostly grown on fields with a very low temporal diversity. To increase crop species diversity, currently minor crops would have to increase in area at the expense of these major crops.

agrobiodiversity | temporal diversity | crop rotation | spatial scale

Variation in crop species diversity has been used to explain differences in the stability of food production (1), pesticide use (2), agroecosystem resilience (3), and natural biodiversity in agroecosystems (4–6). Recent analyses of aggregated data for large regions, such as counties and states in the United States, have shown both losses and gains in crop species diversity, depending on the location, the time period, and the level of spatial aggregation (7–11). It is not clear, however, how knowledge of changes over such large areas is related to agroecosystem function because our understanding of the effects of diversity on agroecosystems comes from studies on the scale of fields and landscapes (12–14). A more general understanding of the scale dependency of crop diversity patterns is therefore needed, as this could support the use of spatially aggregated data to study the effect of diversity in agriculture (15, 16). This is challenging conceptually (17) and practically because of the need for crop distribution data at a sufficiently high spatial resolution. There is also an important (short-term) temporal dimension of diversity that needs to be considered and can only be directly observed at a high spatial resolution: Many fields are planted in a seasonal sequence of multiple crops. These crop rotations can reduce pressure from pathogens, pest, and weeds (18–20) and improve soil quality (21), and it has been argued that these benefits are similar to those ascribed to spatial diversity in natural ecosystems (22), just as a rapid crop varietal turnover in time can compensate for genetic uniformity (13).

In this paper we use 30 m spatial resolution crop distribution data for the conterminous United States between 2008 and 2017

to show how crop species diversity changes with spatial scale. We also demonstrate that temporal diversity and farm-level spatial diversity can be estimated from aggregated spatial diversity data if the effect of spatial scale on diversity is taken into consideration.

Results

Temporal Crop Diversity. Average temporal crop species diversity ($D\tau$; the effective number of species) in the United States is 2.1. About 9% of the cropland has a single crop, 60% has two or fewer crops, and 86% has three or fewer crops in rotation (Fig. 1A). $D\tau$ is relatively high in large parts of North and South Dakota, along the Southern seaboard (from New Jersey to Georgia), in parts of the West Coast states and Idaho, and in northeast Michigan (Fig. 2 and *SI Appendix, Table S1*). Regions dominated by perennial crops, such as Florida and parts of California and Louisiana, have a $D\tau$ of 1, as expected. When not considering perennial crops (Fig. 2B), most areas in the West Coast states and Idaho have a high temporal diversity. Areas with monocropping of annual crops ($D\tau = 1$ in Fig. 2B) are predominant in Oklahoma (wheat), northern Texas (cotton), Montana (wheat), eastern Washington (wheat), and northern California (rice). Wheat has the largest monocrop area (2.9 Mha, 33% of all monocropped area), while 66% of the maize area (23 Mha) and 64% of the soybean area (20 Mha) have a temporal diversity of 2 (*SI Appendix, Table S2*).

The larger the area planted with a crop is, the lower the temporal diversity of the areas it is grown in is (Fig. 3). For annual crops that cover at least 0.01% of the cropland area there is a strong log-linear

Significance

There is considerable debate about the effect of changes in and the need to increase biodiversity in agriculture. The spatial scale dependency of crop diversity has not been formally addressed, and this complicates understanding and synthesis. Crop species diversity also has a temporal diversity component of fundamental importance that has been ignored in diversity assessments. To fill this gap, we develop a framework for understanding the scale dependency of spatial crop species diversity and its relation to temporal diversity using 30 m spatial resolution crop species distribution data for the United States. We show that aggregated diversity data can be downscaled to estimate spatial and temporal diversity at the farm scale. We use the results to discuss diversification strategies.

Author contributions: F.A.M. and R.J.H. designed research; F.A.M. performed research; F.A.M. analyzed data; and F.A.M. and R.J.H. wrote the paper.

The authors declare no competing interest.

This article is a PNAS Direct Submission. C.K.K. is a guest editor invited by the Editorial Board.

Published under the PNAS license.

¹To whom correspondence may be addressed. Email: faramburmerlos@ucdavis.edu.

This article contains supporting information online at <https://www.pnas.org/lookup/suppl/doi:10.1073/pnas.2011702117/-DCSupplemental>.

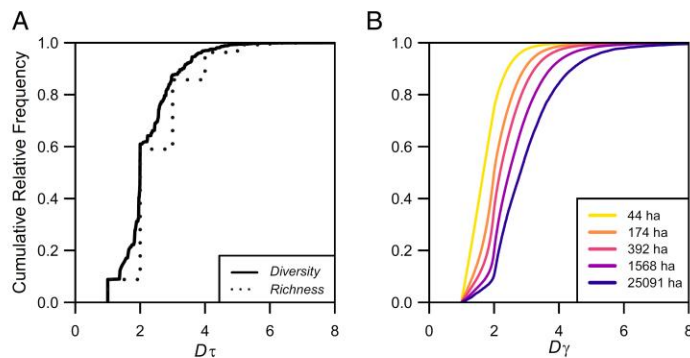


Fig. 1. Temporal (A, $D\tau$) and spatial (B, $D\gamma$) crop species diversity (effective number of crop species) in the conterminous United States for 2008 to 2017. Temporal diversity was computed at 30 m spatial resolution, and spatial diversity was computed at five different observational unit sizes. A also shows the temporal species richness (the number of different species, not accounting for their relative abundance).

decline of temporal diversity with crop area. For crops with less than 0.01% of the area, there is no clear effect of area planted, and $D\tau$ is about 3.7. The downward slope is expected because a crop that covers 100% of an area can only have $D\tau = 1$, and an area with two crops that each cover 50% can only have $D\tau \leq 2$. But the

empirical data are far below this theoretical maximum. The fields with the highest temporal diversity ($D\tau \geq 4$) are mostly planted with crops grown for fresh consumption such as eggplants, lettuce, and carrots.

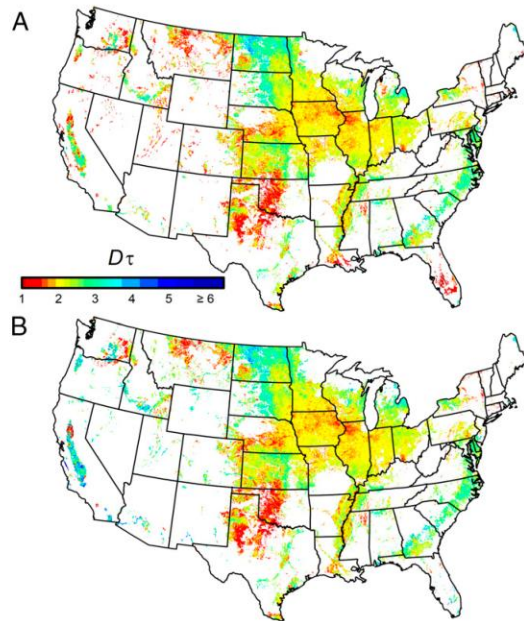


Fig. 2. Temporal crop species diversity ($D\tau$) in the conterminous United States (2008 to 2017) measured as the effective number of crops species in rotation considering (A) all crop species and (B) only annual crops. $D\tau$ was computed at a 30 m resolution and then aggregated to a 3.96 km resolution for display purposes. Aggregated cells with less than 10% of cropland were not considered. In B, 30 m cells classified as perennial crops in four or more years were removed from the calculation of average $D\tau$ for the aggregated cells.

Spatial Crop Diversity. Spatial crop species diversity ($D\gamma$) strongly increases with the size of the observational unit (Figs. 1, 4, and 5). When measured on areas of 44 ha, only 25% of US cropland has a $D\gamma \geq 2$ (that is, two equally abundant crops or more), and 2.5% of the cropland has a $D\gamma \geq 3$ (Figs. 1 and 4A). In contrast, 80% of the cropland has a $D\gamma \geq 2$ when the observational unit is 1,568 ha, and this increases to 90% for units of 25,091 ha (Figs. 1 and 4D). Spatial diversity patterns are highly apparent at this level of aggregation, showing large tracts of low spatial crop species diversity in Florida, southern Louisiana, northern Texas, Oklahoma, and parts of Montana and Washington (Fig. 4D). $D\gamma$ is also low in isolated croplands in western regions where alfalfa is grown in areas dominated by rangelands (SI Appendix, Fig. S1). Most of the Corn Belt (and Nebraska) has $D\gamma \sim 2$. Kansas and the Mississippi Portal (the southern half of the Mississippi basin) have $D\gamma \sim 3$, while the regions with the highest $D\gamma (\geq 4)$ are found along the coasts and borders with Canada and Mexico.

Country-wide average $D\gamma$ monotonically increases as diversity is computed over larger areas (Fig. 5A). $D\gamma$ increases exponentially as it moves away from fields (with generally only one crop at a time) to multiple fields and captures more of the farm-level diversity. When the observational units reach about 400 ha, the increase in $D\gamma$ slows down as neighboring farms are generally similar to each other. $D\gamma$ then increases exponentially again at very large areas (>1 Mha), reaching 5.4 at 411 Mha (Fig. 5A) and 8.1 at the national level.

The average regional-to-local diversity ratio, $D\beta$ (always computed with 392 ha subunits to have a constant definition of “local”), remains low and close to 1 (that is, no difference in diversity) as the regional area increases in size, until the regions considered are as big as a state, at which point it increases exponentially (SI Appendix, Fig. S2). This again shows that crops grown on different farms tend to be similar at the county to state level but not across larger areas. At observational units of intermediate size, such as 25,091 ha, crop species diversity is most strongly associated with farm-level diversity, represented here by $D\alpha$ (local diversity) with 392 ha subunits. For instance, if the United States is divided in square regions of 0.4 Mha (that is, comparable to the size of a county), only a few regions have $D\beta \geq 2$, including parts of California, western South and North Dakota, eastern Montana, and Washington

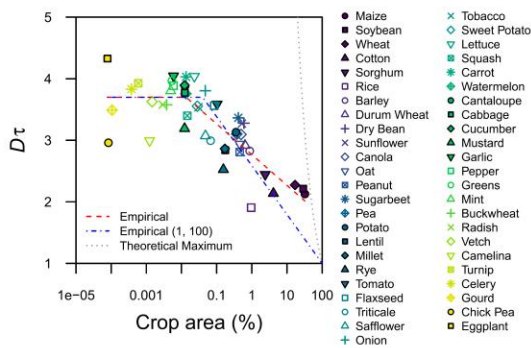


Fig. 3. Mean temporal crop species diversity ($D\tau$, effective number of crop species) by crop as a function of their area planted (percentage of cropland) for annual crops in the conterminous United States. The means are for all 30 m spatial resolution cells in which a crop occurred between 2008 and 2017. The horizontal axis has a logarithmic scale. The red dashed line is a fitted log-linear regression line: $D\tau = \min(3.699; 1.769 - 0.499 \log(\text{area}))$, where area is the area planted as a proportion of total cropland. The blue dot-dashed line is a fitted log-linear regression line forced through (1, 100): $D\tau = \min(3.698; 1 - 0.794 \log(\text{area}))$. The gray dotted line represents the theoretical maximum for a situation in which all crops are in equal area and grown everywhere with the same frequency, $D\tau = 1/\text{area}$.

(SI Appendix, Fig. S3). But $D\alpha$ is still greater than $D\beta$ in most of these regions.

Association between Spatial and Temporal Crop Species Diversity.

The relation between spatial and temporal crop species diversity depends on the size of the observational unit of analysis, and it is strongest between 100 and 400 ha (Fig. 5B), which is about the size of a typical US farm (23). If spatial diversity is measured on smaller areas (<100 ha), $D\tau$ tends to be greater than $D\gamma$, while the opposite occurs at larger areas (>400 ha) (Fig. 5A). Consider the extreme cases: If the spatial diversity were measured at a point (an infinitesimal small area), $D\gamma$ would always be 1 because only one crop could be present, but $D\tau$ would change from place

to place depending on the crop rotation of each site, so no association would exist. At the other extreme, national $D\gamma$ is 8.1, almost four times the national average $D\tau$ of 2.1.

The smallest root-mean-square deviation (RMSD) between $D\tau$ with $D\gamma$ is that measured on areas of 174 ha, although it barely changes in the range of 100 to 400 ha (Fig. 5B). The lowest lack of correlation (and greatest correlation) between $D\tau$ and $D\gamma$ is at an area of 1,568 ha, probably because averaging larger areas reduces noise stemming from variation in field sizes, cropland fraction per observational unit, noise in the data, and other factors. At higher levels of aggregation, however, the lack of correlation rapidly escalates beyond 1 because of the increasingly strong influence of $D\beta$ on $D\gamma$ (SI Appendix, Fig. S2). At the county level, $D\gamma$ is always greater than or equal to average county $D\tau$, and the difference between these two measures is associated with the number of crop species assemblages (cropping systems with different species composition) in each county, measured by $D\beta$ (Fig. 6A). Strong agreement between spatial and temporal diversity at the county level is achieved when $D\beta$ is removed from $D\gamma$ by applying the equality in Eq. 3, ensuring that $D\alpha$ (that is, 174 ha subunit diversity averages, a proxy for farm-level diversity) is properly considered (Fig. 6B).

Discussion

We have analyzed the variation in temporal and spatial crop species diversity in the United States and have shown how these are related. Spatial diversity is most strongly associated with temporal diversity at the farm level. For county to state-sized regions, the total spatial diversity is mainly determined by farm-level diversity, and the diversity among farms at this level of aggregation is low. At the national level, in contrast, the variation among farms and regions is much greater than within them. Understanding the effect of scale on diversity is important because both the processes shaping diversity and the effects of diversity on ecosystem functioning vary with scale. Our analytical approach could be applied to research on other levels of agricultural biodiversity, such as genetic diversity within species (16) and contexts (6, 24), which would also benefit from more formal conceptual frameworks for the analysis of spatial scale.

Our analysis of the scale dependency in crop species diversity allows for improved comparison between regions and countries.

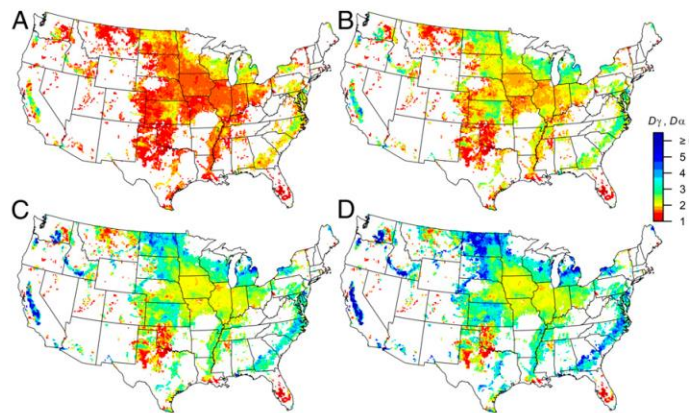


Fig. 4. Spatial crop species diversity (effective number of crop species) in the conterminous United States (2008 to 2017) at four observational unit sizes: (A) 44 ha, (B) 174 ha, (C) 1,568 ha, and (D) 25,091 ha (15.84 km resolution). For comparison, all maps are displayed at a 15.84 km resolution, and smaller units' results were aggregated by computing their weighted average value using Eq. 2. In D, the diversity is the total diversity of each 15.84 km grid cell ($D\gamma$), whereas on the other maps, each grid cell shows the mean effective number of crop species for subunits at the corresponding spatial scale ($D\alpha$). Only cells with more than 5% of crop area are included.

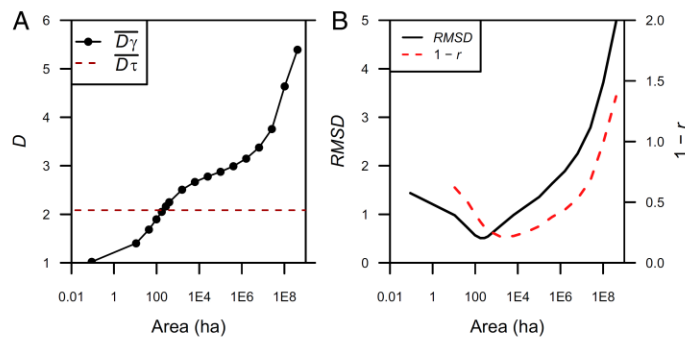


Fig. 5. Scale dependency of spatial crop species diversity and its association with temporal diversity. (A) Average crop species diversity (effective number of crop species) in space (\overline{D}_γ) and time (\overline{D}_τ) for the conterminous United States (2008 to 2017) at different observational unit sizes. (B) Summary statistics for the difference between \overline{D}_γ and \overline{D}_τ as a function of the size of the observational unit. Here, RMSD is the root-mean-squared deviation and $1 - r$ is the lack of positive correlation, where r is Pearson's correlation coefficient. In both plots the horizontal axis has a logarithmic scale.

Departures from the relationship between crop diversity and spatial aggregation level that we described should reflect differences in temporal diversity and/or farm (and field) sizes. Regions with smaller farms and fields would present a first inflection point at smaller areas, while those with more diverse rotations would have it at higher diversity values. Similarly, the second exponential growth phase depends on how different the farms are from each other as larger areas are considered. Data for countries with greater diversity among cropping systems than the United States, perhaps because of greater environmental diversity, would show a steeper increase and reach a higher level. Variation in the relationship between crop dominance and temporal diversity, notably the location of the inflection point and the slope, should also allow for a more quantitative understanding of crop diversity patterns.

Temporal diversity (crop rotation) has been studied in the context of the multiple agronomic benefits it provides (25–29), but farm-level temporal diversity assessments are rare. Our study formally analyzes temporal crop diversity patterns over a large area. It is important to distinguish “temporal diversity” from “changes in spatial diversity over time” (30), which has been used in prior work (6–8). True temporal diversity is a key system property of croplands. There is also temporal diversity in natural ecosystems, which may merit more formal evaluation. For example, the temporal diversity concept might be useful for understanding the role of biodiversity in ecosystems with short-term (fire-driven) succession (31) or variation in species distributions and abundance driven by cycles in ocean temperature (32), masting (33), and annual migration.

Monitoring changes over time in temporal diversity in agriculture is important (34–37), but it requires time series of high spatial resolution crop distribution data that generally do not exist. While the increasing availability of remote sensing-derived cropland classification data will enable future study of temporal crop diversity, we need methods to assess historical changes in temporal crop diversity. Our results suggest that we can do so by using the tight association of temporal and spatial crop diversity for areas close to the median farm size. In the United States, that is between 100 and 400 ha. We have shown that with observational units of that size, temporal crop diversity can be predicted from a single year of high spatial resolution data. If temporal diversity needs to be predicted from more aggregated data, the effective number of cropping system types ($D\beta$) must be considered in order to avoid overestimation. This method should be reliable at intermediate levels of aggregation (such as counties in

the United States), but it should be used with great caution with more aggregated data since the lack of correlation between spatial and temporal diversities increases exponentially as data are aggregated over larger areas. Future work could investigate this further using, for example, environmental dissimilarity to predict cropping system variability within large regions.

A compelling case has been made for increasing the diversity of cropping systems (1, 5, 6, 38–41), and our analysis can help us to understand some important aspects that need to be considered. Minor annual crops tend to be grown in more diverse rotations than major crops. However, minor crops cover, by definition, only a small area. In addition, minor crops are often restricted to specific regions, in part because of favorable environmental conditions and in part because of regional specialization leading to the presence of superior infrastructure for processing and distribution (42). In contrast, major crops are sometimes the only profitable option. For instance, wheat might be the only cost-effective crop in the United States in cold or dry environments (43). Moreover, changes in relative crop prices that favor major crops, such as those caused by an increasing bioethanol demand, have been shown to negatively affect diversity (12). A better understanding of the drivers of crop spatial distribution, crop price

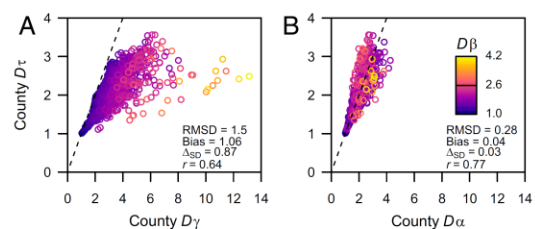


Fig. 6. County-level average temporal crop species diversity (\overline{D}_τ) in the conterminous United States as a function of two spatial diversity measurements. (A) County-level spatial diversity (\overline{D}_γ) and (B) subunit average (174 ha) crop species diversity (\overline{D}_α) for each county. The color of each point indicates the region-to-local diversity ratio ($D\beta$) for each county based on 174 ha subunits. The same color ramp was used for both plots and is shown in B. For both plots, the dashed line represents the identity function ($\overline{D}_\tau = \overline{D}_\gamma$). The root-mean-squared deviation (RMSD), mean bias, difference between standard deviations (Δ_{std}), and Pearson's correlation coefficient (r) for the agreement between \overline{D}_τ and the corresponding spatial diversity type are shown on each plot. Only counties with more than 5% of crop area are included.

effects, and why certain crops present greater temporal diversity than others should inform opportunities for and constraints on the development of more diverse cropping systems.

National-level diversity in the United States is quite low. Despite its large size and wide range of environmental conditions, the United States is in the 29th percentile when comparing country-level crop diversity globally (11). We found that farm-scale diversity is also low in most of the country, in large part because of the great predominance of three major crops. Wheat, maize, and soybean crops cover most of the US cropland, and despite the hundreds of other crops that are grown in the United States, it is not possible to create much more diverse cropping systems unless the area planted with these three dominant commodities decreases drastically. This would require major changes in the food system that would be rather costly in the short term (44). Our analysis suggests that an important approach to increasing farm-scale crop diversity is to provide financial incentives and improved technology for the production of smaller crops such that it becomes more attractive to bring them into rotation with maize, soybean, and/or wheat. This is what the United States looked like in the 1950s when there was a much larger “middle class” of crops, including barley, oats, and sorghum (8). It could also be relevant to consider how to get more variability among neighboring farms, as we showed that this tends to be very low. An increased emphasis on consumption of locally produced fresh food (45) could perhaps play a modest role. Reintegration of crop production and livestock production, that is, with local sourcing of feed, could diversify farms and greatly reduce environmental pollution stemming from concentrated livestock production as well (39, 46). Cover crops constitute another diversification strategy that has gained popularity in recent years, particularly in areas with poor soils and long growing seasons (47). These crops planted to protect the soil and/or avoid leaching of nutrients may provide larger ecosystem services than adding another crop planted for its harvestable product (48).

Acknowledging the scale dependency of spatial diversity and the role of diversity in time is critical for the analysis of diversification strategies and their effects. While both human health and the environment would benefit from more diverse diets and food production (49–51), we must assess how to deploy current crops in space and time. Many authors advocate for high diversity at the field level (38, 52–54), but field-level diversification benefits are context dependent. For instance, intercroops (in-field mixtures of annual crops) are most commonly used in N-deprived systems of developing countries (55), where legume–cereal mixes provide a clear advantage over the monocrop alternatives (56), or when they provide temporal complementarity (57), resembling a crop rotation. However, intercroops are rarely compared against their temporal diversification alternative (22). Temporal diversity allows for greater field-level diversity without running into the practical management problems of intercroops. Furthermore, temporal diversity might be better for the control of soilborne pests and disease (58) and for other ecosystem services as well (27, 59). Diverse crop rotations also foster farm-level spatial diversity, as farmers tend to cultivate all crop rotation components every year, but how this shapes the landscape and its effects on ecosystem services depends on field and farm sizes. For instance, natural biodiversity associated with agriculture increases when the landscape is composed of small fields (<6 ha) and a diverse mosaic of crops (5). This composite of small and diverse fields implies high spatial diversity even when measured on units of 44 ha. In most of the United States, however, diversity is very low at this level because of the combination of large fields (60, 61) and low temporal diversity. Even the most diverse regions of the United States present a relatively low diversity when considering observational units of 392 ha or smaller.

Beyond farms and landscapes, national-level crop diversity has been associated with food production stability (1). While there

can be benefits to high crop diversity at the national level, this is different from having high crop diversity at the farm and landscape levels. We showed that the diversity among cropping systems ($D\beta$) can be a far greater determinant of national-level diversity than the diversity within them ($D\alpha$) because $D\beta$ increases exponentially at higher aggregation levels. $D\beta$ might also have a stronger stability effect on national food production than $D\alpha$ because yields of different cropping systems and regions are usually less correlated among each other than yields within the same cropping system (62). Therefore, identifying the role of $D\alpha$ and $D\beta$ on the diversity–stability relation is necessary in order to better understand the relation between crop diversity and food production stability at the farm level. Downscaling spatial diversity to farm level by removing the effect of $D\beta$ would allow for using average farm-level diversity, which is likely a more relevant measure when investigating the relation between crop diversity and other agroecosystem properties.

Materials and Methods

Data Source and Preparation. We used the Cropland Data Layers (CDLs) annual crop-specific land cover classifications for the conterminous United States (63, 64). Each CDL has a spatial resolution of 30 m and classifies each raster cell as cropland or not and each cropland cell as 1 of 106 crop classes, which can either be a single crop or a double crop (e.g., winter wheat/soybean). We used the 10 years of CDLs (from 2008 to 2017) that were available at the beginning of this project. Early CDL years have been reprocessed and rereleased, bringing them to a similar level of accuracy as later years (Cohen’s kappa coefficient ~ 0.83), which constitutes a significant improvement for our multiyear analyses. The typical crop field in the United States ranges between 16 and 65 ha (61), much larger than the CDL spatial resolution (0.09 ha), and the CDL data have been used to study changes in crop rotations (34–37), suggesting that the CDLs provide high enough spatial and temporal resolution to assess temporal diversity. CDL-derived spatial diversity estimates at the county level and those obtained based on the US Department of Agriculture Census of Agriculture showed strong agreement between both datasets (root-mean-square error (RMSE) = 3% of Shannon entropy index average, *SI Appendix*, Fig. S4).

We aggregated CDL classes by species. For example, corn, sweet corn, popcorn, and ornamental corn were grouped as maize (*SI Appendix*, Table S3). Each double-crop type remained as a different category, and both species within the double crop were fully considered for the calculation of spatial and temporal crop diversity. Only land that was classified as cropland for more than 5 years was considered. That threshold was chosen for two reasons: 1) to avoid the influence of areas cropped only for a few years on temporal diversity estimations and 2) as a data-cleaning process since most land that is only occasionally classified as cropland is probably never used for that purpose.

Spatial and Temporal Diversity. We follow the definition and partition of diversity proposed by Jost (65) and reviewed by Tuomisto (66). A true diversity (D) quantifies the effective number of types of entities, which in this case refers to crop species. The effective number of crop species in space (D_T) or time (D_t) is the number of equally abundant virtual crop species that has the same entropy as the actual crop species given their mean relative abundance. D is calculated as an exponent of the Shannon entropy index (H) (65, 66):

$$D = \exp\left(-\sum_{i=1}^S p_i \ln p_i\right) = \exp(H), \quad [1]$$

where p_i is the proportion of cropland area covered with crop species i and S is the number of crop species.

We computed D_T for square grid cells of different spatial resolutions covering the conterminous United States. A grid cell represents an observational unit, which can have different sizes according to the spatial resolution. The median crop field size in the United States considering the fraction of cropland area is 35 ha (61), and the median farm size is 445 ha (23). We used a series of spatial resolutions that were aggregates of the original 30 m grid cells, selecting six resolutions at field to farm scales (from 0.33 to 1.98 km in steps of 0.33 km) and an additional 10 resolutions by increasing the cell sizes exponentially by multiplying 0.99 km with 2^x (in which x can take any integer value between 2 and 11), that is, a sequence of resolutions of 0.33, 0.66, 0.99, 1.32, 1.65, 1.98, 3.96, 7.92, 15.8, 31.7, 63.4, 127, 253, 507, 1,014, and 2,028 km, which yields observational units of 11, 44, 98, 174, 272, 392, 1,568, 6,273, 25,091, 0.1×10^6 , 0.4×10^6 , 1.6×10^6 , 6.4×10^6 , 26×10^6 , 103×10^6 , and 411×10^6 ha.

When an observational unit is divided into smaller subunits, its total ("regional") spatial diversity, D_T , can be partitioned into its α and β components (67), with D_α referring to the local diversity and D_β referring to the regional-to-local diversity ratio. Both components depend on the definition of "local," which might be set by the aggregation level of the input data (e.g., farm, county, or state data) or might be arbitrarily selected if higher-resolution data are available. Here, for all observational units with an area greater than or equal to 1,568 ha, their total diversity (D_T) was partitioned into D_α (local diversity) and D_β (regional-to-local diversity ratio) by applying Eqs. 2 and 3 and using all grids with smaller cells whose borders perfectly fit within the observational units (in other words, the division between resolutions is without remainder). For example, the 15.84 km resolution grid was partitioned using the 0.33, 0.66, 0.99, 1.32, 1.98, and 3.96 km cells as subunits, and different α and β diversities estimations were obtained for all those subunit sizes:

$$D_\alpha = \exp \left[- \sum_{j=1}^N \left(w_j \sum_{i=1}^S (p_{ij} \ln p_{ij}) \right) \right], \quad [2]$$

$$D_\beta = D_T / D_\alpha. \quad [3]$$

In Eq. 2, N is the number of subunits in a given area, and w_j is the weight of subunit j , estimated as the number of cropland pixels within the subunit divided by the total number of cropland pixels in that area. D_α is thus the weighted mean effective number of crop species of the subunits, while D_β expresses how many times as diverse the observational unit is compared with the average diversity of its subunits (66).

Temporal crop species diversity (D_T) was calculated with 10 years of data (2008 to 2017) with Eq. 1 at a 30 m spatial resolution and then aggregated to the same resolutions used for D_T by applying Eq. 4 in order to maintain an equivalent relation between spatial and temporal diversity:

$$D_{T(r)} = \exp \left(\frac{\sum_{i=1}^n \ln D_{T(30)}}{n} \right). \quad [4]$$

In Eq. 4, n is the number of 30 m cropland grid cells for a cell at resolution r . In other words, instead of averaging temporal diversity values at 30 m resolution, $D_{T(r)}$ (at the resolution r) is computed as the exponent of the average of the Shannon index for temporal crop diversity. Accordingly, 10 year

averages of D_T , D_α , and D_β were computed as the exponent of the weighted average of the Shannon index of each year in order to ensure the equality in Eq. 3 at all levels of aggregation. Back transforming diversities to the Shannon index when averaging and aggregating to other resolutions is necessary because entropies have better mathematical properties than diversities (which also happens with coefficients of variation compared to standard deviations), and it would be wrong to simply average diversity values (65).

Postprocessing and Analysis. Diversity estimates based on very low crop area have greater uncertainty and, on average, lower diversity values. For that reason, observational units with a crop area lower than certain thresholds were removed from analysis. These thresholds ranged from 11 to 0.5% (lower percentages for larger observational unit sizes) and were defined, for each resolution, as the crop area in which the last segment of a two-piece linear spline of D_T as a function of crop area (%) no longer yields a significant positive slope ($P > 0.01$; *SI Appendix, Fig. S5*).

Then, D_T , D_α , and D_β within the conterminous United States were mapped, and correlations among different levels and types of crop species diversities were assessed in order to examine the association between the spatial and temporal dimensions of crop species diversity. We measured the level of (dis)agreement between D_T and D_α at different aggregation

levels with the root-mean-square deviation (RMSD) = $\sqrt{\frac{1}{n} \sum_{i=1}^n (D_{T_i} - D_{\alpha_i})^2}$ and

its components: bias ($Bias = \overline{D_T} - \overline{D_\alpha}$), the difference between population standard deviations ($\Delta_{SD} = SD_{D_T} - SD_{D_\alpha}$), and the lack of positive correlation ($1 - r$, where r is Pearson's correlation coefficient). Note that $RMSD^2 = Bias^2 + \Delta_{SD}^2 + (2 \times SD_{D_T} \times SD_{D_\alpha} \times (1 - r))$ (68). We evaluated how county-level spatial diversity relates to county average D_α . We compared the agreement between county D_α averages and 1) county D_T and 2) county D_α based on 174 ha subunits.

All data analysis was done with R (69), and the scripts used for this study are available at https://github.com/AramburuMerlos/cropdiv_usa.

Data Availability. All study data are included in the article and *SI Appendix*.

ACKNOWLEDGMENTS. F.A.M. was supported by the Fulbright Program and the Argentine Ministry of Education.

1. D. Renard, D. Tilman, National food production stabilized by crop diversity. *Nature* **571**, 257–260 (2019).
2. A. E. Larsen, F. Noack, Identifying the landscape drivers of agricultural insecticide use leveraging evidence from 100,000 fields. *Proc. Natl. Acad. Sci. U.S.A.* **114**, 5473–5478 (2017).
3. A. C. Gaudin *et al.*, Increasing crop diversity mitigates weather variations and improves yield stability. *PLoS One* **10**, e0113261 (2015).
4. C. Kremen, A. M. Merenlender, Landscapes that work for biodiversity and people. *Science* **362**, eaau6020 (2018).
5. S. Sirami *et al.*, Increasing crop heterogeneity enhances multitrophic diversity across agricultural regions. *Proc. Natl. Acad. Sci. U.S.A.* **116**, 16442–16447 (2019).
6. I. Perfecto, J. Vandermeer, The agroecological matrix as alternative to the land-sparing/agriculture intensification model. *Proc. Natl. Acad. Sci. U.S.A.* **107**, 5786–5791 (2010).
7. J. Aguilar *et al.*, Crop species diversity changes in the United States: 1978–2012. *PLoS One* **10**, e0136580 (2015).
8. R. J. Hijmans, H. Choe, J. Perlman, Spatiotemporal patterns of field crop diversity in the United States, 1870–2012. *Agric. Environ. Lett.* **1**, 160022 (2016).
9. D. Renard, E. M. Bennett, J. M. Rhemtulla, Agro-biodiversity has increased over a 95 year period at sub-regional and regional scales in southern Quebec, Canada. *Environ. Res. Lett.* **11**, 124024 (2016).
10. J. C. Smith, A. Ghosh, R. J. Hijmans, Agricultural intensification was associated with crop diversification in India (1947–2014). *PLoS One* **14**, e0225555 (2019).
11. M. A. Aizen *et al.*, Global agricultural productivity is threatened by increasing pollinator dependence without a parallel increase in crop diversification. *Glob. Chang. Biol.* **25**, 3516–3527 (2019).
12. D. A. Landis, M. M. Gardiner, W. van der Werf, S. M. Swinton, Increasing corn for biofuel production reduces biocontrol services in agricultural landscapes. *Proc. Natl. Acad. Sci. U.S.A.* **105**, 20552–20557 (2008).
13. M. J. Swift, A.-M. Izac, M. van Noordwijk, Biodiversity and ecosystem services in agricultural landscapes—Are we asking the right questions? *Agric. Ecosyst. Environ.* **104**, 113–134 (2004).
14. T. Tschantke, A. M. Klein, A. Kruess, I. Steffan-Dewenter, C. Thies, Landscape perspectives on agricultural intensification and biodiversity–ecosystem service management. *Ecol. Lett.* **8**, 857–874 (2005).
15. B. B. Lin, Resilience in agriculture through crop diversification: Adaptive management for environmental change. *Bioscience* **61**, 183–193 (2011).
16. K. L. Mercer *et al.*, "Crop evolutionary agroecology: Genetic and functional dimensions of agrobiodiversity and associated knowledge" in *Agrobiodiversity: Integrating Knowledge for a Sustainable Future*, K. S. Zimmerer, S. de Haan, Eds. (Strüngmann Forum Reports, MIT Press, 2019), pp. 20–62.
17. S. A. Levin, The problem of pattern and scale in ecology: The Robert H. MacArthur Award Lecture. *Ecology* **73**, 1943–1967 (1992).
18. D. G. Bullock, Crop rotation. *Crit. Rev. Plant Sci.* **11**, 309–326 (1992).
19. E. A. Curl, Control of plant diseases by crop rotation. *Bot. Rev.* **29**, 413–479 (1963).
20. M. Liebman, E. Dyck, Crop rotation and intercropping strategies for weed management. *Ecol. Appl.* **3**, 92–122 (1993).
21. L. K. Tiemann, A. S. Grandy, E. E. Atkinson, E. Marin-Spiotta, M. D. McDaniel, Crop rotational diversity enhances belowground communities and functions in an agroecosystem. *Ecol. Lett.* **18**, 761–771 (2015).
22. R. F. Denison, *Darwinian Agriculture: How Understanding Evolution Can Improve Agriculture* (Princeton University Press, 2012).
23. J. M. MacDonald, P. Korb, R. A. Hoppe, *Farm Size and the Organization of US Crop Farming* (US Department of Agriculture Economic Research Service, Washington, DC, 2013).
24. S. A. Wood *et al.*, Functional traits in agriculture: Agrobiodiversity and ecosystem services. *Trends Ecol. Evol.* **30**, 531–539 (2015).
25. J. M. Krupinsky, K. L. Bailey, M. P. McMullen, B. D. Gossen, T. K. Turkington, Managing plant disease risk in diversified cropping systems. *Agron. J.* **94**, 198–209 (2002).
26. M. Liebman *et al.*, Ecologically sustainable weed management: How do we get from proof-of-concept to adoption? *Ecol. Appl.* **26**, 1352–1369 (2016).
27. M. D. McDaniel, L. K. Tiemann, A. S. Grandy, Does agricultural crop diversity enhance soil microbial biomass and organic matter dynamics? A meta-analysis. *Ecol. Appl.* **24**, 560–570 (2014).
28. L. L. Renwick, T. M. Bowles, W. Deen, A. C. Gaudin, "Potential of increased temporal crop diversity to improve resource use efficiencies: Exploiting water and nitrogen linkages" in *Agroecosystem Diversity*, G. Lemaire, P. C. de Faccio Carvalho, S. Kronberg, S. Recous, Eds. (Elsevier, 2019), pp. 55–73.
29. G. A. Studdert, H. E. Echeverria, Crop rotations and nitrogen fertilization to manage soil organic carbon dynamics. *Soil Sci. Soc. Am. J.* **64**, 1496–1503 (2000).
30. M. L. Rosenzweig, *Species Diversity in Space and Time* (Cambridge University Press, 1995).
31. M. I. Shafi, G. A. Yarranton, Diversity, floristic richness, and species evenness during a secondary (post-fire) succession. *Ecology* **54**, 897–902 (1973).

32. J. A. Santora *et al.*, Impacts of ocean climate variability on biodiversity of pelagic forage species in an upwelling ecosystem. *Mar. Ecol. Prog. Ser.* **580**, 205–220 (2017).
33. W. D. Koenig, J. M. H. Knops, The mystery of masting in trees: Some trees reproduce synchronously over large areas, with widespread ecological effects, but how and why? *Am. Sci.* **93**, 340–347 (2005).
34. J. Ren, J. B. Campbell, Y. Shao, Spatial and temporal dimensions of agricultural land use changes, 2001–2012, east-central Iowa. *Agric. Syst.* **148**, 149–158 (2016).
35. C. A. Seifert, M. J. Roberts, D. B. Lobell, Continuous corn and soybean yield penalties across hundreds of thousands of fields. *Agron. J.* **109**, 541–548 (2017).
36. J. D. Plourde, B. C. Pijanowski, B. K. Pekin, Evidence for increased monoculture cropping in the central United States. *Agric. Ecosyst. Environ.* **165**, 50–59 (2013).
37. A. Stern, P. C. Doraiswamy, E. R. Hunt, Changes of crop rotation in Iowa determined from the United States Department of Agriculture, National Agricultural Statistics Service Cropland Data Layer product. *J. Appl. Remote Sens.* **6**, 063590 (2012).
38. C. Kremen, A. Iles, C. Bacon, Diversified farming systems: An agroecological, systems-based alternative to modern industrial agriculture. *Ecol. Soc.* **17**, 44 (2012).
39. G. Lemaire, P. C. de Faccio Carvalho, S. Kronberg, S. Recous, *Agroecosystem Diversity: Reconciling Contemporary Agriculture and Environmental Quality* (Academic Press, 2018).
40. J. Pretty *et al.*, Global assessment of agricultural system redesign for sustainable intensification. *Nat. Sustain.* **1**, 441–446 (2018).
41. S. Spiegel *et al.*, Evaluating strategies for sustainable intensification of US agriculture through the Long-Term Agroecosystem Research Network. *Environ. Res. Lett.* **13**, 034031 (2018).
42. G. E. Roesch-McNally, J. G. Arbuckle, J. C. Tyndall, Barriers to implementing climate resilient agricultural strategies: The case of crop diversification in the US Corn Belt. *Glob. Environ. Chang.* **48**, 206–215 (2018).
43. E. G. Smith, R. P. Zentner, C. A. Campbell, R. Lemke, K. Brandt, Long-term crop rotation effects on production, grain quality, profitability, and risk in the Northern Great Plains. *Agron. J.* **109**, 957–967 (2017).
44. R. Trostle, *Global Agricultural Supply and Demand: Factors Contributing to the Recent Increase in Food Commodity Prices* (DIANE Publishing, rev. ed., 2010).
45. G. Berti, C. Mulligan, Competitiveness of small farms and innovative food supply chains: The role of food hubs in creating sustainable regional and local food systems. *Sustainability* **8**, 616 (2016).
46. G. Lemaire, F. Gastal, A. Franzluebbers, A. Chabbi, Grassland-cropping rotations: An avenue for agricultural diversification to reconcile high production with environmental quality. *Environ. Manage.* **56**, 1065–1077 (2015).
47. C. A. Seifert, G. Azzari, D. B. Lobell, Satellite detection of cover crops and their effects on crop yield in the midwestern United States. *Environ. Res. Lett.* **13**, 064033 (2018).
48. H. Blanco-Canqui *et al.*, Cover crops and ecosystem services: Insights from studies in temperate soils. *Agron. J.* **107**, 2449–2474 (2015).
49. D. Tilman, M. Clark, Global diets link environmental sustainability and human health. *Nature* **515**, 518–522 (2014).
50. T. Beal, E. Massiot, J. E. Arsenault, M. R. Smith, R. J. Hijmans, Global trends in dietary micronutrient supplies and estimated prevalence of inadequate intakes. *PLoS One* **12**, e0175554 (2017).
51. C. Lachat *et al.*, Dietary species richness as a measure of food biodiversity and nutritional quality of diets. *Proc. Natl. Acad. Sci. U.S.A.* **115**, 127–132 (2018).
52. S. J. Risch, D. Andow, M. A. Altieri, Agroecosystem diversity and pest control: Data, tentative conclusions, and new research directions. *Environ. Entomol.* **12**, 625–629 (1983).
53. M. A. Altieri, The significance of diversity in the maintenance of the sustainability of traditional agroecosystems. *ILEIA Newsl.* **3**, 3–7 (1987).
54. G. Conway, *The Doubly Green Revolution: Food for All in the Twenty-First Century* (Cornell University Press, 1998).
55. A. S. Lithourgidis, C. A. Dordas, C. A. Damalas, D. N. Vlachostergios, Annual intercrops: An alternative pathway for sustainable agriculture. *Aust. J. Crop Sci.* **5**, 396–410 (2011).
56. Y. Yu, T.-J. Stomph, D. Makowski, L. Zhang, W. van der Werf, A meta-analysis of relative crop yields in cereal/legume mixtures suggests options for management. *Field Crops Res.* **198**, 269–279 (2016).
57. Y. Yu, T.-J. Stomph, D. Makowski, W. van der Werf, Temporal niche differentiation increases the land equivalent ratio of annual intercrops: A meta-analysis. *Field Crops Res.* **184**, 133–144 (2015).
58. X.-M. Xu, A simulation study on managing plant diseases by systematically altering spatial positions of cultivar mixture components between seasons. *Plant Pathol.* **60**, 857–865 (2011).
59. G. Peter, A. Runge-Metzger, Monocropping, intercropping or crop rotation? An economic case study from the West African Guinea savannah with special reference to risk. *Agric. Syst.* **45**, 123–143 (1994).
60. S. Fritz *et al.*, Mapping global cropland and field size. *Glob. Chang. Biol.* **21**, 1980–1992 (2015).
61. L. Yan, D. P. Roy, Conterminous United States crop field size quantification from multi-temporal Landsat data. *Remote Sens. Environ.* **172**, 67–86 (2016).
62. P. Calviño, J. Monzon, Farming systems of Argentina: Yield constraints and risk management. *Crop Physiol. Appl. Genet. Improv. Agron.* **51**, 70 (2009).
63. USDA National Agricultural Statistics Service, Cropland Data Layer. <https://nassgeodata.gmu.edu/CropScape/>. Accessed 6 April 2018.
64. C. Boryan, Z. Yang, R. Mueller, M. Craig, Monitoring US agriculture: The US Department of Agriculture, National Agricultural Statistics Service, Cropland Data Layer Program. *Geocarto Int.* **26**, 341–358 (2011).
65. L. Jost, Entropy and diversity. *Oikos* **113**, 363–375 (2006).
66. H. Tuomisto, A diversity of beta diversities: Straightening up a concept gone awry. Part 1. Defining beta diversity as a function of alpha and gamma diversity. *Ecography* **33**, 2–22 (2010).
67. L. Jost, Partitioning diversity into independent alpha and beta components. *Ecology* **88**, 2427–2439 (2007).
68. K. Kobayashi, M. U. Salam, Comparing simulated and measured values using mean squared deviation and its components. *Agron. J.* **92**, 345–352 (2000).
69. R. Core Team, *R: A Language and Environment for Statistical Computing* (R Foundation for Statistical Computing, Vienna, Austria, 2019).



Supplementary Information for

The relation between spatial and temporal crop species diversity

Fernando Aramburu Merlos ^{a,b,*} and Robert J. Hijmans^a

^a Department of Environmental Science and Policy, University of California Davis, Davis, California, United States of America

^b Instituto Nacional de Tecnología Agropecuaria (INTA), Unidad Integrada Balcarce, Ruta 226, km 73.5, CC 276, CP 7620, Balcarce, Buenos Aires, Argentina.

* corresponding author.

Email: faramburumerlos@ucdavis.edu

This PDF file includes:

Figures S1 to S5
Tables S1 to S2

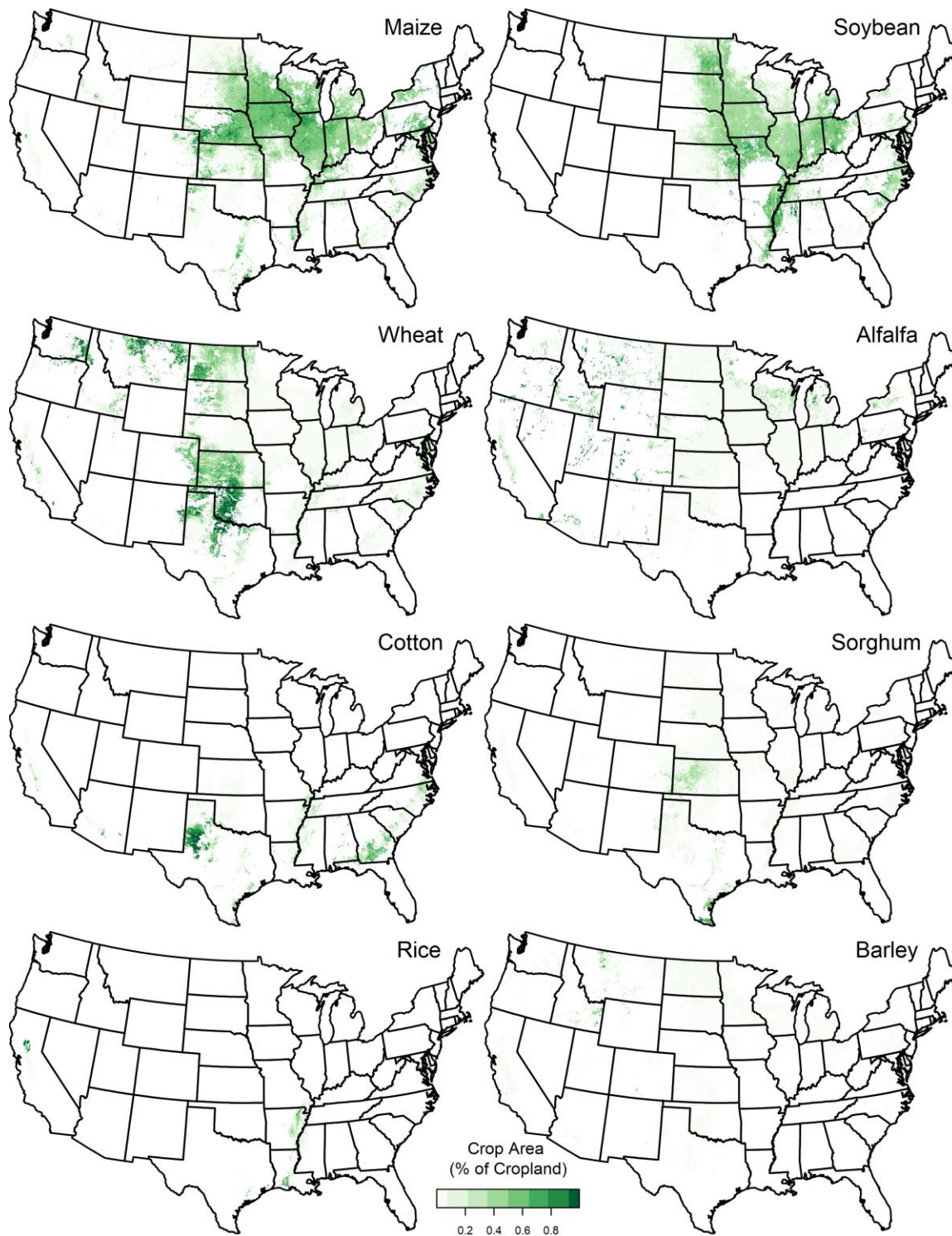


Fig. S1. Crop area of the eight most abundant crop species in the United States, expressed as percentage of the total cropland (3.96 km spatial resolution).

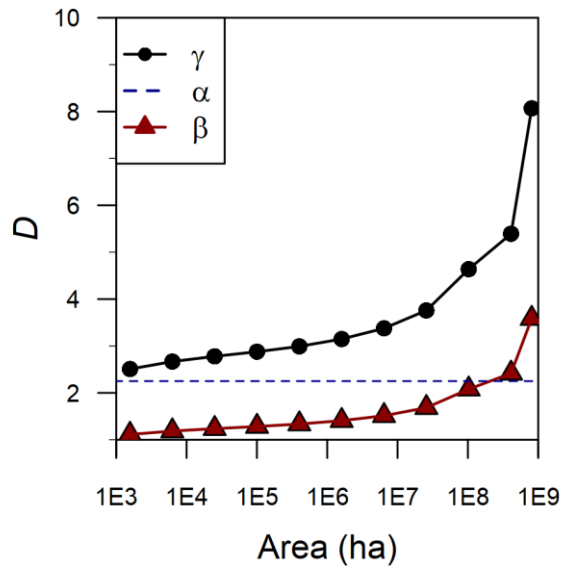


Fig. S2. Average crop species diversity in space (D_γ) for the conterminous United States for observational units equal or larger than 1568 ha. D_γ was divided in its D_α and D_β components based on 392 ha subunits. The horizontal axis has a logarithmic scale. National level diversity values (Area = 8.08×10^8 ha) are also shown.

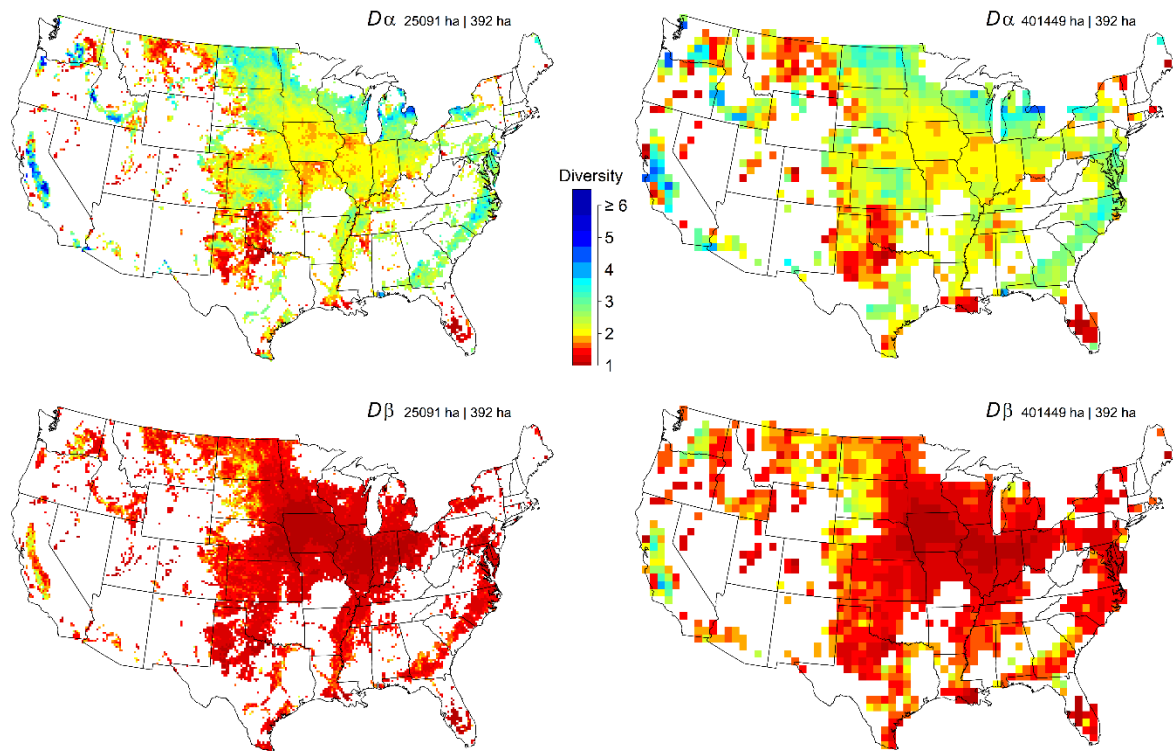


Fig. S3. Alpha ($D\alpha$) and beta ($D\beta$) crop species diversities of the conterminous United States calculated based on 392 ha subunits (i.e. local scale) for two observational unit sizes: 25091 and 401449 ha (regional scale). $D\alpha$ represents the weighted average crop species diversity of the subunits and $D\beta$ the regional to local diversity ratio.

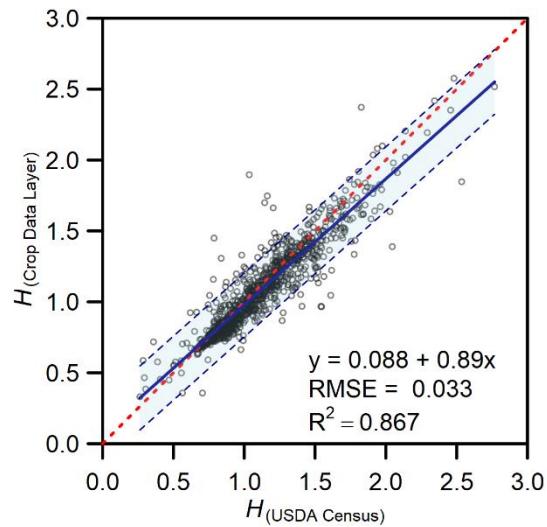


Fig. S4. County-level crop species Shannon Entropy index (H) for the conterminous United States computed with data from the 2012 USDA Census of Agriculture (USDA Census) against county-level H derived from the 2012 Crop Data Layer (CDL). Only counties with more than 20% of crop area were considered for the calculations, comprising 1085 entropy estimations for each data set. The red dashed line shows the identity function, the blue solid line shows the fitted linear regression, and the blue dashed lines indicate the confidence interval for the prediction of a new observation of H_{CDL} .

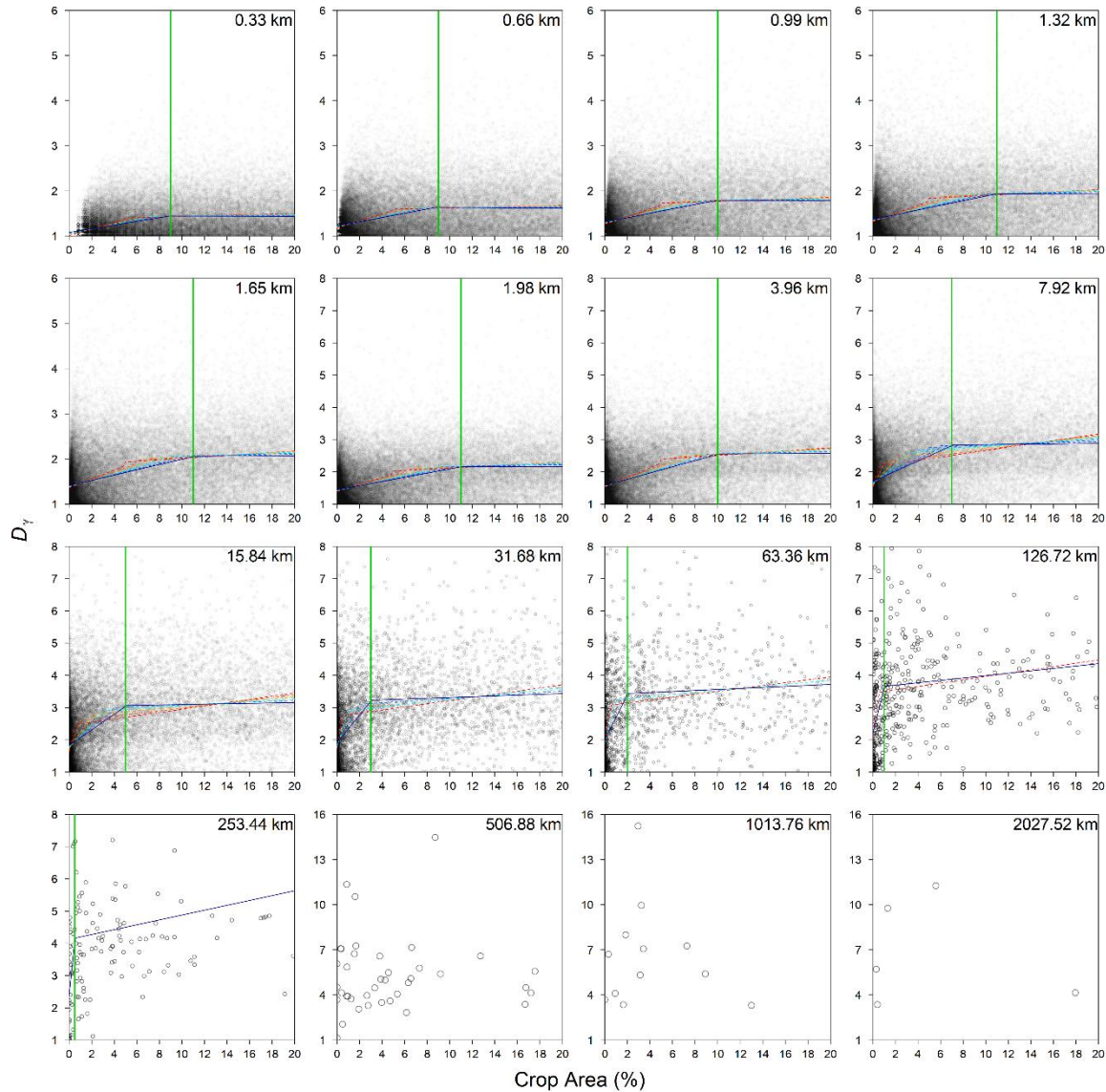


Fig. S5. Threshold selection for removal of cells with a low proportion of cropland. Each plot represents a different spatial resolution. For each resolution, gamma diversity (D_γ) is plotted as a function of cell crop area (%). Several two-piece linear splines were fitted changing the location of their unique knot, adding one percent at each iteration until the second spline no longer yielded a significant positive slope. The knot position for the last spline was used as the crop area threshold. The solid blue line is the last spline with no significant positive slope in the second piece (P -value > 0.01). The vertical green line indicates the last spline-knot position and the value used as threshold for the given resolution (e.g. 0.99 km: 10%; 31.68 km: 5%; 126.72 km: 2%). The dashed lines in red to light blue are the preceding splines with significant positive slopes (P -value < 0.01). Note that for resolutions lower than 507 km (areas > 25.7 Mha) no threshold was used as there was no significant association between D_γ and crop area.

Table S1. Percentage of cropland area under mono- or perennial crops ($D\tau = 1$) and other summary statistics of temporal crop species diversity ($D\tau$) for each state in the conterminous US.

State	$D\tau = 1$ (%)	1 st quartile	Median	Mean	3 rd quartile
Alabama	3	2	2.6	2.7	3.4
Arizona	14	1.5	2.4	2.6	3.4
Arkansas	7	1.8	2	2.2	2.6
California	22	1.4	2.3	2.5	3.4
Colorado	18	1.5	2	2	2.6
Connecticut	66	1	1	1.3	1.5
Delaware	1	2.3	2.8	2.8	3.2
Florida	55	1	1	1.5	1.9
Georgia	7	1.9	2.6	2.7	3.4
Idaho	12	1.6	2.3	2.4	3
Illinois	3	1.8	2	2	2
Indiana	2	2	2	2	2
Iowa	4	1.9	2	1.9	2
Kansas	6	1.9	2.1	2.3	2.8
Kentucky	3	2	2	2.3	2.9
Louisiana	14	1.5	2	2	2.6
Maine	27	1	2.6	2.6	3.6
Maryland	1	2.4	2.8	2.7	3
Massachusetts	30	1	1.5	1.7	2
Michigan	5	2	2.5	2.5	3
Minnesota	3	2	2	2.3	2.6
Mississippi	8	1.6	2	2.2	2.6
Missouri	4	1.9	2	2.1	2.5
Montana	27	1	1.7	1.9	2.5
Nebraska	6	1.8	2	2	2
Nevada	53	1	1	1.4	1.6
New Hampshire	72	1	1	1.2	1.4
New Jersey	6	1.8	2.4	2.6	3.1
New Mexico	21	1.4	1.9	2.1	2.6
New York	12	1.7	2	2.3	2.7
North Carolina	2	2.3	2.8	2.8	3.3
North Dakota	2	2	2.7	2.9	3.6
Ohio	2	2	2	2.2	2.6
Oklahoma	36	1	1.5	1.7	2
Oregon	27	1	1.9	2.2	2.9
Pennsylvania	12	1.6	2	2.1	2.6
Rhode Island	34	1	1.5	1.6	2
South Carolina	2	2.4	2.9	2.9	3.5
South Dakota	2	2	2.5	2.5	2.9
Tennessee	6	1.8	2.4	2.4	2.9
Texas	20	1.4	1.9	2	2.5
Utah	36	1	1.5	1.7	2
Vermont	66	1	1	1.3	1.5
Virginia	5	2	2.6	2.5	3
Washington	25	1.4	1.9	2.2	2.8
West Virginia	18	1.5	2	2	2.6
Wisconsin	5	1.8	2	2.3	2.7
Wyoming	28	1	1.8	2	2.6

Table S2. Frequency distribution (%) of temporal crop species diversity (D_t) for annual crops and their corresponding crop area (ha). For area, M indicates millions and k thousands.

Crop	D_t range							Area
	= 1	(1,2]	(2,3]	(3,4]	(4,5]	(5,6]	(6,11]	
Maize	5	66	22	6	1	0	0	34.8M
Soybean	2	64	26	7	1	0	0	31.2M
Wheat	16	31	36	13	3	0	0	18.2M
Cotton	15	42	28	12	3	0	0	4.4M
Sorghum	2	42	39	15	2	0	0	2.6M
Rice	21	55	19	5	1	0	0	1M
Barley	3	28	32	24	11	3	1	936k
Durum Wheat	2	21	37	25	11	3	1	687k
Dry Bean	0	11	34	36	16	3	1	644k
Sunflower	0	10	36	36	14	3	1	563k
Canola	0	19	35	29	14	3	1	530k
Oat	3	19	35	29	11	3	1	499k
Peanut	1	29	36	23	10	2	0	485k
Sugarbeet	0	5	38	40	14	2	0	444k
Pea	0	18	36	27	14	4	1	402k
Potato	1	17	35	29	14	3	1	383k
Lentil	0	21	44	25	8	2	0	188k
Millet	0	26	41	23	8	2	0	184k
Rye	6	39	27	18	8	2	0	167k
Tomato	0	8	26	33	22	8	3	110k
Flaxseed	0	7	27	34	23	7	2	91k
Triticale	0	23	33	26	12	4	1	72k
Safflower	0	23	32	26	13	4	2	52k
Onion	2	7	19	33	25	11	4	51k
Tobacco	0	6	28	37	21	7	1	33k
Sweet Potato	0	9	26	34	22	8	2	30k
Lettuce	0	2	16	34	30	13	5	25k
Squash	0	8	38	27	16	7	3	16k
Carrot	0	4	19	29	28	13	6	14k
Watermelon	0	6	24	34	21	10	5	14k
Cantaloupe	0	5	21	31	26	11	5	14k
Cabbage	0	4	25	35	24	9	4	13k
Cucumber	0	3	20	36	28	10	3	13k
Mustard	0	15	33	31	15	5	1	13k
Garlic	0	7	14	30	29	13	6	6.4k
Pepper	0	10	20	26	24	13	7	6.4k
Greens	0	5	19	31	26	13	6	5.7k
Mint	0	8	22	30	24	11	5	5.3k
Buckwheat	0	11	27	27	22	9	4	4k
Radish	0	12	25	28	20	9	5	3.1k
Vetch	0	12	28	26	19	10	5	1.6k
Camelina	0	20	34	31	11	3	1	1.3k
Turnip	0	7	21	27	25	13	7	634
Celery	0	9	23	27	22	13	6	407
Gourd	0	6	36	33	14	4	7	114
Chick Pea	0	7	41	50	1	1	1	90
Eggplant	0	5	17	23	23	18	14	84

Table S3 Crop Data Layer (CDL) crop classes and their corresponding scientific names and common names as used in this paper. CDL classes with the same common name were aggregated. For example, corn, sweet corn and pop-corn were aggregated as maize.

CDL class	Common name	Scientific Name	CDL class	Common name	Scientific Name
Corn	Maize	<i>Zea mays</i>	Switchgrass	Switchgrass	<i>Panicum virgatum</i>
Cotton	Cotton	<i>Gossypium hirsutum</i>	Cherries	Cherry	<i>Prunus avium</i>
Rice	Rice	<i>Oryza sativa</i>	Peaches	Peach/Nectarine	<i>Prunus persica</i>
Sorghum	Sorghum	<i>Sorghum bicolor</i>	Apples	Apple	<i>Malus pumila</i>
Soybeans	Soybean	<i>Glycine max</i>	Grapes	Grape	<i>Vitis vinifera</i>
Sunflower	Sunflower	<i>Helianthus annuus</i>	Christmas Trees	Christmas Tree	<i>Picea spp.</i>
Peanut	Peanut	<i>Arachis hypogaea</i>	Citrus	Citrus	<i>Citrus spp.</i>
Tobacco	Tobacco	<i>Nicotiana tabacum</i>	Pecans	Pecan	<i>Carya illinoensis</i>
Sweet Corn	Maize	<i>Zea mays</i>	Almonds	Almond	<i>Prunus dulcis</i>
Pop or Orn Corn	Maize	<i>Zea mays</i>	Walnuts	Walnut	<i>Juglans regia</i>
Mint	Mint	<i>Mentha spp.</i>	Pears	Pear	<i>Pyrus spp.</i>
Barley	Barley	<i>Hordeum vulgare</i>	Pistachios	Pistachio	<i>Pistacia vera</i>
Durum Wheat	Durum Wheat	<i>Triticum durum</i>	Triticale	Triticale	<i>Triticosecale</i>
Spring Wheat	Wheat	<i>Triticum aestivum</i>	Carrots	Carrot	<i>Daucus carota</i>
Winter Wheat	Wheat	<i>Triticum aestivum</i>	Asparagus	Asparagus	<i>Asparagus officinalis</i>
Rye	Rye	<i>Secale cereale</i>	Garlics	Garlic	<i>Allium sativum</i>
Oats	Oat	<i>Avena sativa</i>	Cantaloupe	Cantaloupe	<i>Cucumis melo</i>
Millet	Millet	<i>Pennisetum glaucum</i>	Prunes	Prune	<i>Prunus spp.</i>
Speltz	Wheat	<i>Triticum aestivum</i>	Olives	Olive	<i>Olea europaea</i>
Canola	Canola	<i>Brassica napus</i>	Oranges	Orange	<i>Citrus sinensis</i>
Flaxseed	Flaxseed	<i>Linum usitatissimum</i>	Honeydew Melons	Cantaloupe	<i>Cucumis melo</i>
Safflower	Safflower	<i>Carthamus tinctorius</i>	Brocolis	Cabbage	<i>Brassica oleracea</i>
Rape Seeds	Canola	<i>Brassica napus</i>	Peppers	Pepper	<i>Capsicum annum</i>
Mustards	Mustard	<i>Brassica spp.</i>	Pomegranates	Pomegranate	<i>Punica granatum</i>
Alfalfa	Alfalfa	<i>Medicago sativa</i>	Nectarines	Peach/Nectarine	<i>Prunus persica</i>
Camelina	Camelina	<i>Camelina sativa</i>	Plums	Plum	<i>Prunus spp.</i>
Buckwheat	Buckwheat	<i>Fagopyrum esculentum</i>	Strawberries	Strawberry	<i>Fragaria x ananassa</i>
Sugarbeet	Sugarbeet	<i>Beta vulgaris</i>	Squash	Squash	<i>Cucurbita spp.</i>
Dry Beans	Dry Bean	<i>Phaseolus spp.</i>	Apricots	Apricot	<i>Prunus armeniaca</i>
Potatoes	Potato	<i>Solanum tuberosum</i>	Vetch	Vetch	<i>Vicia villosa</i>
Sugarcane	Sugarcane	<i>Saccharum officinarum</i>	Lettuce	Lettuce	<i>Lactuca sativa</i>
Sweet Potatoes	Sweet Potato	<i>Ipomoea batatas</i>	Pumpkins	Squash	<i>Cucurbita spp.</i>
Watermelons	Watermelon	<i>Citrullus lanatus</i>	Blueberries	Blueberry	<i>Vaccinium spp.</i>
Onions	Onion	<i>Allium cepa</i>	Cabbages	Cabbage	<i>Brassica oleracea</i>
Cucumbers	Cucumber	<i>Cucumis sativus</i>	Cauliflower	Cabbage	<i>Brassica oleracea</i>
Chick Peas	Chick Pea	<i>Cicer arietinum</i>	Celery	Celery	<i>Apium graveolens</i>
Lentils	Lentil	<i>Lens culinaris</i>	Radish	Radish	<i>Raphanus sativus</i>
Peas	Pea	<i>Pisum sativum</i>	Turnips	Turnip	<i>Brassica rapa</i>
Tomatoes	Tomato	<i>Lycopersicon esculentum</i>	Eggplant	Eggplant	<i>Solanum melongena</i>
Caneberries	Caneberry	<i>Phylloctepes gracilis</i>	Gourd	Gourd	<i>Cucurbita spp.</i>
Hops	Hop	<i>Humulus lupulus</i>	Cranberries	Cranberry	<i>Vaccinium spp.</i>

CHAPTER 2

Potential, attainable, and current levels of global crop diversity

Environmental Research Letters, 17(4) 044071.

ENVIRONMENTAL RESEARCH
LETTERS

LETTER



Potential, attainable, and current levels of global crop diversity

OPEN ACCESS

RECEIVED
24 December 2021REVISED
22 February 2022ACCEPTED FOR PUBLICATION
30 March 2022PUBLISHED
8 April 2022

Original content from
this work may be used
under the terms of the
Creative Commons
Attribution 4.0 licence.

Any further distribution
of this work must
maintain attribution to
the author(s) and the title
of the work, journal
citation and DOI.

Fernando Aramburu Merlos^{1,2,*}  and Robert J Hijmans¹ ¹ Department of Environmental Science and Policy, University of California Davis, Davis, CA, United States of America² Instituto Nacional de Tecnología Agropecuaria (INTA, Unidad Integrada Balcarce), Ruta 226, km 73.5, CC 276, CP 7620 Balcarce, Buenos Aires, Argentina

* Author to whom any correspondence should be addressed.

E-mail: faramburumerlos@ucdavis.edu**Keywords:** attainable diversity, potential diversity, diversity gap, crop distribution, crop suitability, crop diversification, agroecology
Supplementary material for this article is available [online](#)**Abstract**

High levels of crop species diversity are considered beneficial. However, increasing diversity might be difficult because of environmental constraints and the reliance on a few major crops for most food supply. Here we introduce a theoretical framework of hierarchical levels of crop diversity, in which the environmental requirements of crops limit potential diversity, and the demand for agricultural products further constrain attainable crop diversity. We estimated global potential, attainable, and current crop diversity for grid cells of 86 km². To do so, we first estimated cropland suitability values for each of 171 crops, with spatial distribution models to get estimations of relative suitability and with a crop model to estimate absolute suitability. We then used a crop allocation algorithm to distribute the required crop area to suitable cropland. We show that the attainable crop diversity is lower in temperate and continental areas than in tropical and coastal regions. The diversity gap (the difference between attainable and current crop diversity) is particularly large in most of the Americas and relatively small in parts of Europe and East Asia. By filling these diversity gaps, crop diversity could double on 84% of the world's agricultural land without changing the aggregate amount of global food produced. It follows that while there are important regional differences in attainable diversity, specialization of farms and regions is the main reason for low levels of local crop diversity across the globe, rather than our high reliance on a few crops.

1. Introduction

High crop species diversity is considered important for agriculture sustainability (Jones *et al* 2021) because of its positive association with food production stability and resilience (Gaudin *et al* 2015, Renard and Tilman 2019). However, it is unclear how much diversity would be enough or desirable and how this varies between locations. Not all crops can grow everywhere, and what may be considered low diversity in one region could be beyond what is ecologically possible in another region. Moreover, only a few crops provide the vast majority of our food supply, which *a priori* imposes a severe demand-side constraint on diversification (Cassman and Grassini 2020, Renard and Tilman 2021). Even though it could be desirable to reduce the importance of the most

dominant crops (Tilman and Clark 2014), vast areas would still be needed to produce staple crops such as wheat, rice, and cassava, but not for many other crops that are only useful in relatively small quantities. Thus, to understand current diversity patterns and assess opportunities for diversification, it is essential to consider both ecological constraints (which crops can be grown in a location) and economic constraints (how much demand is there for these crops).

To allow for such analysis, we need a framework to determine what levels of crop species diversity are possible to compare these with the actual situation. Here we provide and apply such a framework inspired by concepts from production ecology and the work on crop yield gaps (van Ittersum *et al* 2013). We first define different theoretical levels of crop diversity (maximal, potential, and attainable)

and then calculate their present values (circa 2010) for 86 km² grid cells for the entire world. The theoretical levels of diversity depend on estimates of crop-specific cropland suitability that we computed in two ways: using spatial distribution models (SDMs) (relative suitability) and rule-based crop models (absolute suitability). We then used a crop allocation algorithm to predict potential and attainable crop distributions and calculate the corresponding diversity level. Finally, we contrasted these levels to current patterns of diversity and computed diversity gaps.

2. Theoretical levels of crop diversity

Crop diversity (D) has been defined as the effective number of different crop species planted in a given area (Jost 2006). The term effective refers to the number of equally abundant virtual species that has the same entropy as the actual species when considering their relative abundance.

To better interpret patterns in current crop diversity (cD), we define three new theoretical concepts: maximum, potential, and attainable crop diversity (figure 1). Maximum diversity (mD) results from planting all crops that can be grown in an area in equal proportion. It has very limited relevance, and while we include it in our framework, we do not discuss it further. Potential diversity (pD) is reached when the area planted with each crop is a function of crop-specific cropland suitability (the proportion of land planted to the best-adapted crops is largest). Attainable diversity (aD) is obtained if all crops are planted to maximize D while considering crop-specific cropland suitability, as well as the demand for different crops and the interspecific competition for land. The main difference between aD and pD is that aD is constrained to meet crop-specific total demand (for any purpose, including food, feed, fiber, and industrial use). We define crop-specific 'demand' as equal to each crop's total current production (supply). Thus, aD can be reached without changing total consumption and crop diversity at the global level (or, more generally, in the entire study region in question, which could be a country). Therefore, by definition, at the global (study region) level, aD equals cD , but this is not true at lower levels of aggregation (areas within the study region). pD is directly proportional to the number of crops considered, as it assumes that any crop can take an equal amount of land. In contrast, aD is less sensitive to the omission of rare crops.

Lastly, we define the diversity gap (Dg) as the difference between the aD and cD , expressed as a percentage of aD . We refer to all factors reducing crop diversity from its attainable to its current level with the broad term specialization, which includes many factors not directly controlled by farmers, such as access to market, technology, and know-how (figure 1).

3. Methods

3.1. Data

We used crop distribution data from two sources: 'SPAM' (IFPRI 2019) and 'Monfreda' (Monfreda *et al* 2008). These data sets include gridded, at a 5 arc-minutes spatial resolution, crop-specific physical (SPAM) and harvested (SPAM and Monfreda) areas (the same physical area may be harvested more than once per year) that were generated by downscaling regional (national and subnational) crop statistics over the available cropland area. SPAM includes data for 42 crop categories (33 individual crops and nine crop groups), while Monfreda provides data for 175 crops. We merged both data sets prioritizing SPAM crop physical area to end with a total of 171 crops. See section S.3.1 (available online at stacks.iop.org/ERL/17/044071/mmedia) in the supplementary material for further details on these data sets, how they were merged, and an assessment of their quality.

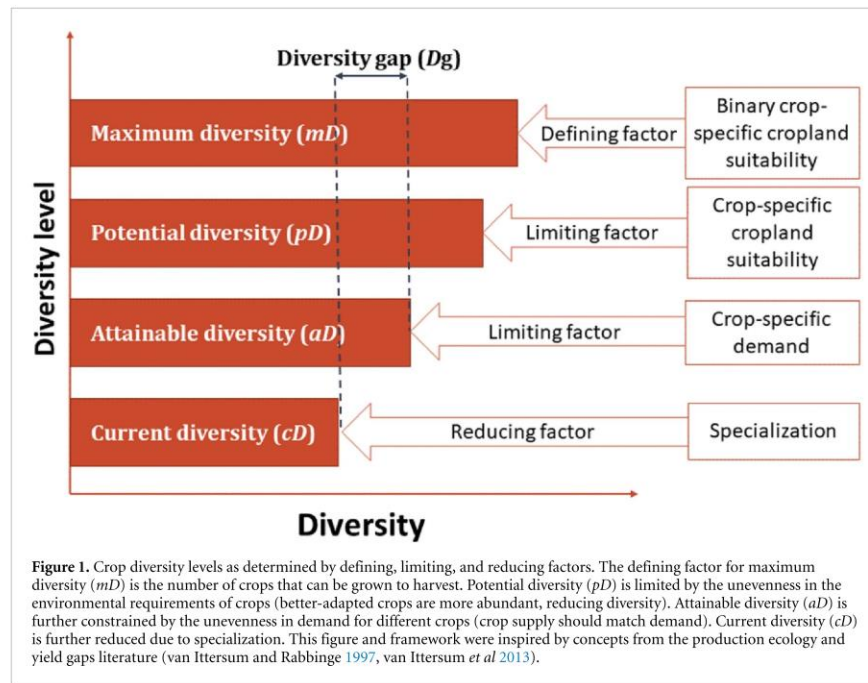
Cropland suitability predictors were derived from Soil Grids (soil pH, Hengl *et al* 2017), AQUASTAT (irrigation availability, FAO 2016), and WorldClim (climatic and bioclimatic variables, Fick and Hijmans 2017). All variables were aggregated to 5 min spatial resolution (about 9 × 9 km at the Equator) to match the crop data, and crop suitability and allocation were computed at that spatial resolution.

3.2. Crop suitability

We applied two modeling approaches to estimate crop-specific cropland suitability. We used a SDM approach to compute 'relative' suitability and a rule-based model to compute 'absolute' suitability.

SDMs are commonly used to predict relative environmental suitability by assessing the similarity between the conditions at a site of interest and the conditions at locations of known occurrence or abundance (Elith and Leathwick 2009). We refer to this approach as 'relative' suitability because of the (implicit) effect of competition on species distributions: any crop observed abundance is a function of the suitability of a site for that crop, but also for other crops. Here, we predicted the suitability of all cropland for each crop using the crop distribution data as the response variable, bioclimatic, soil pH, and irrigation variables as predictors, and three algorithms: Maxent, Random Forest regression, and Boosted Regression Trees. See section S.3.2 in the supplementary material for details on SDMs methods.

We used the ECOCROP model (Hijmans and Graham 2006, Hijmans 2021) to predict 'absolute suitability', which indicates where a species can be grown without major environmental constraints. ECOCROP is a rule-based model that estimates absolute environmental suitability for each species or sub-species from a combination of dynamic (monthly)



and static predictors, including monthly average and minimum temperature, monthly precipitation, and soil pH. For all variables, default parameters indicate the extreme minimum and maximum value beyond which the crop cannot grow (suitability is zero) and a minimum and maximum optimal value within which suitability is one. Between extreme and optimal values, suitability is determined with linear interpolation between zero and one. See section S.3.3 in the supplementary material for ECOCROP model calibration and usage details.

3.3. Crop allocation

We developed a cross-entropy-based spatial allocation algorithm to compute potential and attainable crop distributions, using each crop's relative or absolute cropland suitability as priors. It is described in detail in section S.3.4 in the supplementary material. Similar algorithms have been used to downscale regional crop area data to generate current and historical global crop distribution maps (You *et al* 2014, Jackson *et al* 2019). Potential diversity only considers adaptation and does not consider demand; thus, areas allocated to each crop are proportional to the crop-specific cropland suitability. In contrast, for attainable diversity, the total global demand for each crop is considered, and we used our allocation algorithm to distribute required areas for each crop to their most suitable cropland.

3.4. Diversity and diversity gap calculation

We quantified crop diversity (D) as the effective number of crop categories, which is the inverse of the weighted average of their proportional abundances and indicates the number of equally-abundant virtual crops with the same entropy as the actual crops (Jost 2006, Tuomisto 2010). We computed these averages as the exponent of the Shannon entropy, using nominal weights (each crop affects the mean based on their relative proportion) to avoid over or underrepresenting rare crops (equation (1)).

$${}^1D = \exp\left(-\sum_{j=1}^n (p_j \ln p_j)\right) \quad (1)$$

where p_j is the proportion of crop area occupied by crop j and n is the total number of crops.

We also computed diversity with the inverse of the Simpson index (2D), which gives more weight to the most dominant species. The differences between these two approaches are described in section S.4.2 in the supplementary material.

Because of diversity scale-dependency (Aramburu Merlos and Hijmans 2020), we transformed the current and allocated crop areas to raster with equal-area grid-cells, using the Equal Earth map projection (Šavrič *et al* 2019). We chose a 9.26×9.26 km spatial resolution (ca 86 km²) to match the largest grid cells of the original (longitude/latitude) raster data (i.e. at the Equator). We then

computed crop diversity for each 86 km² grid cell (local diversity) and at the country level (total national diversity).

Moreover, the local-diversity-average ($\overline{D\alpha}$) (Jost 2007, Tuomisto 2010) was computed for each country and diversity level with (equation (2)), in which m is the number of cells in a given country, and w_j is the weight of cell j , computed as the cropland area in cell j divided by the total cropland of that country. Note that this is the local (86 km² cell) average national diversity and different from the total national diversity, $D\gamma$, used in most global crop species diversity analyses (Renard and Tilman 2019, Aguiar *et al* 2020).

$$D\alpha = \exp \left[- \sum_{j=1}^m \left(w_j \sum_{i=1}^n (p_{ij} \ln p_{ij}) \right) \right]. \quad (2)$$

Diversity gaps (D_g) were computed as the difference between aD , averaged across the two methods used to compute aD , and cD , relative to aD and multiplied by 100 to express D_g as a percentage.

$$D_g (\%) = \frac{(aD - cD)}{aD} \times 100. \quad (3)$$

3.5. Software

All the analysis was done in R (R Core Team 2020), including data preparation, modeling, allocation algorithm, data analysis, and mapping, with the packages listed in section S.3.5 in the supplementary material. The code is available on GitHub (<https://github.com/aramburumerlos/globcropdiv>).

4. Results

4.1. Current diversity

There are large extents with high levels of current cD in East Asia (China, the Korean peninsula, and Japan), Sub Saharan Africa except for the driest regions, and the Mediterranean, especially Portugal, Italy, and western Turkey. cD is also high in other parts of Europe (such as the Netherlands and Belarus), parts of India, New Zealand's North Island, Peru and Central Chile in South America, the Caribbean islands, and the west coast of the United States (figure 2 and supplementary figure S1). In contrast, cD is very low in most other parts of the Americas: Argentina, Uruguay, and Brazil (dominated by soybean), Mexico (maize), and the central United States (maize and soybean in the east, wheat in the west); central Asia: Afghanistan and Kazakhstan (wheat); and in parts of Southeast Asia: Thailand and Cambodia (rice), and Malaysia (oil palm) (figures 2 and 3(a)). These regions have one or two major crops covering more than 50% of the cropland area (supplementary figures S2 and S3).

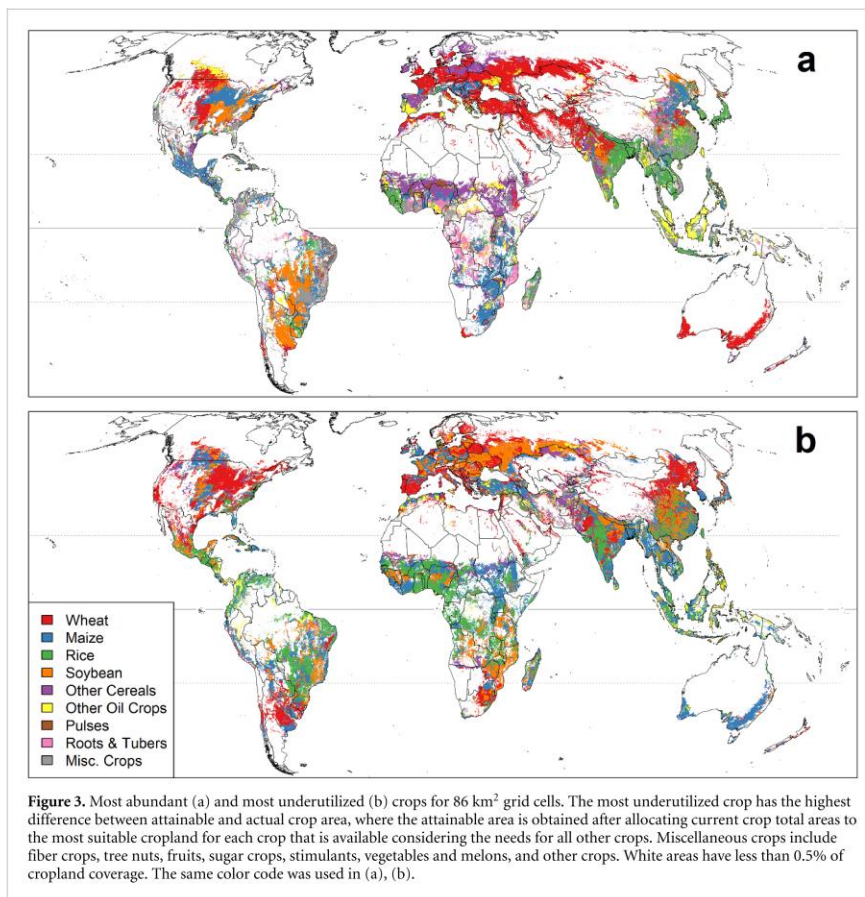
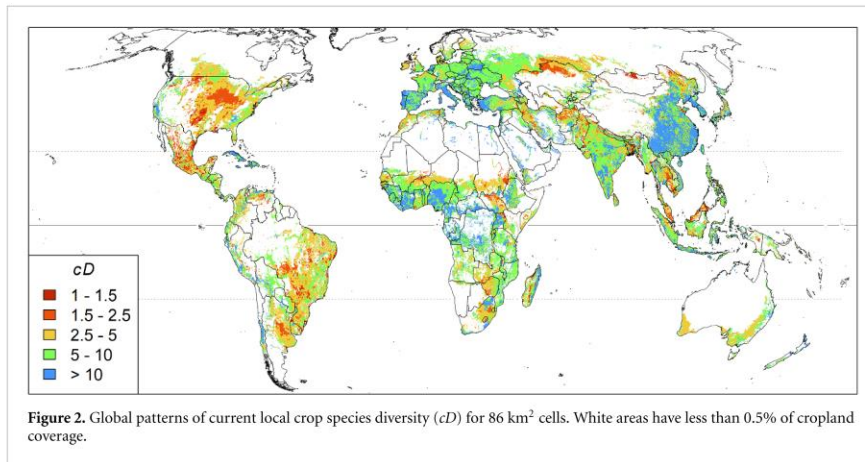
cD is highest (around 20 effective crops) around the Equator and the Tropic of Cancer (Northern tropic, 23° N), from where it linearly decreases when going northwards (figures 2 and 4), dropping to four at around 64° N. In contrast, south of the Equator, crop diversity decreases rapidly with latitude and reaches eight around the Tropic of Capricorn (23° S). It then remains stable until 40° S, and there is not much cropland further south (supplementary figure S4). The difference in cD between the southern and northern hemispheres (figure 4) is strongly associated with the lower amount of cropland in the southern hemisphere, most of which is low diversity cropland in South America. In contrast, in the northern hemisphere, there is more high diversity cropland in Europe and East Asia than low diversity cropland in North America (supplementary figures S4 and S5).

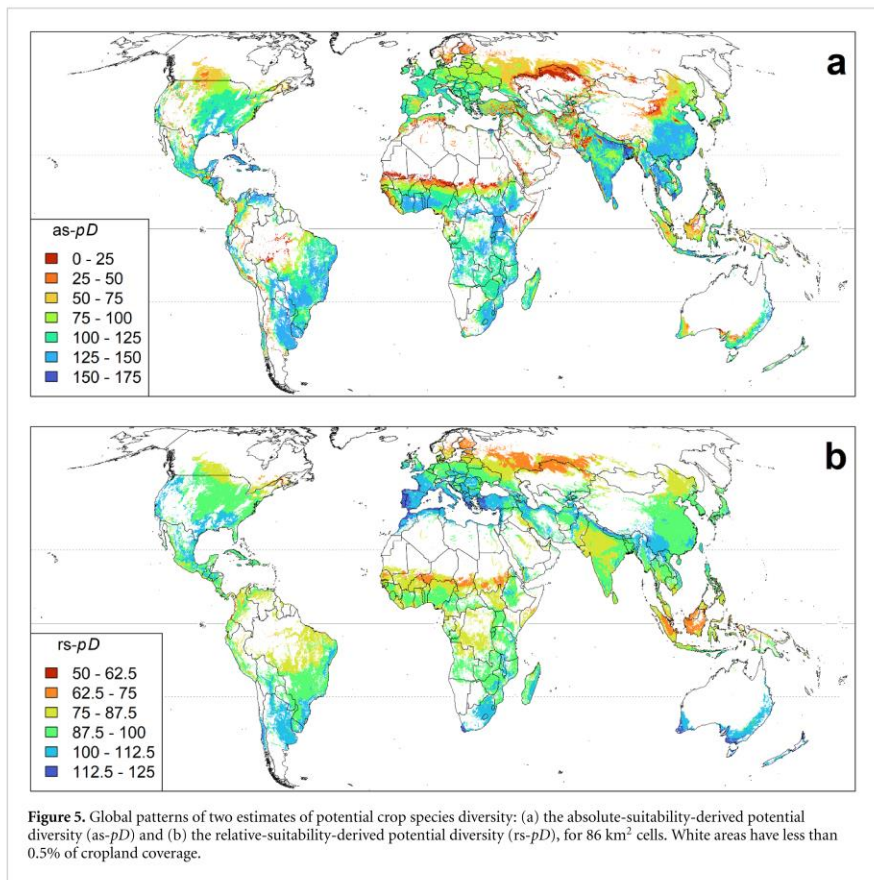
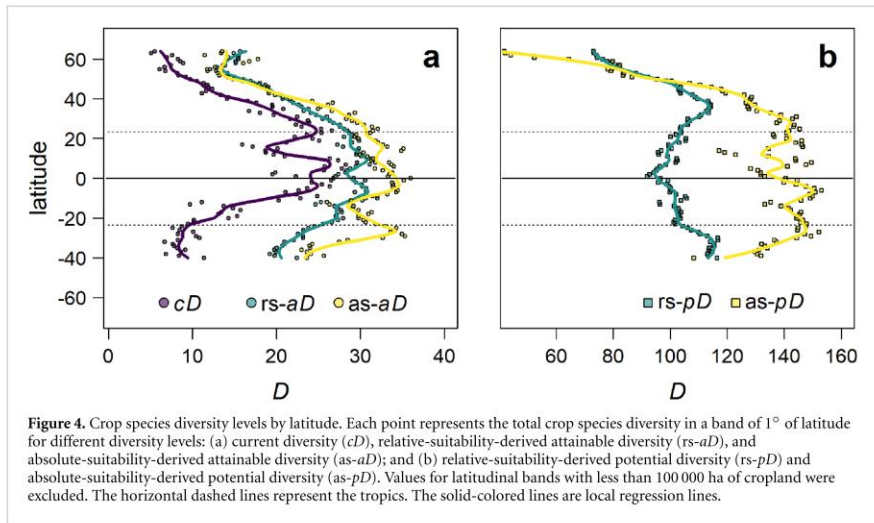
The countries with the most extreme (high or low) local diversity average ($c\overline{D\alpha}$) are small countries with little cropland area (e.g. Grenada and Western Sahara, supplementary table S1), perhaps because crop diversity sample variance is higher at small sampling units (Aramburu Merlos and Hijmans 2020). When only considering countries with at least 0.1 Mha of cropland, Israel stands out for its high $c\overline{D\alpha}$ of 19.5. Lebanon, Italy, Taiwan, Portugal, Cuba, and Republic of Congo, also have high $c\overline{D\alpha}$ values (12–14.5). About half of these countries (88 out of 151) has a $c\overline{D\alpha}$ between 4 and 8, while only 6 have a $c\overline{D\alpha}$ lower than 3, including two countries with much cropland (>10 Mha), Kazakhstan and the USA. These values are considerably lower than the current total country-level diversity ($cD\gamma$). For instance, less than 5% of these countries have a $c\overline{D\alpha}$ greater than 12, but 40% have a $cD\gamma$ greater than 12 effective crops (supplementary table S1).

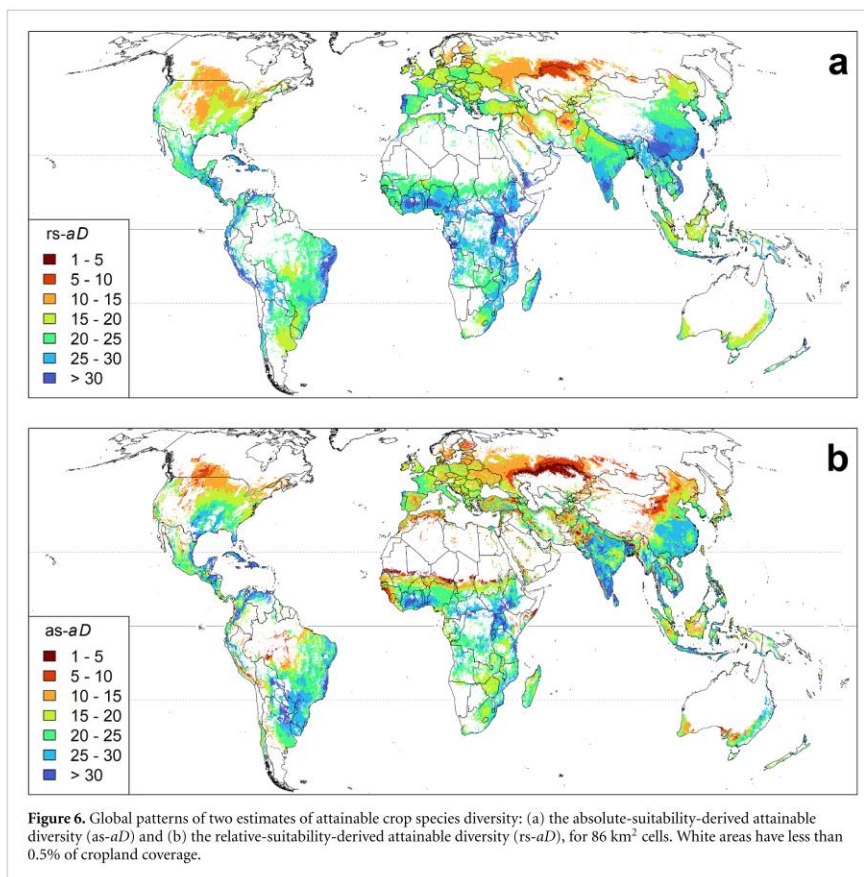
4.2. Potential and attainable diversity

The values for pD strongly depend on the suitability estimation method used (figures 4, 5 and supplementary figure S6). In contrast, the aD values derived from the two suitability methods are remarkably similar and considerably lower than pD (figures 4, 6 and supplementary figures S8 and S9). The differences in pD and aD due to the suitability estimation methods are described and discussed in supplementary section S.4.1.

Irrespective of the method used, aD is higher in the tropics than temperate regions, and outside the tropics, higher in coastal than continental regions. aD is highest in Sub Saharan Africa, southern India, some regions of Southeast Asia, eastern Brazil, northern South America, and the Caribbean. In subtropical and temperate areas, aD is high in East Asia, New Zealand's North Island, Chile, the US southeast and west coast, and parts of the Mediterranean region (e.g. Portugal and Italy). aD is very low in Kazakhstan, Mongolia, Russia, the Baltic States, Scandinavia, Canada, and the northern US (figure 6







and supplementary table S1). The annual average temperature strongly affects *aD*: it increases linearly from -10°C until it reaches a plateau at about 20°C to 25°C and slightly decreases at higher temperatures (supplementary figure S10).

4.3. Global diversity gaps

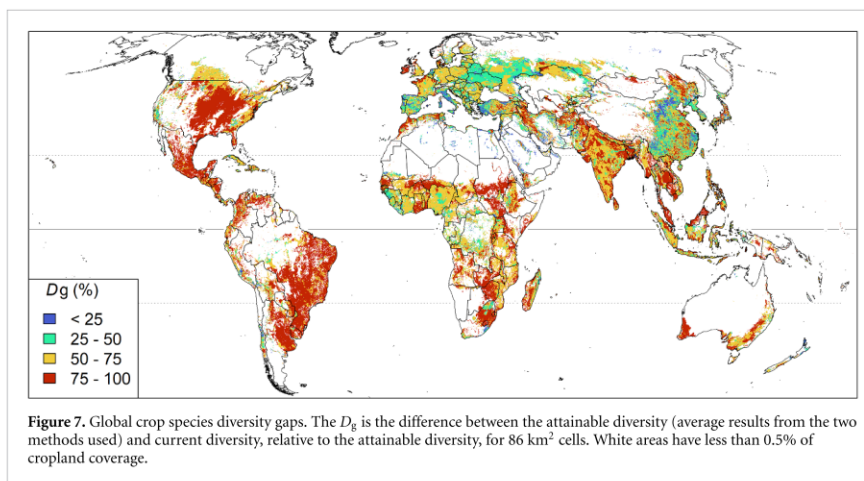
Nearly 84% of the world's cropland has a D_g that is $>50\%$; thus, it has less than half of the crop diversity that it would have if crops were planted to maximize diversity while considering their suitability and current food demand (figure 7). The D_g is especially high in the Americas (82% on average) except for the Andean region, the Caribbean Islands, the US west coast, and Canada. Africa (72%), Asia (71%), and Oceania (76%) also have large D_g values but with much spatial variability. The D_g is relatively small in Europe (56%), especially in the Mediterranean, Eastern Europe, and the Netherlands.

Cropland with a low *cD* tends to have a high D_g (supplementary figure S12). For instance, about 40% of the world's cropland has a *cD* lower than 5. Of this

low *cD* cropland, 80% have a $D_g > 75\%$, while less than one percent have a $D_g < 50\%$. In contrast, virtually all the 10% most diverse cropland (*cD* > 12) has a $D_g < 60\%$, and 80% of it has a $D_g < 50\%$.

At the national level, Israel stands out for its low local-average D_g of 14%. Lebanon (30%) and only ten other countries with more than 0.1 Mha of cropland have an average D_g below 50%, while about half have an average D_g higher than 70% (supplementary table S1). However, at the country level, diversity gaps are significantly smaller when considering total diversity (D_T) instead of local diversity averages (D_α) (paired *t*-test, $P < 0.01$), illustrating the scale-dependency of diversity.

One strategy to reduce diversity gaps can be to increase the area of the 'most under-utilized' crops, that is, crops showing the highest differences between their attainable and actual crop proportion (figure 3(b) and supplementary figure S13). These crops are primarily major crops because the attainable area (proportion) in a grid cell tends to be greater for these crops than crops with little demand. For



instance, the most abundant crop worldwide, wheat, is also one of the most under-utilized, particularly in the US Corn Belt, northeast China, and parts of Europe and Argentina.

5. Discussion

5.1. Specialization and diversification

We assessed global crop diversity gaps considering both ecological and demand constraints to attainable levels of crop diversity. Even when considering the world's heavy reliance on a few major crops for food supply (Cassman and Grassini 2020, Renard and Tilman 2021), our results show vast opportunities for crop diversification: crop species diversity could be doubled on five-sixths of the world's croplands if we only consider environmental constraints and total demand for crops.

There are various reasons why local specialization currently reduces crop diversity this much. While there can be economic benefits to some level of diversification at the farm level, such as risk reduction (Gaudin *et al* 2015), pest and weed pressure mitigation (Davis *et al* 2012), and soil fertility improvement (Tiemann *et al* 2015), these benefits are context-specific and may not be large enough to justify the increase in costs and complexity of managing additional crops (Roesch-McNally *et al* 2018). For example, the benefits of diversification may strongly depend on which crops are added to a cropping system, and further research could investigate opportunities for 'functional diversification'. If increasing farm-level crop diversity is too challenging, it may be possible to increase regional diversity by having different farms specializing in different crops. The effect of this diversification strategy would depend on how farm sizes and configuration shape the landscape (Sirami *et al* 2019), and while this might in some

cases reduce transportation costs by decreasing the distance between production and consumption, there could also be a reduced benefit of economies of scale (for example, producing tomatoes near tomato processing plants) and other losses of efficiency associated with regional specialization. At the national level, the opportunity for diversification may be reduced due to policies to assure that a large part of the staple food is produced internally, as imports may be considered less reliable unless there is sufficient land available for new crops (Arsenault *et al* 2015).

When considering opportunities for increasing crop diversity, an important question is which crops should be grown more. For example, while some regions could increase the area with specialty crops, such increases might reduce crop diversity elsewhere if there is no increased demand for those crops. In contrast, given current crop-specific supplies and demands, the most effective strategy to increase crop diversity in a large area might be to reduce the proportion of the most dominant crops and plant more of the most under-utilized crop, which is often a suitable major crop not widely planted in that area. Furthermore, a drastic change in global demand, perhaps through changing diets, could affect attainable and actual diversity, but it is hard to imagine a diet not dominated by starch-producing crops such as wheat, maize, rice, and cassava.

While we focused on crop species diversity, other diversification strategies, such as rotations with cover crops, grassland-cropland integration, and agroforestry, should also be considered when seeking better ecosystem services provision through diversification, particularly in regions where the attainable crop diversity is low (Garrity *et al* 2010, Lemaire *et al* 2015). The best choice will depend on the magnitude of the constraints to diversity and the targeted services to be improved.

5.2. Constraints on crop diversity

Most studies on crop diversity do not consider the environmental constraints that might limit farmers' opportunities for diversification (Kremen and Miles 2012, Renard and Tilman 2019), and very little attention has been given to drivers of crop species diversity (Roesch-McNally *et al* 2018, Goslee 2020). Our analysis of environmental effects on attainable diversity can shed light on some important questions related to crop diversity (Wood 1998), especially the extent to which crop diversity can be increased (Cassman and Grassini 2020). Crop species diversity tends to be greater in tropical than in temperate areas and in coastal than in continental regions, and there is a clear limit to increasing crop diversity in cold environments. Therefore, it is not sensible to expect or call for similar levels of diversity across very different regions, and it cannot be assumed that all countries have the same diversity potential (Jones *et al* 2021), just as is the case with crop yield potential.

Furthermore, there is high spatial variability in current crop diversity that environmental models of attainable diversity cannot explain. This high spatial heterogeneity in diversity and diversity gaps could be related to factors affecting farmers' cropping decisions, such as spatial variation in market access, prices, risk, and policies. Understanding how these factors lead to specialization or limit diversification using spatially explicit models is needed to determine to which extent closing the diversity gap is economically feasible and identify policies that strongly affect diversity, particularly for regions with the highest diversity gaps (Socolar *et al* 2021). Moreover, while increasing diversity may be beneficial in some cases, closing diversity gaps might not always be necessary, such as in regions with high diversity and extremely high potential. Nevertheless, the diversity gap concept is helpful as it allows us to better contrast and compare crop diversity in different regions and investigate what shapes these patterns.

5.3. Diversity gaps

Diversity gaps are smaller in Europe and other areas dominated by relatively small family farms that tend to have higher crop diversity (Ricciardi *et al* 2021). This farm size-crop diversity inverse relationship might be associated with a higher proportion of minor crops in smaller farms (e.g. pulses, roots, tubers, and fruits) (Ricciardi *et al* 2018). Minor crops tend to be planted in more diverse cropping systems and are less likely to take most of the cropland of a region (Aramburu Merlos and Hijmans 2020). This association between minor crops and crop diversity might also explain the small diversity gaps in regions specializing in horticultural crops, such as the US west coast and the Netherlands. In Europe, relatively low D_g may be further supported by agricultural policies that promote diverse landscapes (Stoate *et al* 2009). Gaps are also relatively small in countries that rely less

on international markets (Cuba, North Korea) and in places that face high transportation costs (Caribbean islands, desert oases), where most of the production is for local consumption. In contrast, diversity gaps are very high in the sparsely populated plains with a relatively recent agricultural expansion in the Americas (Graesser *et al* 2018). Farms in these regions have larger fields and focus on major crops for export in low diversity cropping systems (Aramburu Merlos and Hijmans 2020).

5.4. Assessing potential and attainable diversity

Diversity gaps can only be calculated after defining appropriate theoretical levels of diversity. Although our approach could be refined, it seems clear that attainable diversity (aD) is a much more robust and meaningful diversity benchmark than potential diversity (pD). aD not only accounts for total demand, making it insensitive to the omission of rare crops, but also it is less sensitive to changes in the suitability estimation method. pD estimates depend on how crop-specific suitability indices relate to each other between crops, whereas aD estimates only depend on the relative score of the cropland within each crop. However, there might be cases in which it is interesting to assess the potential diversity of a region. In such a case, the suitability estimation method should be carefully selected. Any suitability estimation method that depends on observed data is constrained by the current diversity level of the area of study and data availability for minor crops. Some examples include those methods that rely on crop distribution data (i.e. SDMs) and those that use observed diversity data to fit quantile regressions (Goslee 2020). Quantile regression methods are notably inadequate for potential diversity estimations because farmers generally do not aim at reaching the highest levels of diversity possible. Crop models are more suited for estimating potential diversity because current diversity levels do not affect them.

5.5. Local versus country-level diversity

Crop diversity in space depends on the area of the unit at which diversity estimations are made (Aramburu Merlos and Hijmans 2020). Much analysis of crop diversity and effects relies on national statistics (Khoury *et al* 2014, Mahaut *et al* 2021), in which the country-total diversity (D_γ) is computed. However, most interest in diversification is related to expected effects at farm or landscape levels (Sirami *et al* 2019). Here we provide estimations of diversity and diversity gaps at a 9.26×9.26 km resolution (8575 ha), which allows us to compute local-average diversity ($D\alpha$) for each country, which is consistently lower than D_γ and results in larger gaps. $D\alpha$ estimates are more appropriate for studying crop diversity's effects on agroecosystem services and processes, such

as pollination (Aizen *et al* 2019), associated biodiversity (Sirami *et al* 2019), and biological pests control (Tschardt *et al* 2005). In addition, spatial crop diversity at this resolution is highly correlated with crop rotation diversity because different fields are in different stages of their crop rotation (Aramburu Merlos and Hijmans 2020). While there can be benefits of diversity at the national level (Renard and Tilman 2019), the national to local-average diversity ratio (i.e. $D\beta$), an indicator of regional heterogeneity, should also be considered when assessing diversity effects on the stability of food production (Mahaut *et al* 2021).

6. Conclusions

In this paper, we have contributed to a better understanding of spatial patterns of global crop diversity and opportunities for diversification. By defining theoretical levels of crop diversity, we created a way to compute diversity gaps, the difference between attainable diversity and actual diversity. The (relative) diversity gap is more informative than just the actual diversity because it accounts for environmental variation and limits set by demand. We have shown that even within the limits of the very skewed current levels of production for different crops, crop diversity could increase enormously. However, given the economic benefits of specialization, it remains an important question what the value of diversification could be in different regions and cropping systems, and, where more diversity is desirable, what incentives could be provided to achieve this.


Data availability statement

The data that support the findings of this study are openly available at the following URL/DOI: <https://github.com/aramburumerlos/globcropdiv>.

Conflict of interest

The authors declare no competing interest.

ORCID iDs

Fernando Aramburu Merlos 

<https://orcid.org/0000-0003-0957-7482>

Robert J Hijmans  <https://orcid.org/0000-0001-5872-2872>

References

- Aguar S, Teixeira M, Garibaldi L A and Jobbágy E G 2020 Global changes in crop diversity: trade rather than production enriches supply *Glob. Food Secur.* **26** 100385
- Aizen M A *et al* 2019 Global agricultural productivity is threatened by increasing pollinator dependence without a parallel increase in crop diversification *Glob. Change Biol.* **25** 3516–27

- Aramburu Merlos F and Hijmans R J 2020 The scale dependency of spatial crop species diversity and its relation to temporal diversity *Proc. Natl Acad. Sci. USA* **117** 26176–82
- Arsenault J E, Hijmans R J and Brown K H 2015 Improving nutrition security through agriculture: an analytical framework based on national food balance sheets to estimate nutritional adequacy of food supplies *Food Secur.* **7** 693–707
- Cassman K G and Grassini P 2020 A global perspective on sustainable intensification research *Nat. Sustain.* **3** 262–8
- Davis A S, Hill J D, Chase C A, Johanns A M and Liebman M 2012 Increasing cropping system diversity balances productivity, profitability and environmental health *PLoS One* **7** e47149
- Elith J and Leathwick J R 2009 Species distribution models: ecological explanation and prediction across space and time *Annu. Rev. Ecol. Evol. Syst.* **40** 677–97
- FAO 2016 AQUASTAT website (Food and Agriculture Organization of the United Nations (FAO)) (available at: www.fao.org/nr/water/aquastat/irrigationmap/index10.stm)
- Fick S E and Hijmans R J 2017 WorldClim 2: new 1-km spatial resolution climate surfaces for global land areas *Int. J. Climatol.* **37** 4302–15
- Garrity D P, Akinnifesi F K, Ajayi O C, Weldesemayat S G, Mowo J G, Kalinganire A, Larwanou M and Bayala J 2010 Evergreen agriculture: a robust approach to sustainable food security in Africa *Food Secur.* **2** 197–214
- Gaudin A C, Tolhurst T N, Ker A P, Janovicek K, Tortora C, Martin R C and Deen W 2015 Increasing crop diversity mitigates weather variations and improves yield stability *PLoS One* **10** e0113261
- Goslee S C 2020 Drivers of agricultural diversity in the contiguous United States *Front. Sustain. Food Syst.* **4** 75
- Graesser J, Ramankutty N and Coomes O T 2018 Increasing expansion of large-scale crop production onto deforested land in sub-Andean South America *Environ. Res. Lett.* **13** 084021
- Hengl T *et al* 2017 SoilGrids 250m: global gridded soil information based on machine learning *PLoS One* **12** e0169748
- Hijmans R J and Graham C H 2006 The ability of climate envelope models to predict the effect of climate change on species distributions *Glob. Change Biol.* **12** 2272–81
- Hijmans R 2021 Recocrop: implementation of the ecocrop model for estimating adaptation of plants to environments (available at: <https://github.com/cropmodels/Recocrop/>)
- IFPRI 2019 Global spatially-disaggregated crop production statistics data for 2010 Version 2.0 (available at: <https://dataverse.harvard.edu/dataset.xhtml?persistentId=doi:10.7910/DVN/PRFF8V>)
- Jackson N D, Konar M, Debaere P and Estes L 2019 Probabilistic global maps of crop-specific areas from 1961 to 2014 *Environ. Res. Lett.* **14** 094023
- Jones S K, Estrada-Carmona N, Juventia S D, Dulloo M E, Laporte M-A, Villani C and Remans R 2021 Agrobiodiversity index scores show agrobiodiversity is underutilized in national food systems *Nat. Food* **2** 712–23
- Jost L 2006 Entropy and diversity *Oikos* **113** 363e375
- Jost L 2007 Partitioning diversity into independent alpha and beta components *Ecology* **88** 2427–39
- Khouri C K, Bjorkman A D, Dempewolf H, Ramirez-Villegas J, Guarino L, Jarvis A, Rieseberg L H and Struik P C 2014 Increasing homogeneity in global food supplies and the implications for food security *Proc. Natl Acad. Sci. USA* **111** 4001–6
- Kremen C and Miles A 2012 Ecosystem services in biologically diversified versus conventional farming systems: benefits, externalities, and trade-offs *Ecol. Soc.* **17** 40
- Lemaire G, Gastal F, Franzluebbers A and Chabbi A 2015 Grassland-cropping rotations: an avenue for agricultural diversification to reconcile high production with environmental quality *Environ. Manage.* **56** 1065–77
- Mahaut L, Violle C and Renard D 2021 Complementary mechanisms stabilize national food production *Sci. Rep.* **11** 4922

- Monfreda C, Ramankutty N and Foley J A 2008 Farming the planet: 2. Geographic distribution of crop areas, yields, physiological types, and net primary production in the year 2000 *Glob. Biogeochem. Cycles* **22** GB1022
- R Core Team 2020 R: A language and environment for statistical computing (R Foundation for Statistical Computing)
- Renard D and Tilman D 2019 National food production stabilized by crop diversity *Nature* **571** 257
- Renard D and Tilman D 2021 Cultivate biodiversity to harvest food security and sustainability *Curr. Biol.* **31** R1154–8
- Ricciardi V, Mehrabi Z, Wittman H, James D and Ramankutty N 2021 Higher yields and more biodiversity on smaller farms *Nat. Sustain.* **4** 651–7
- Ricciardi V, Ramankutty N, Mehrabi Z, Jarvis L and Chookolingo B 2018 How much of the world's food do smallholders produce? *Glob. Food Secur.* **17** 64–72
- Roesch-McNally G E, Ar buckle J G and Tyndall J C 2018 Barriers to implementing climate resilient agricultural strategies: the case of crop diversification in the US corn belt *Glob. Environ. Change* **48** 206–15
- Šavrič B, Patterson T and Jenny B 2019 The equal Earth map projection *Int. J. Geogr. Inf. Sci.* **33** 454–65
- Sirami C, Gross N, Baillod A B, Bertrand C, Carrié R, Hass A, Henckel L, Miguet P, Vuillot C and Alignier A 2019 Increasing crop heterogeneity enhances multitrophic diversity across agricultural regions *Proc. Natl Acad. Sci. USA* **116** 16442–7
- Socolar Y, Goldstein B R, de Valpine P and Bowles T M 2021 Biophysical and policy factors predict simplified crop rotations in the US Midwest *Environ. Res. Lett.* **16** 054045
- Stoate C, Báldi A, Beja P, Boatman N D, Herzog I, van Doorn A, de Snoo G R, Rakosy L and Ramwell C 2009 Ecological impacts of early 21st century agricultural change in Europe—a review *J. Environ. Manage.* **91** 22–46
- Tiemann L K, Grandy A S, Atkinson E E, Marin-Spiotta E and McDaniel M D 2015 Crop rotational diversity enhances belowground communities and functions in an agroecosystem *Ecol. Lett.* **18** 761–71
- Tilman D and Clark M 2014 Global diets link environmental sustainability and human health *Nature* **515** 518–22
- Tscharntke T, Klein A M, Kruess A, Steffan-Dewenter I and Thies C 2005 Landscape perspectives on agricultural intensification and biodiversity—ecosystem service management *Ecol. Lett.* **8** 857–74
- Tuomisto H 2010 A diversity of beta diversities: straightening up a concept gone awry. Part 1. Defining beta diversity as a function of alpha and gamma diversity *Ecography* **33** 2–22
- van Ittersum M K, Cassman K G, Grassini P, Wolf J, Tittonell P and Hochman Z 2013 Yield gap analysis with local to global relevance—a review *Field Crops Res.* **143** 4–17
- van Ittersum M K and Rabbinge R 1997 Concepts in production ecology for analysis and quantification of agricultural input-output combinations *Field Crops Res.* **52** 197–208
- Wood D 1998 Ecological principles in agricultural policy: but which principles? *Food Policy* **23** 371–81
- You L, Wood S, Wood-Sichra U and Wu W 2014 Generating global crop distribution maps: from census to grid *Agric. Syst.* **127** 53–60

SUPPLEMENTARY MATERIAL

Potential, attainable, and current levels of global crop diversity

Fernando Aramburu Merlos*^{a,b} and Robert J. Hijmans^a

^a Department of Environmental Science and Policy, University of California Davis, Davis, California, United States of America.

^b Instituto Nacional de Tecnología Agropecuaria (INTA), Unidad Integrada Balcarce, Ruta 226, km 73.5, CC 276, CP 7620, Balcarce, Buenos Aires, Argentina.

Table of Contents

S.1. Supplementary Figures	2
S.1.1. Figures S1 to S5 (current crop distributions and diversity)	2
S.1.2. Figures S6 and S7(potential crop diversity)	6
S.1.3. Figures S8 to S10 (attainable crop diversity)	8
S.1.4. Figure S11 to S13 (diversity gaps)	10
S.1.5. Figure S14 (data quality index)	12
S.2. Supplementary Tables	13
S.3. Supplementary Methods	24
S.3.1. Current crop distribution data	24
3 S.3.2. Development of spatial distribution models for relative crop suitability estimation	25
S.3.2.1. Response variable.	25
S.3.2.2. Predictors	26
S.3.2.3. Model selection, tuning, and averaging	26
S.3.3. ECOCROP model calibration and running	27
S.3.4. Crop allocation algorithm and crop potential and attainable distribution	28
S.3.4.1. Algorithm description	28
S.3.4.2. Crop distribution assumptions and considerations	30
S.3.5. R packages used in the analysis	31
S.4. Supplementary Results	32
S.4.1. Differences in potential and attainable diversity between suitability estimation methods	32
S.4.2. Crop diversity as the inverse of the Simpson index (2D)	33
S.5. Supplementary references	34

S.1. Supplementary Figures

S.1.1. Figures S1 to S5 (current crop distributions and diversity)

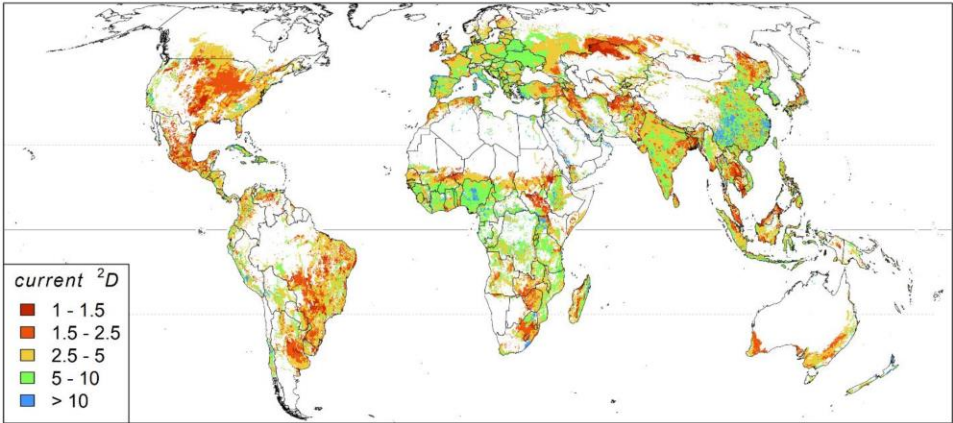


Figure S1. Global patterns of current local crop species diversity (*current*²*D*) computed as the inverse of the Simpson index for 86 km² cells. White areas have less than 0.5% of cropland coverage.

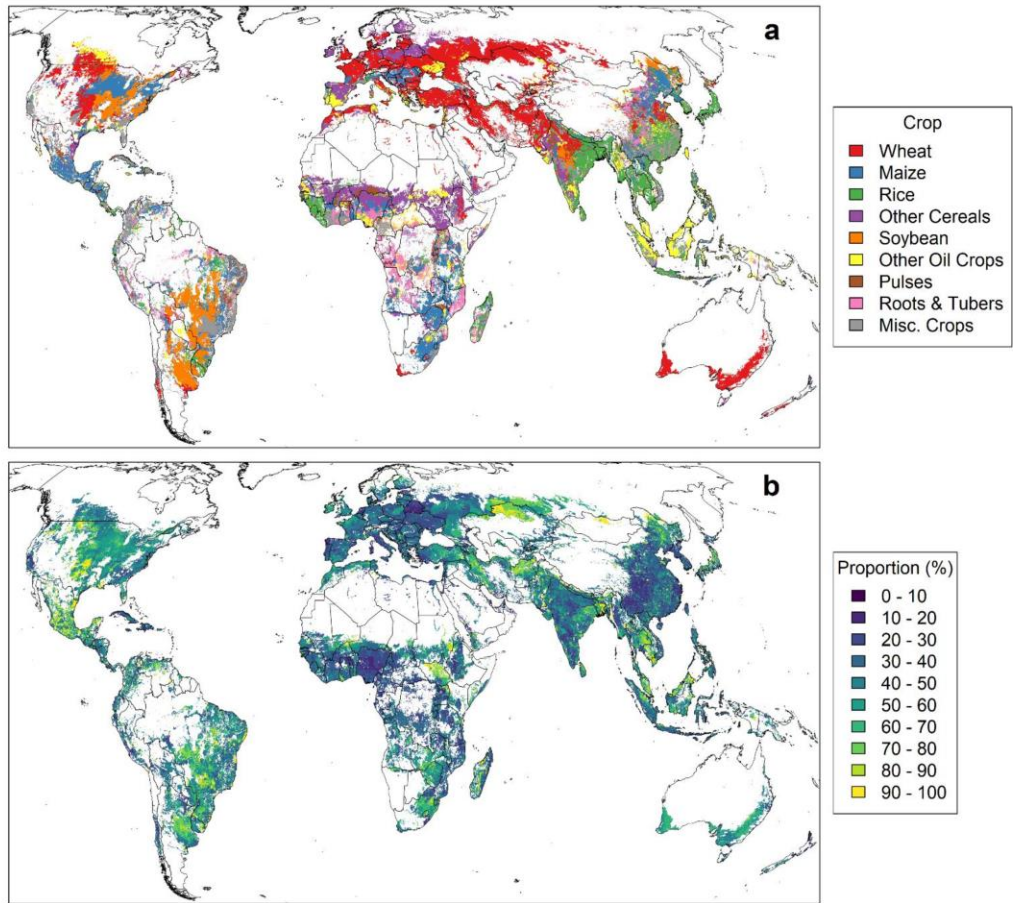


Figure S2. Most abundant crop (a) and the cropland proportion covered by the most abundant crop (b) for 86 km² cells. Miscellaneous crops include fiber crops, tree nuts, fruits, sugar crops, stimulants, vegetables and melons, and other crops. White areas have less than 0.5% of cropland coverage.

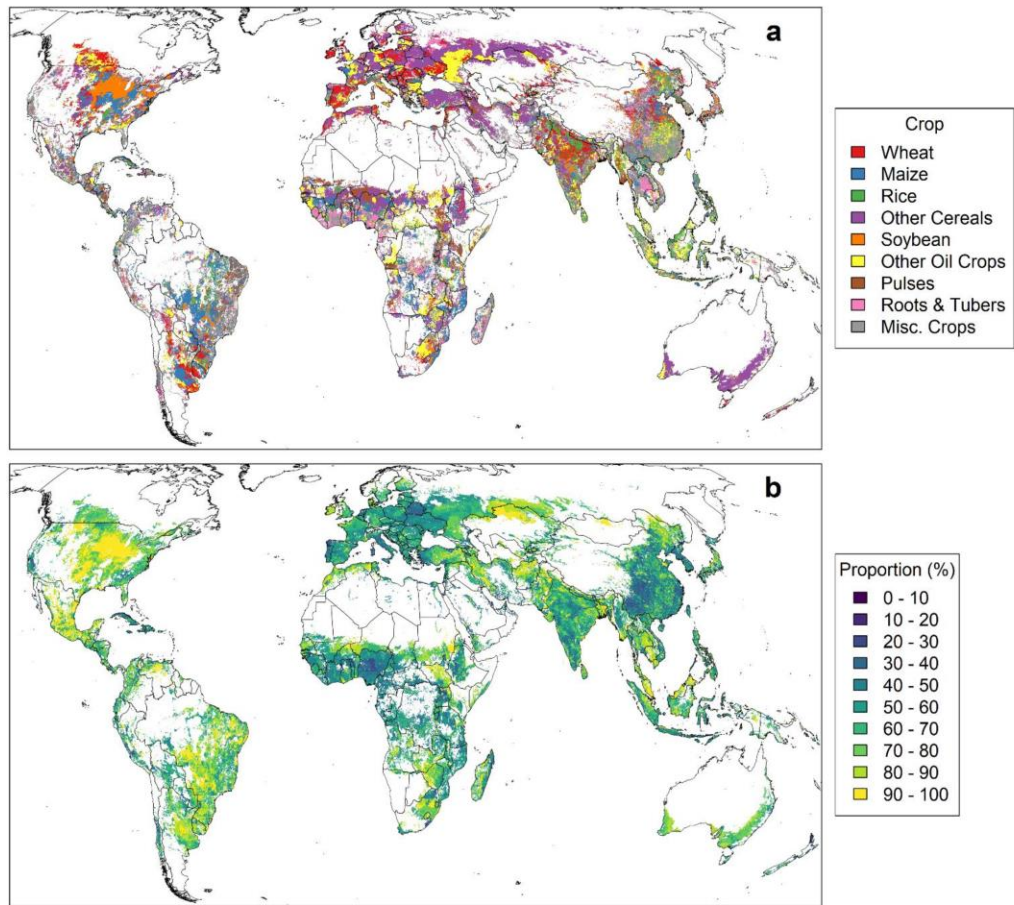


Figure S3. Second most abundant crop (a) and the cropland proportion covered by the two most abundant crops (b) for 86 km² cells. Miscellaneous crops include fiber crops, tree nuts, fruits, sugar crops, stimulants, vegetables and melons, and other crops. White areas have less than 0.5% of cropland coverage.

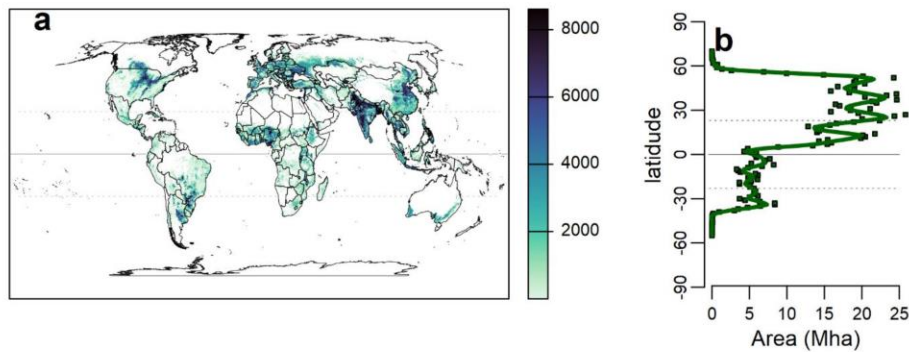


Figure S4. **(a)** Global distribution of current cropland area (ha) (9.26×9.26 km resolution). **(b)** Cropland area (Mha) as a function of latitude; each point represents the total cropland area (Mha) in a band of 1° of latitude, and the solid dark green line is a local regression line.

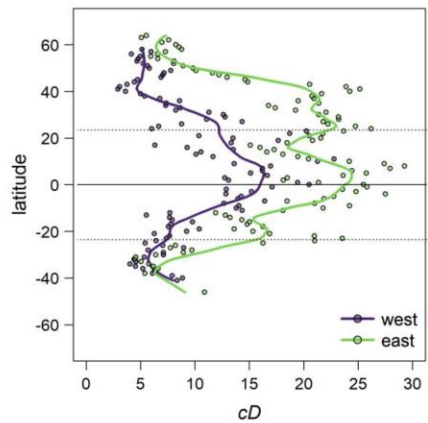


Figure S5. Crop species diversity by latitude for two regions: west from meridian -30° (the Americas and part of Polynesia) and east from meridian -30° (Africa, Eurasia, rest of Oceania). Each point represents the total current crop species diversity in a band of 1° of longitude for each region. Values for latitudinal bands with less than 50,000 ha of cropland were excluded. The horizontal dashed lines represent the Tropics. The solid-colored lines are local regression lines for the two regions (purple: west, light green: east).

S.1.2. Figures S6 and S7(potential crop diversity)

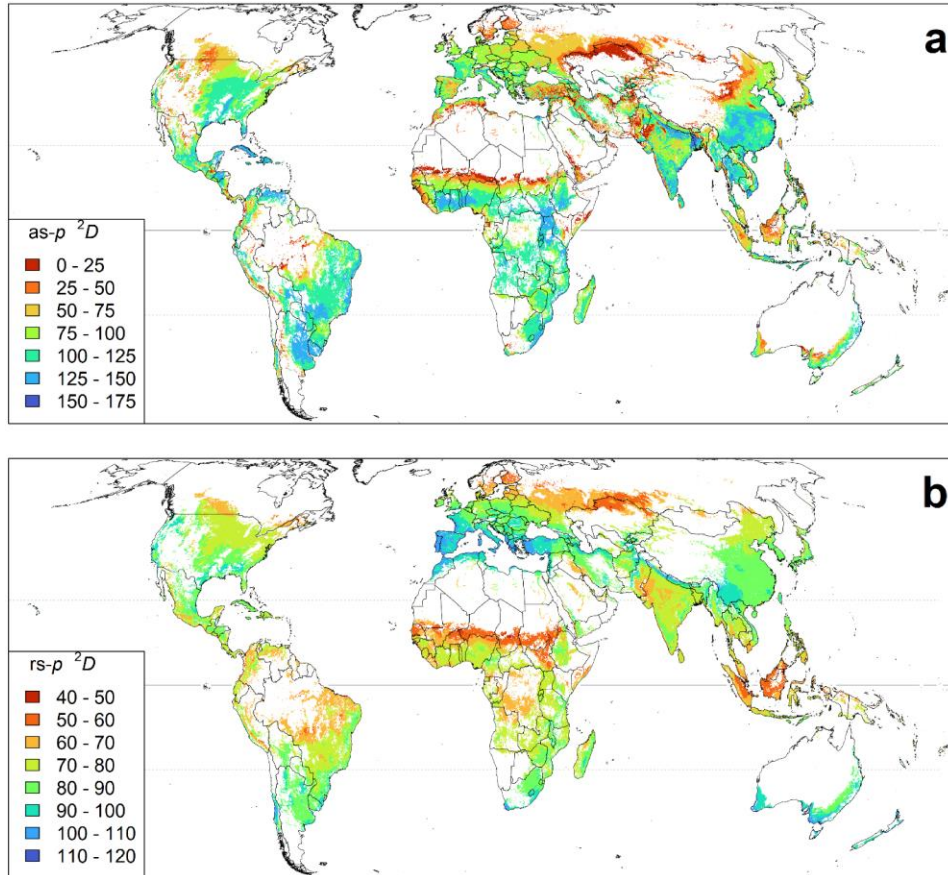


Figure S6. Global patterns of potential crop species diversity computed as the inverse of the Simpson index for two potential diversity estimation methods: (a) the absolute-suitability-derived potential diversity ($as-p^2D$) and (b) the relative-suitability-derived potential diversity ($rs-p^2D$), for 86 km^2 cells. White areas have less than 0.5% of cropland coverage.

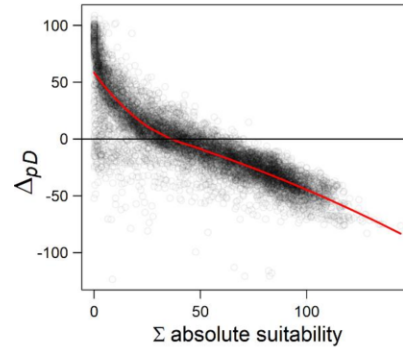


Figure S7. Differences in potential diversity estimates between methods (ΔpD) as a function of cell total absolute suitability. ΔpD is equal to pD derived from relative suitability indices minus pD derived from absolute suitability indices. Each point represents a 9.26×9.26 km grid cell. A random sample of 10,000 cells (12% of all raster cells) was used for this plot. The red line is a local regression line.

S.1.3. Figures S8 to S10 (attainable crop diversity)

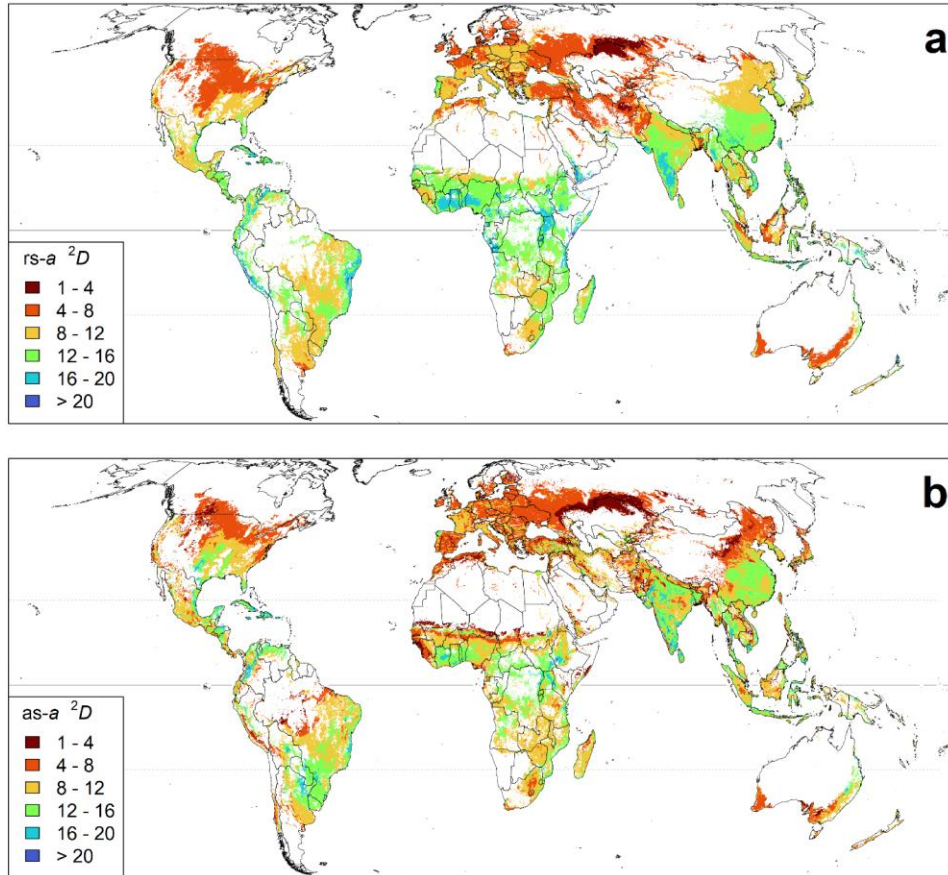


Figure S8. Global patterns of attainable crop species diversity computed as the inverse of the Simpson index for two attainable diversity estimation methods: (a) the absolute-suitability-derived attainable diversity (*as-pD*) and (b) the relative-suitability-derived attainable diversity (*rs-pD*), for 86 km² cells. White areas have less than 0.5% of cropland coverage.

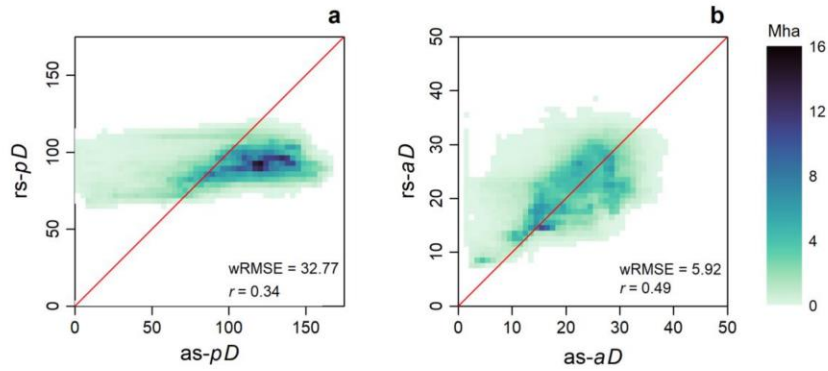


Figure S9. Relation between crop species diversity values as derived from two types of suitability indices (relative and absolute) for two diversity levels (attainable and potential). (a) Absolute-suitability-derived potential diversity ($as-pD$) versus relative-suitability-derived potential diversity ($rs-pD$). (b) Absolute-suitability-derived attainable diversity ($as-aD$) versus relative-suitability-derived attainable diversity ($rs-aD$). The color gradient indicates the cropland area (Mha) under each D estimation combination. The red line represents the identity function. The area-weighted root mean squared error (wRMSE) and Pearson's correlation coefficient are shown for each comparison.

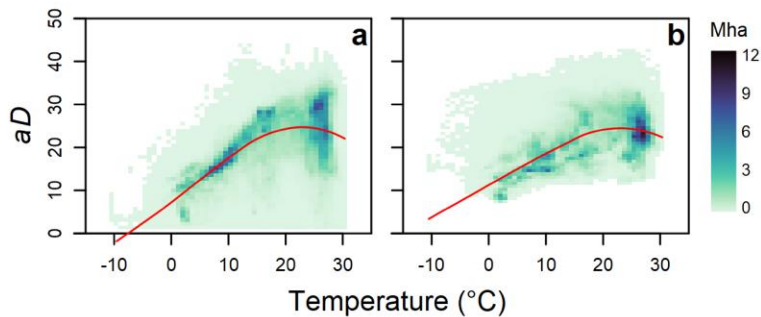


Figure S10. Attainable crop species diversity (aD) as a function of the annual average temperature ($^{\circ}C$) for two estimates of aD (a) the absolute-suitability-derived attainable diversity and (b) the relative-suitability-derived attainable diversity. aD was computed at all 5-arc minute cells (about 9×9 km at the Equator) with at least 0.5% of cropland. The color gradient indicates each Dg- cD combination's cropland area (Mha). The red lines are local regression lines.

S.1.4. Figure S11 to S13 (diversity gaps)

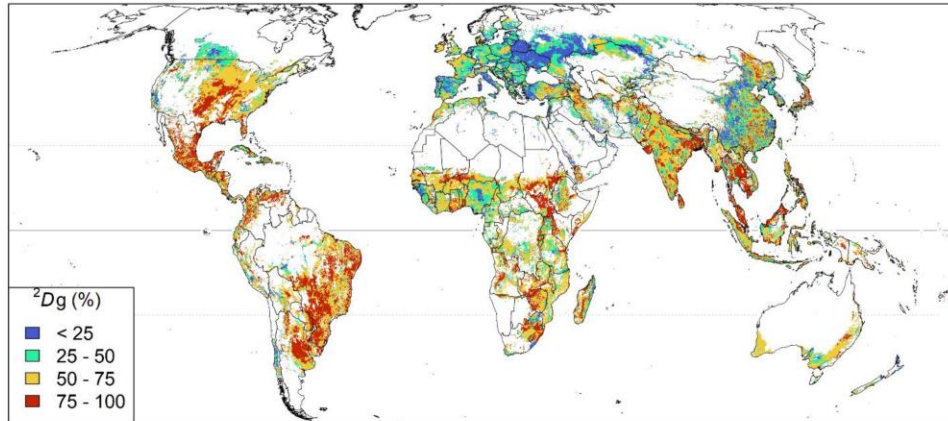


Figure S11. Global crop species diversity gaps when diversity is computed as the inverse of the Simpson index. The diversity gap (Dg) is the difference between the attainable diversity (average results from the two methods used) and current diversity, relative to the attainable diversity, for 86 km² cells. White areas have less than 0.5% of cropland coverage.

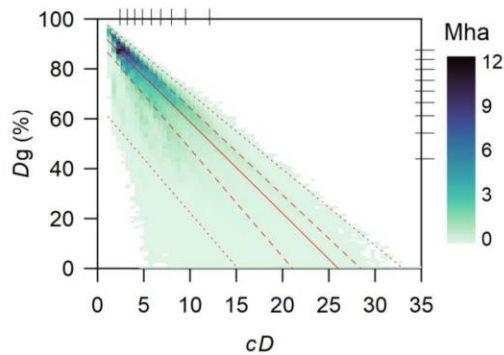


Figure S12. Crop species diversity gaps (Dg , %) as a function of current crop species diversity (cD) for 5-arc minute cells (about 9×9 km at the Equator). The color gradient indicates each Dg - cD combination's cropland area (Mha). The red lines are quantile regression lines (dotted: 0.01 and 0.99 quantiles, dashed: first and third quartiles, solid: median). The marginal lines on the top and right axes show the cD and Dg area-based quantile distribution in one-tenth increments (i.e., 0.1, 0.2, 0.3... 0.9).

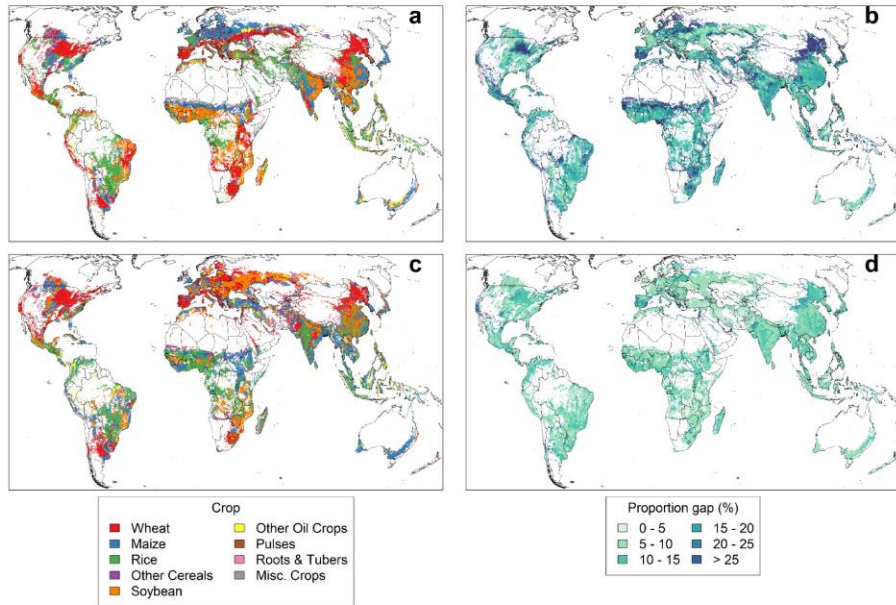


Figure S13. (a) & (c) Most under-utilized crop, with the highest difference between attainable and actual crop proportion; and (b) & (d) proportion gap (difference between attainable and actual proportions). Attainable crop proportion refers to proportions obtained after allocating current crop total areas in their most suitable cropland. (a) & (b) show results derived from absolute suitability and (c) & (d) from relative suitability. Miscellaneous crops include fiber crops, tree nuts, fruits, sugar crops, stimulants, vegetables and melons, and other crops. White areas have less than 0.5% of cropland coverage.

S.1.5. Figure S14 (data quality index)

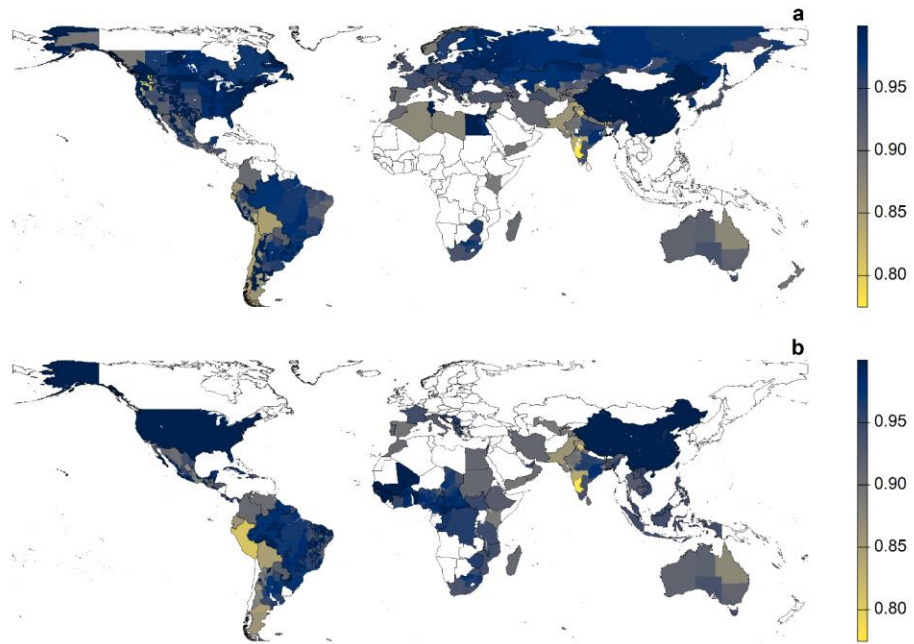


Figure S14. Data quality index (DQI) of two crop areas derived from Monfreda *et al* (2008): (a) apple DQI and (b) mango DQI. White countries or regions are those from which no apple (a) or mango (b) crop area was reported.

S.2. Supplementary Tables

Table S1. Country local diversity average ($D\alpha$) and total diversity ($D\gamma$) for current (cD) and attainable (aD) crop species diversity levels and their corresponding diversity gap (Dg , %). Local diversity average refers to the weighted average of all 86km² cropland cells inside a country. aD is the average attainable diversity estimated with two methods. Dg is the difference between aD and cD , expressed as a percentage of aD . For cropland area, M refers to millions and k to thousands of ha.

Country	Continent	$D\alpha$			$D\gamma$			Cropland (ha)
		cD	aD	$Dg(\%)$	cD	aD	$Dg(\%)$	
India	Asia	6.3	24.2	74	23.2	29.1	20	164.4 M
China	Asia	8.6	21.6	60	24.7	26.0	5	142.1 M
United States	N. America	2.9	16.9	83	6.5	19.5	66	96.6 M
Brazil	S. America	3.3	23.6	86	9.9	27.9	65	65.0 M
Russia	Europe	5.4	11.6	54	7.7	12.9	40	52.2 M
Nigeria	Africa	9.1	24.4	63	18.9	30.4	38	37.1 M
Indonesia	Asia	6.8	21.9	69	16.6	24.7	33	30.6 M
Argentina	S. America	3.2	21.7	85	6.0	23.5	74	28.6 M
Canada	N. America	4.2	12.2	65	7.3	13.2	44	25.7 M
Ukraine	Europe	8.4	15.8	46	9.7	16.9	42	24.3 M
Australia	Oceania	4.2	17.1	75	5.9	20.4	71	23.8 M
Pakistan	Asia	4.2	17.2	75	8.9	20.4	56	20.6 M
Thailand	Asia	4.3	24.7	83	8.3	27.3	70	18.7 M
Turkey	Asia	8.0	18.2	56	11.8	22.7	48	18.2 M
Kazakhstan	Asia	2.5	7.1	65	3.2	8.4	62	17.9 M
Myanmar	Asia	5.5	24.2	77	11.4	28.5	60	16.6 M
France	Europe	6.2	20.1	69	9.1	21.1	57	14.0 M
Mexico	N. America	3.3	23.1	86	12.4	29.2	58	13.9 M
Iran	Asia	5.6	17.2	68	10.2	22.9	56	13.1 M
Spain	Europe	9.5	19.3	51	15.5	21.1	27	12.5 M
Ethiopia	Africa	8.1	27.2	70	19.5	31.3	38	11.2 M
Tanzania	Africa	7.0	26.4	74	21.5	30.0	28	11.1 M
Philippines	Asia	6.0	24.5	76	12.1	27.3	56	10.5 M
Bangladesh	Asia	3.2	24.6	87	5.5	26.3	79	10.5 M
Poland	Europe	7.6	18.6	59	9.1	19.7	54	10.4 M
Sudan	Africa	2.6	20.2	87	4.6	26.1	82	9.8 M
Germany	Europe	6.1	17.1	64	7.7	17.9	57	9.1 M
Vietnam	Asia	5.9	26.6	78	12.9	29.3	56	8.9 M

Country	Continent	$D\alpha$			$D\gamma$			Cropland (ha)
		cD	aD	$Dg(\%)$	cD	aD	$Dg(\%)$	
Niger	Africa	3.9	17.7	78	4.3	22.4	81	8.9 M
Côte d'Ivoire	Africa	10.8	28.8	63	14.9	31.3	53	7.6 M
Romania	Europe	7.6	18.0	58	8.9	18.8	53	7.5 M
Morocco	Africa	4.3	18.5	77	8.7	21.9	60	7.3 M
Mozambique	Africa	7.3	25.7	72	13.0	28.3	54	6.7 M
Ghana	Africa	5.8	27.9	79	13.7	31.2	56	6.6 M
DRC	Africa	8.5	26.3	68	14.7	29.2	50	6.3 M
Burkina Faso	Africa	5.7	22.2	74	7.8	23.7	67	6.2 M
Malaysia	Asia	2.5	19.4	87	4.0	20.7	81	6.0 M
Italy	Europe	12.7	22.1	43	23.0	23.7	3	5.8 M
Cameroon	Africa	9.5	25.3	62	23.8	32.7	27	5.8 M
Mali	Africa	5.4	20.7	74	8.0	23.7	66	5.7 M
South Africa	Africa	4.4	21.0	79	9.0	23.4	62	5.3 M
Egypt	Africa	9.2	20.8	56	20.9	23.9	13	5.1 M
Kenya	Africa	5.8	27.4	79	13.9	33.5	59	5.0 M
Paraguay	S. America	4.1	24.6	83	5.7	25.5	78	4.9 M
Uganda	Africa	7.9	30.4	74	18.7	32.5	42	4.6 M
Syria	Asia	6.6	16.5	60	9.5	19.9	52	4.6 M
Nepal	Asia	7.2	23.6	70	10.5	26.1	60	4.4 M
United Kingdom	Europe	5.5	18.3	70	6.4	19.2	67	4.3 M
Algeria	Africa	5.4	16.7	68	9.2	19.2	52	4.2 M
Angola	Africa	5.4	24.6	78	9.2	27.7	67	4.0 M
Hungary	Europe	8.3	17.7	53	9.5	18.3	48	3.9 M
Chad	Africa	6.3	20.3	69	9.6	24.3	60	3.8 M
Malawi	Africa	6.9	24.3	72	11.0	25.9	58	3.8 M
Colombia	S. America	5.0	26.1	81	17.4	32.1	46	3.7 M
Guinea	Africa	8.8	19.8	56	12.6	23.5	47	3.6 M
Belarus	Europe	10.4	17.2	40	11.6	17.8	35	3.6 M
Uzbekistan	Asia	5.3	19.4	73	6.4	21.3	70	3.6 M
Tunisia	Africa	7.2	18.1	60	11.9	21.4	44	3.5 M
Cambodia	Asia	2.9	23.6	88	4.2	25.3	83	3.4 M
South Sudan	Africa	4.5	26.7	83	6.5	29.5	78	3.2 M
Afghanistan	Asia	3.7	13.9	73	5.3	21.5	75	3.1 M
Peru	S. America	7.2	26.0	72	24.8	35.1	29	3.1 M
Bulgaria	Europe	6.7	18.2	63	7.6	19.3	61	3.0 M

Country	Continent	$D\alpha$			$D\gamma$			Cropland (ha)
		cD	aD	$Dg(\%)$	cD	aD	$Dg(\%)$	
Madagascar	Africa	5.5	24.1	77	12.5	29.8	58	3.0 M
Zimbabwe	Africa	4.8	22.0	78	7.5	23.1	67	3.0 M
Serbia	Europe	7.4	18.4	60	9.7	18.9	49	2.9 M
Bolivia	S. America	6.8	26.3	74	16.0	33.0	51	2.9 M
Senegal	Africa	4.2	19.0	78	6.0	22.1	73	2.8 M
Iraq	Asia	6.6	15.1	56	8.0	20.2	60	2.8 M
Greece	Europe	9.2	21.5	57	14.7	22.7	35	2.6 M
Japan	Asia	7.3	21.5	66	13.4	25.1	46	2.6 M
North Korea	Asia	11.9	21.6	45	14.5	22.4	35	2.5 M
Ecuador	S. America	7.4	25.5	71	18.4	31.9	42	2.4 M
Zambia	Africa	4.4	21.9	80	8.0	23.2	66	2.2 M
Czech Republic	Europe	6.6	17.6	62	7.5	17.9	58	2.2 M
Guatemala	N. America	5.7	24.3	77	12.4	29.1	57	2.1 M
Sri Lanka	Asia	5.0	26.7	81	8.9	31.0	71	2.0 M
Venezuela	S. America	4.4	27.3	84	15.3	30.0	49	2.0 M
Benin	Africa	5.9	27.7	79	12.0	29.7	59	2.0 M
Uruguay	S. America	4.2	23.3	82	6.1	23.9	74	1.8 M
Cuba	N. America	12.4	29.9	59	16.2	30.7	47	1.7 M
Togo	Africa	8.0	28.1	71	11.2	30.5	63	1.7 M
Denmark	Europe	4.5	16.0	72	5.2	16.6	69	1.6 M
Moldova	Europe	7.7	17.5	56	10.4	18.0	42	1.6 M
Turkmenistan	Asia	3.2	17.0	81	4.9	19.5	75	1.6 M
Sierra Leone	Africa	8.2	18.0	54	9.8	19.1	49	1.5 M
Taiwan	Asia	13.0	27.4	52	21.6	30.9	30	1.5 M
Laos	Asia	4.4	21.8	80	6.6	23.7	72	1.5 M
Lithuania	Europe	6.2	13.8	55	7.2	13.9	49	1.4 M
Haiti	N. America	9.9	30.2	67	15.7	32.4	51	1.4 M
Azerbaijan	Asia	4.6	21.1	78	7.9	22.7	65	1.4 M
South Korea	Asia	11.3	23.8	52	18.1	24.6	26	1.3 M
Burundi	Africa	7.5	29.7	75	12.3	30.9	60	1.3 M
Portugal	Europe	13.5	25.7	48	20.4	27.2	25	1.2 M
Chile	S. America	9.7	23.0	58	22.0	26.2	16	1.2 M
Rwanda	Africa	5.4	29.7	82	14.1	31.8	56	1.2 M
Finland	Europe	4.9	13.5	64	5.8	14.5	60	1.2 M
Sweden	Europe	5.9	14.4	59	7.4	17.0	57	1.2 M

Country	Continent	$D\alpha$			$D\gamma$			Cropland (ha)
		cD	aD	$Dg(\%)$	cD	aD	$Dg(\%)$	
Austria	Europe	9.4	18.4	49	12.4	19.1	35	1.2 M
Yemen	Asia	6.2	23.5	74	11.6	28.8	60	1.1 M
Slovakia	Europe	8.1	17.6	54	9.3	18.3	49	1.1 M
Honduras	N. America	5.5	28.6	81	8.8	31.1	72	1.1 M
Nicaragua	N. America	5.3	27.3	81	8.4	31.4	73	1.0 M
Papua New Guinea	Oceania	5.2	22.4	77	13.3	25.5	48	975 k
Central African Republic	Africa	11.8	27.6	57	16.4	30.4	46	945 k
Dominican Republic	N. America	8.5	29.6	71	16.8	33.3	49	899 k
Kyrgyzstan	Asia	6.4	16.9	62	10.1	18.6	45	892 k
Tajikistan	Asia	7.2	19.9	64	9.4	24.4	62	829 k
Croatia	Europe	8.4	18.4	54	10.3	19.2	46	824 k
Libya	Africa	9.9	19.5	49	16.4	25.7	36	804 k
El Salvador	N. America	6.0	23.4	74	7.6	24.3	69	732 k
Somalia	Africa	3.9	21.6	82	5.8	27.9	79	701 k
Latvia	Europe	6.1	13.5	55	6.3	13.7	54	698 k
Saudi Arabia	Asia	8.5	16.2	47	17.3	21.6	20	634 k
Eritrea	Africa	5.9	24.3	76	8.7	30.0	71	626 k
Bosnia and Herzegovina	Europe	9.9	17.6	44	12.3	18.1	32	606 k
Liberia	Africa	9.6	20.5	53	11.6	22.5	49	591 k
Belgium	Europe	7.8	18.5	58	11.2	19.3	42	588 k
Netherlands	Europe	10.1	20.2	50	14.5	21.0	31	553 k
Costa Rica	N. America	5.5	23.3	76	17.9	26.3	32	486 k
Estonia	Europe	5.8	13.3	56	6.1	13.5	55	411 k
Gambia	Africa	5.6	19.5	71	6.6	20.0	67	399 k
Guinea-Bissau	Africa	5.3	17.5	70	11.5	18.6	38	399 k
Namibia	Africa	3.6	21.5	83	5.6	22.2	75	381 k
Georgia	Asia	7.4	21.3	65	14.6	24.5	40	371 k
Mauritania	Africa	5.0	15.1	67	8.5	22.3	62	366 k
Macedonia	Europe	10.7	18.3	42	20.2	19.3	-5	336 k
Congo	Africa	12.4	25.9	52	15.8	28.0	44	336 k
Norway	Europe	4.8	14.9	68	7.6	16.3	53	321 k
Ireland	Europe	3.7	18.7	80	4.1	19.8	79	310 k
Panama	N. America	7.1	23.4	70	11.7	25.6	54	307 k
Israel	Asia	19.5	22.8	14	26.3	24.1	-9	304 k
Mongolia	Asia	1.5	10.0	85	2.2	11.4	81	303 k

Country	Continent	$D\alpha$			$D\gamma$			Cropland (ha)
		cD	aD	$Dg(\%)$	cD	aD	$Dg(\%)$	
Albania	Europe	9.7	23.2	58	13.2	24.3	45	287 k
Armenia	Asia	7.2	15.6	54	10.1	17.1	41	269 k
New Zealand	Oceania	10.1	23.4	57	26.4	27.3	3	262 k
Gabon	Africa	11.5	24.5	53	13.4	27.8	52	240 k
Switzerland	Europe	8.4	18.1	54	11.2	18.4	39	240 k
Lebanon	Asia	14.1	20.3	31	23.4	21.7	-8	223 k
Guyana	S. America	4.5	22.9	80	5.8	24.0	76	222 k
Lesotho	Africa	3.1	20.2	84	4.4	20.7	79	208 k
East Timor	Asia	5.9	29.0	80	9.1	30.6	70	194 k
Botswana	Africa	3.4	23.1	85	6.7	24.4	73	190 k
Jordan	Asia	8.1	18.4	56	18.0	22.0	18	184 k
Kosovo	Europe	5.6	18.9	71	6.1	19.2	68	164 k
Eswatini	Africa	4.1	25.6	84	7.1	27.0	74	160 k
Jamaica	N. America	11.9	31.6	62	14.8	34.0	56	149 k
United Arab Emirates	Asia	9.4	19.4	52	12.7	22.2	43	144 k
Slovenia	Europe	9.2	19.1	52	10.8	19.9	46	142 k
Bhutan	Asia	6.4	23.8	73	18.4	29.0	37	139 k
Fiji	Oceania	4.5	25.0	82	7.6	25.8	71	120 k
Equatorial Guinea	Africa	8.1	23.4	65	10.2	25.1	59	93 k
Vanuatu	Oceania	2.7	22.9	88	3.6	23.3	84	85 k
Belize	N. America	9.8	30.1	68	11.0	30.9	64	78 k
Solomon Islands	Oceania	5.9	20.8	72	7.5	21.3	65	78 k
Suriname	S. America	2.0	23.2	91	2.5	24.0	90	62 k
Oman	Asia	11.1	22.3	50	17.8	24.9	28	55 k
Mauritius	Africa	2.2	30.0	93	2.5	30.3	92	53 k
Montenegro	Europe	12.1	20.9	42	18.8	22.6	17	46 k
Cyprus	Asia	11.4	19.5	42	15.3	20.1	24	45 k
Cabo Verde	Africa	7.0	30.0	77	7.2	34.0	79	41 k
Puerto Rico	N. America	5.8	29.4	80	8.5	32.0	73	39 k
Luxembourg	Europe	6.2	17.3	64	6.8	17.6	61	35 k
Sao Tome and Principe	Africa	5.2	28.1	81	5.7	29.4	81	29 k
Trinidad and Tobago	S. America	18.1	27.9	35	24.3	28.7	15	28 k
Brunei	Asia	5.0	17.4	71	7.9	17.8	56	26 k
Dominica	N. America	18.7	30.0	38	22.1	30.2	27	20 k
Northern Cyprus	Asia	9.8	19.7	50	12.3	20.2	39	20 k

Country	Continent	$D\alpha$			$D\gamma$			Cropland (ha)
		cD	aD	$Dg(\%)$	cD	aD	$Dg(\%)$	
Guadeloupe	N. America	8.9	30.6	71	12.6	30.9	59	18 k
Kuwait	Asia	19.3	13.3	-45	28.1	21.4	-31	14 k
Martinique	N. America	7.2	29.7	76	8.3	30.2	72	12 k
New Caledonia	Oceania	17.0	30.9	45	21.1	32.3	35	12 k
Djibouti	Africa	5.9	22.2	73	9.8	27.7	65	10 k
Malta	Europe	23.4	22.9	-2	23.5	23.0	-2	10 k
French Guiana	S. America	8.4	20.6	59	10.8	21.2	49	10 k
Åland	Europe	9.3	18.1	48	10.2	19.2	47	8 k
Bahamas	N. America	16.2	32.1	50	16.8	32.3	48	7 k
Grenada	N. America	26.8	30.4	12	27.1	30.5	11	6 k
Guam	Asia	1.9	25.2	93	1.9	25.3	93	6 k
Barbados	N. America	6.2	29.9	79	6.3	30.0	79	6 k
Qatar	Asia	20.4	21.9	7	21.9	25.2	13	5 k
Saint Lucia	N. America	12.4	28.0	56	12.9	28.0	54	5 k
Saint Vincent	N. America	16.5	27.8	41	16.8	27.8	40	4 k
Singapore	Asia	3.0	21.4	86	4.0	21.4	81	4 k
French Polynesia	Oceania	2.6	29.1	91	2.6	30.4	91	4 k
Western Sahara	Africa	1.0	18.2	94	1.1	38.1	97	3 k
Niue	Oceania	5.4	26.9	80	5.4	26.9	80	3 k
Micronesia	Oceania	2.2	12.6	82	2.2	12.9	83	2 k
Palestine	Asia	23.9	22.7	-5	24.9	23.7	-5	2 k
Bahrain	Asia	22.4	26.5	15	25.4	26.6	4	2 k
Akrotiri and Dhekelia	Asia	11.0	19.4	43	13.1	19.7	34	2 k
Tonga	Oceania	17.9	26.5	33	17.9	28.1	36	2 k
Antigua and Barbuda	N. America	14.3	32.6	56	15.3	32.8	53	1 k
Wallis and Futuna	Oceania	4.6	22.2	79	4.6	22.2	79	1 k
Iceland	Europe	1.2	13.4	91	1.3	14.8	91	607
Kiribati	Oceania	2.0	27.7	93	2.0	27.7	93	545
Saint Kitts and Nevis	N. America	16.0	32.2	50	16.1	32.3	50	521
Liechtenstein	Europe	10.5	28.4	63	10.5	28.4	63	169
Seychelles	Africa	2.6	25.9	90	2.6	27.9	91	149
Andorra	Europe	15.4	16.3	6	20.6	17.0	-21	66
Cayman Islands	N. America	1.8	29.4	94	1.8	29.4	94	29

Table S2. Crops included in crop diversity calculations, their source, and corresponding names reported by Monfreda, SPAM, and FAOSTAT. The groups were used for supplementary figures S2, S3, & S13.

Crop	Source	Monfreda	SPAM	FAO	Group
wheat	SPAM	wheat	wheat	wheat	Wheat
maize	SPAM	maize	maize	maize	Maize
rice	SPAM	rice	rice	rice	Rice
barley	SPAM	barley	barley	barley	Other Cereals
pearl millet	SPAM	millet	pearl millet	millet	Other Cereals
small millet	SPAM	millet	small millet	millet	Other Cereals
popcorn	Monfreda	popcorn	other cereals	Popcorn	Other Cereals
rye	Monfreda	rye	other cereals	Rye	Other Cereals
oats	Monfreda	oats	other cereals	Oats	Other Cereals
buckwheat	Monfreda	buckwheat	other cereals	Buckwheat	Other Cereals
canaryseed	Monfreda	canaryseed	other cereals	Canary seed	Other Cereals
cerealnes	Monfreda	cerealnes	other cereals	cerealnes, nes	Other Cereals
sorghum	SPAM	sorghum	sorghum	sorghum	Other Cereals
soybean	SPAM	soybean	soybean	soybean	Soybean
coconut	SPAM	coconut	coconut	coconut	Other Oil Crops
groundnut	SPAM	groundnut	groundnut	groundnut, with shell	Other Oil Crops
oilpalm	SPAM	oilpalm	oilpalm	palmoil	Other Oil Crops
rapeseed	SPAM	rapeseed	rapeseed	rapeseed	Other Oil Crops
sesame	SPAM	sesame	sesameseed	sesame seed	Other Oil Crops
sunflower	SPAM	sunflower	sunflower	sunflower seed	Other Oil Crops
olive	Monfreda	olive	other oil crops	Olives	Other Oil Crops
karite	Monfreda	karite	other oil crops	Karite Nuts (Sheanuts)	Other Oil Crops
castor	Monfreda	castor	other oil crops	Castor oil seed	Other Oil Crops
tung	Monfreda	tung	other oil crops	Tung Nuts	Other Oil Crops
safflower	Monfreda	safflower	other oil crops	Safflower seed	Other Oil Crops
mustard	Monfreda	mustard	other oil crops	Mustard seed	Other Oil Crops
poppy	Monfreda	poppy	other oil crops	Poppy seed	Other Oil Crops
melonseed	Monfreda	melonseed	other oil crops	Melonseed	Other Oil Crops
kapokseed	Monfreda	kapokseed	other oil crops	Kapokseed in Shell	Other Oil Crops
linseed	Monfreda	linseed	other oil crops	Linseed	Other Oil Crops
hempseed	Monfreda	hempseed	other oil crops	Hempseed	Other Oil Crops
oilseednes	Monfreda	oilseednes	other oil crops	Oilseeds, Nes	Other Oil Crops
bean	SPAM	bean	bean	beans, dry	Pulses
chickpea	SPAM	chickpea	chickpea	chickpea	Pulses
cowpea	SPAM	cowpea	cowpea	cowpea	Pulses
lentil	SPAM	lentil	lentil	lentils	Pulses
pigeonpea	SPAM	pigeonpea	pigeonpea	pigeon pea	Pulses

broadbean	Monfreda	broadbean	other pulses	Broad beans, horse beans, dry	Pulses
pea	Monfreda	pea	other pulses	Peas, dry	Pulses
bambara	Monfreda	bambara	other pulses	Bambara beans	Pulses
vetch	Monfreda	vetch	other pulses	Vetches	Pulses
lupin	Monfreda	lupin	other pulses	Lupins	Pulses
pulsesnes	Monfreda	pulsesnes	other pulses	pulsesnes, nes Pulses	Pulses
yautia	Monfreda	yautia	other roots	Yautia (cocoyam)	Roots & Tubers
taro	Monfreda	taro	other roots	Taro (cocoyam)	Roots & Tubers
rootnes	Monfreda	rootnes	other roots	Roots and Tubers, nes	Roots & Tubers
cassava	SPAM	cassava	cassava	cassava	Roots & Tubers
potato	SPAM	potato	potato	potato	Roots & Tubers
sweetpotato	SPAM	sweetpotato	sweet potato	sweet potato	Roots & Tubers
yam	SPAM	yam	yams	yam	Roots & Tubers
flax	Monfreda	flax	other fibre crops	Flax fibre and tow	Fiber Crops
hemp	Monfreda	hemp	other fibre crops	Hemp Tow Waste	Fiber Crops
kapokfiber	Monfreda	kapokfiber	other fibre crops	Kapok Fibre	Fiber Crops
jute	Monfreda	jute	other fibre crops	Jute	Fiber Crops
jutelikefiber	Monfreda	jutelikefiber	other fibre crops	Other Bastfibres	Fiber Crops
ramie	Monfreda	ramie	other fibre crops	Ramie	Fiber Crops
sisal	Monfreda	sisal	other fibre crops	Sisal	Fiber Crops
agave	Monfreda	agave	other fibre crops	Agave Fibres Nes	Fiber Crops
abaca	Monfreda	abaca	other fibre crops	Manila Fibre (Abaca)	Fiber Crops
coir	Monfreda	coir	other fibre crops	Coir	Fiber Crops
fibrenes	Monfreda	fibrenes	other fibre crops	Fibre Crops Nes	Fiber Crops
cotton	SPAM	cotton	cotton	seed cotton	Fiber Crops
orange	Monfreda	orange	temperate fruit	Oranges	Fruits
tangetc	Monfreda	tangetc	temperate fruit	Tangerines, mandarins, clem.	Fruits
lemonlime	Monfreda	lemonlime	temperate fruit	Lemons and limes	Fruits
grapefruitetc	Monfreda	grapefruitetc	temperate fruit	Grapefruit (inc. pomelos)	Fruits
citrusnes	Monfreda	citrusnes	temperate fruit	Citrus fruit, nes	Fruits
apple	Monfreda	apple	temperate fruit	Apples	Fruits
pear	Monfreda	pear	temperate fruit	Pears	Fruits
quince	Monfreda	quince	temperate fruit	Quinces	Fruits
apricot	Monfreda	apricot	temperate fruit	Apricots	Fruits
sourcherry	Monfreda	sourcherry	temperate fruit	Sour cherries	Fruits
cherry	Monfreda	cherry	temperate fruit	Cherries	Fruits
peachetc	Monfreda	peachetc	temperate fruit	Peaches and nectarines	Fruits
plum	Monfreda	plum	temperate fruit	Plums and sloes	Fruits

stonefruitnes	Monfreda	stonefruitnes	temperate fruit	Stone fruit, nes	Fruits
strawberry	Monfreda	strawberry	temperate fruit	Strawberries	Fruits
rasberry	Monfreda	rasberry	temperate fruit	Raspberries	Fruits
gooseberry	Monfreda	gooseberry	temperate fruit	Gooseberries	Fruits
currant	Monfreda	currant	temperate fruit	Currants	Fruits
blueberry	Monfreda	blueberry	temperate fruit	Blueberries	Fruits
cranberry	Monfreda	cranberry	temperate fruit	Cranberries	Fruits
berrynes	Monfreda	berrynes	temperate fruit	Berries Nes	Fruits
grape	Monfreda	grape	temperate fruit	Grapes	Fruits
kiwi	Monfreda	kiwi	temperate fruit	Kiwi fruit	Fruits
fruitnes	Monfreda	fruitnes	temperate fruit	Fresh Nes Fruit	Fruits
fig	Monfreda	fig	tropical fruit	Figs	Fruits
mango	Monfreda	mango	tropical fruit	Mangoes, mangosteens, guavas	Fruits
avocado	Monfreda	avocado	tropical fruit	Avocados	Fruits
pineapple	Monfreda	pineapple	tropical fruit	Pineapples	Fruits
date	Monfreda	date	tropical fruit	Dates	Fruits
persimmon	Monfreda	persimmon	tropical fruit	Persimmons	Fruits
cashewapple	Monfreda	cashewapple	tropical fruit	Cashewapple	Fruits
papaya	Monfreda	papaya	tropical fruit	Papayas	Fruits
tropicalnes	Monfreda	tropicalnes	tropical fruit	tropicalnes, tropical fresh nes Fruit	Fruits
banana	SPAM	banana	banana	banana	Fruits
plantain	SPAM	plantain	plantain	plantain	Fruits
brazil	Monfreda	brazil	rest of crops	Brazil nuts, with shell	Treenuts
cashew	Monfreda	cashew	rest of crops	Cashew nuts, with shell	Fruits
chestnut	Monfreda	chestnut	rest of crops	Chestnuts	Fruits
almond	Monfreda	almond	rest of crops	Almonds, with shell	Fruits
walnut	Monfreda	walnut	rest of crops	Walnuts, with shell	Fruits
pistachio	Monfreda	pistachio	rest of crops	Pistachios	Fruits
hazelnut	Monfreda	hazelnut	rest of crops	Hazelnuts, with shell	Fruits
nutnes	Monfreda	nutnes	rest of crops	Nuts, nes	Fruits
maizefor	Monfreda	maizefor	rest of crops	maizefor	Forage Crops
sorghumfor	Monfreda	sorghumfor	rest of crops	sorghumfor	Forage Crops
ryefor	Monfreda	ryefor	rest of crops	ryefor	Forage Crops
grassnes	Monfreda	grassnes	rest of crops	grassnes	Forage Crops
clover	Monfreda	clover	rest of crops	clover	Forage Crops
alfalfa	Monfreda	alfalfa	rest of crops	alfalfa	Forage Crops
legumenes	Monfreda	legumenes	rest of crops	legumenes	Forage Crops

cabbagefor	Monfreda	cabbagefor	rest of crops	cabbagefor	Forage Crops
turnipfor	Monfreda	turnipfor	rest of crops	turnipfor	Forage Crops
beetfor	Monfreda	beetfor	rest of crops	beetfor	Forage Crops
carrotfor	Monfreda	carrotfor	rest of crops	carrotfor	Forage Crops
swedefor	Monfreda	swedefor	rest of crops	swedefor	Forage Crops
mixedgrass	Monfreda	mixedgrass	rest of crops	mixedgrass	Forage Crops
kolanut	Monfreda	kolanut	rest of crops	Kolanuts	Other Crops
areca	Monfreda	areca	rest of crops	Arecanuts	Other Crops
hop	Monfreda	hop	rest of crops	Hops	Other Crops
pepper	Monfreda	pepper	rest of crops	Pepper (Piper spp.)	Other Crops
pimento	Monfreda	pimento	rest of crops	Chillies and peppers, dry	Other Crops
vanilla	Monfreda	vanilla	rest of crops	Vanilla	Other Crops
cinnamon	Monfreda	cinnamon	rest of crops	Cinnamon (canella)	Other Crops
clove	Monfreda	clove	rest of crops	Cloves	Other Crops
nutmeg	Monfreda	nutmeg	rest of crops	Nutmeg, mace and cardamoms	Other Crops
aniseetc	Monfreda	aniseetc	rest of crops	Anise, badian, fennel, corian	Other Crops
ginger	Monfreda	ginger	rest of crops	Ginger	Other Crops
spicenes	Monfreda	spicenes	rest of crops	Spices, nes	Other Crops
peppermint	Monfreda	peppermint	rest of crops	Peppermint	Other Crops
pyrethrum	Monfreda	pyrethrum	rest of crops	Pyrethrum, Dried	Other Crops
rubber	Monfreda	rubber	rest of crops	Natural rubber	Other Crops
gums	Monfreda	gums	rest of crops	Gums Natural	Other Crops
quinoa	Monfreda	quinoa	other cereals	Quinoa	Other Crops
fonio	Monfreda	fonio	other cereals	Fonio	Stimulants
mate	Monfreda	mate	rest of crops	mate	Stimulants
arabica coffee	SPAM	coffee	arabica coffee	coffee	Stimulants
cocoa	SPAM	cocoa	cocoa	cocoa	Stimulants
robusta coffee	SPAM	coffee	robusta coffee	coffee	Stimulants
tea	SPAM	tea	tea	tea	Stimulants
tobacco	SPAM	tobacco	tobacco	tobacco leaves	Stimulants
sugarbeet	SPAM	sugarbeet	sugarbeet	sugarbeet	Sugar Crops
sugarcane	SPAM	sugarcane	sugarcane	sugar cane	Sugar Crops
sugarnes	Monfreda	sugarnes	rest of crops	Sugar crops, nes	Sugar Crops
watermelon	Monfreda	watermelon	tropical fruit	Watermelons	Veg. & Melons
melonetc	Monfreda	melonetc	tropical fruit	Other melons (inc. cantaloupes)	Veg. & Melons
cabbage	Monfreda	cabbage	vegetables	Cabbages and other brassicas	Veg. & Melons
artichoke	Monfreda	artichoke	vegetables	Artichokes	Veg. & Melons
asparagus	Monfreda	asparagus	vegetables	Asparagus	Veg. & Melons

lettuce	Monfreda	lettuce	vegetables	Lettuce and chicory	Veg. & Melons
spinach	Monfreda	spinach	vegetables	Spinach	Veg. & Melons
tomato	Monfreda	tomato	vegetables	Tomatoes	Veg. & Melons
cauliflower	Monfreda	cauliflower	vegetables	Cauliflowers and broccoli	Veg. & Melons
pumpkinetc	Monfreda	pumpkinetc	vegetables	Pumpkins, squash and gourds	Veg. & Melons
cucumberetc	Monfreda	cucumberetc	vegetables	Cucumbers and gherkins	Veg. & Melons
eggplant	Monfreda	eggplant	vegetables	Eggplants (aubergines)	Veg. & Melons
chilleetc	Monfreda	chilleetc	vegetables	Chillies and peppers, green	Veg. & Melons
greenonion	Monfreda	greenonion	vegetables	Onions (inc. shallots), green	Veg. & Melons
onion	Monfreda	onion	vegetables	Onions, dry	Veg. & Melons
garlic	Monfreda	garlic	vegetables	Garlic	Veg. & Melons
greenbean	Monfreda	greenbean	vegetables	Beans, green	Veg. & Melons
greenpea	Monfreda	greenpea	vegetables	Peas, green	Veg. & Melons
greenbroadbean	Monfreda	greenbroadbean	vegetables	Leguminous vegetables, nes	Veg. & Melons
stringbean	Monfreda	stringbean	vegetables	String beans	Veg. & Melons
carrot	Monfreda	carrot	vegetables	Carrots and turnips	Veg. & Melons
okra	Monfreda	okra	vegetables	Okra	Veg. & Melons
greencorn	Monfreda	greencorn	vegetables	Maize, green	Veg. & Melons
chicory	Monfreda	chicory	vegetables	Chicory roots	Veg. & Melons
carob	Monfreda	carob	vegetables	Carobs	Veg. & Melons
vegetablenes	Monfreda	vegetablenes	vegetables	Vegetables fresh nes	Veg. & Melons

S.3. Supplementary Methods

S.3.1. Current crop distribution data

We merged two current global gridded crop distribution data sets: “SPAM” (IFPRI 2019) and “Monfreda” (Monfreda *et al* 2008). SPAM has data for 42 crop categories circa the year 2010, nine of which are groups of crops (such as tropical fruit, other cereal, remaining crops), while Monfreda provides data for 175 crops circa the year 2000. First, we disaggregated the nine SPAM crop groups by identifying the Monfreda’s crops corresponding to each group and transforming the Monfreda’s crop harvested areas so that the sum of all crop areas within one group matched the physical area reported in SPAM for that group and raster cell (supplementary table S2). Then, we merged the crop physical area data of the 33 (individual) crops from SPAM with the 138 area-transformed Monfreda crops for a total of 171 crops.

These two data sets were obtained by downscaling “regional” statistics over some remote sensing-derived gridded cropland map. Both used a combination of FAO’s national statistics and other sub-national statistics from a myriad of sources as input data and corrected the sub-national statistics to match FAO national reports before downscaling from region to grid. However, the SPAM data set can be considered more accurate because it is based on more detailed sub-national data and considers spatial variation in biophysical conditions. In contrast, Monfreda *et al* (2008) uniformly allocated the area of each crop in a region across the cropland in that region. When there is high environmental heterogeneity within the cropland of a region, it is unlikely that all the included environmental space is equally suitable for any species. Thus, we computed a DQI for crops derived from Monfreda data that is inversely proportional to the spatial variation in precipitation and temperature within the region’s cropland (first or second level national sub-division) from which the original data was obtained. For each crop and region, the DQI was computed as $1 - \max(CV_{rain}, CV_{GDD})/4$, where CV_{rain} is the spatial standard deviation in annual precipitation (mm) of the cropland in the region over the average annual precipitation of the same cropland area plus 100mm, and CV_{GDD} is the spatial coefficient of variation of growing degree days (C, base 0). Grid cells in which more than 50% of the cropland is equipped with irrigation were omitted when calculating regional CV_{rain} (figure S14).

S.3.2. Development of spatial distribution models for relative crop suitability estimation

S.3.2.1. Response variable.

Spatial distribution models (SDMs) predict the relative suitability of a crop species from crop distribution data. Random Forest and Boosted Regression Trees use relative crop abundance data as the response variable. Maxent, in contrast, requires a binary (presence-background) response variable, so we derived presence data from the crop abundance data. For that purpose, we compared five sampling methods for obtaining presence (occurrence) data from gridded abundance data that differed in the probability weight of sampled cells. For each method, the probability weights were computed as follows:

- (i) Equal weight for all cells where the crop is present.

$$w_{ij} = \begin{cases} 1 & \text{if } area_{ij} > 0 \\ 0 & \text{if } area_{ij} = 0 \end{cases}$$

- (ii) Weight equal to the relative crop abundance of each cell.

$$w_{ij} = \frac{area_{ij}}{\sum_{j=1}^n area_{ij}}$$

- (iii) Weight is proportional to each cell's crop relative abundance but with a penalty based on a data quality index (DQI, section S1) for the given cell and crop.

$$w_{ij} = \frac{area_{ij}}{\sum_{j=1}^n area_{ij}} \times DQI$$

- (iv) Weight equal to the absolute crop abundance of each cell.

$$w_{ij} = area_{ij}$$

- (v) Weight is proportional to each cell's crop absolute abundance but with a penalty based on a data quality index (DQI, section S1) for the given crop.

$$w_{ij} = area_{ij} \times DQI$$

Where w_{ij} is the weight of cell i for crop j , $area_{ij}$ is the area of crop i in cell j , and n is the total number of crops. So, then, the probability of cell i being sample as a crop j occurrence (P_{ij}) is:

$$P_{ij} = \frac{w_{ij}}{\sum_{i=1}^m w_{ij}}$$

Where m is the number of cells.

From the five methods considered to derive presence data, methods 2 (for SPAM-derived crops) and 3 (for Monfreda derived crops) were consistently the best methods determined by the regional cross-validation approach (see below). Thus, we used these methods to derive the presence-background data used in the Maxent models.

After model prediction, we used the clog-log transformation (Guillera-Arroita *et al.* 2014, Phillips *et al.* 2017) to transform Maxent predictions to presence probability (i.e., relative abundance) to evaluate Maxent prediction accuracy against relative abundance data.

S.3.2.2. Predictors

We considered the 19 WorldClim bioclimatic variables plus some additional bioclimatic variables of agronomic importance as climatic predictors of crop relative suitability. These additional bioclimatic variables were growing degree days (GDD), aridity indices (annual average and values for the warmest, coldest, wettest, and driest quarter), and potential evapotranspiration seasonality (Metzger *et al.* 2013). All bioclimatic variables were evaluated through correlation and principal component analyses to discard highly correlated variables. We retained 17 bioclimatic variables for modeling and used them with soil pH and irrigation availability as SDMs' predictors.

S.3.2.3. Model selection, tuning, and averaging

We aimed to select models that capture the generalities of the relations between the environment and the species rather than the algorithm that best reproduces the observed abundance patterns (and, for our purposes, overfits the data). Model selection by k-fold cross-validation can lead to overfitting when there is high spatial autocorrelation, as in this case (Hijmans 2012). Thus, to maximize the models' ability to extrapolate to a different geographical region, we divided the world into six regions and tested the prediction accuracy in a region left out in model training, repeating the process for each of the six regions. The six regions were (i) South America, (ii)

North America + the Caribbean, (iii) Sub-Saharan Africa, (iv) northern Africa + Europe + western Asia, (v) Southeast Asia + Oceania, and (vi) central and eastern Asia. We tuned and tested the algorithms on the six most evenly distributed crops across regions: bean, cotton, maize, mango, tobacco, and wheat.

After selecting the tuning parameters that returned the best extrapolation results for each of the three algorithms across the six crops and regions, we ran these models for each of the 171 crops to estimate the worldwide crop-specific cropland relative suitability. Finally, we integrated all model results into one global cropland relative suitability estimation per crop by computing the weighted average of the three algorithms using the root mean squared error improvement over the null model (training data average) as weight.

S.3.3. ECOCROP model calibration and running

We calibrated the ECOCROP model parameters for all crops to reduce possible errors in the database and the *omission* error; that is, the model should predict that an environment is suitable if a crop is widely grown in it. However, we did not want to reduce *commission* errors because a crop not planted in an environment does not mean that it cannot be grown there. Thus, we did not narrow the default parameters but, instead, relaxed the environmental limits until at least 95% of the observed crop area of a given crop was included within the predicted environmental range of the species. Similarly, we relaxed the minimum and maximum optimum values of each parameter to ensure that at least 50% of the crop area was included within the limits of optimum environmental conditions. First, we calibrated each static predictor (e.g., soil pH and annual precipitation), one at a time. Second, we calibrated all dynamic predictors (e.g., killing and average temperatures) at once following a “greedy” approach, that is, by relaxing all environmental limits and detecting the parameter that allowed for a greater increase in crop area coverage. This process was repeated until 95% of the actual crop area was included within a species’ environmental limits.

We then ran Ecocrop for all the species and subspecies included in each of the 171 crop categories for both rainfed (i.e., water-limited) and irrigated (no water limitation) conditions. Next, we computed the maximum suitability value of any (sub-) species within one crop category for each raster cell and water condition. Finally, we calculated rainfed and irrigated suitability weighted average with irrigation availability per cell as weight, assuming that all crops can have equal access to the available irrigation.

S.3.4. Crop allocation algorithm and crop potential and attainable distribution

One of the foundations of our diversity gap framework is the crop allocation algorithm that we used to estimate attainable diversity (aD). This algorithm distributes each crop's total area in the available cropland with crop suitability indices as priors.

S.3.4.1. Algorithm description

First, to better represent the expected relative abundance of each crop per cell, crop-specific cropland suitability indices are normalized such that they sum to one in each grid cell.

$$NS_{ij} = S_{ij} / \sum_{j=1}^n S_{ij} \quad (\text{Eq. 1})$$

Where NS is the normalized suitability for crop j in cell i ; S_{ij} is the (relative or absolute) suitability value, and n is the total number of crops. Normalizing absolute suitability indices over cells is necessary because the expected proportion of crop j in cell i depends on its relative rather than its absolute suitability. For example, a given area might be very suitable for a crop, but the expected proportion planted with the crop could be small if the area is also highly suitable for many other crops. By contrast, it is expected that a crop occupies all cropland (proportion = 1) when it is the only feasible option (only crop with absolute suitability > 0), even if its absolute suitability is low.

For the estimation of pD , allocated areas are equal to the normalized suitability indices times total cell cropland for the corresponding crops and cells because it assumes that crops are grown

based on their adaptation only and not on their demand. In contrast, each crop's current global area was used to estimate aD . When cropland suitability is the same for two crops, a major crop (high total demand) is expected to be more abundant than a minor crop. Crops with narrow environmental ranges might be more abundant, too, because they might have very few other areas to which they can be allocated. Therefore, to allocate crop areas for estimating aD , a crop relative abundance factor (RAF) is computed for each crop as the ratio between their required (world total) and the available (niche) area.

$$RAF_j = \frac{\sum_{i=1}^m A_{ij}}{\sum_{i=1}^m (NS_{ij} \times \sum_{j=1}^n A_{ij})} \quad (\text{Eq. 2})$$

Where A_{ij} is the actual area of crop j in cell i and m is the total number of cells. Note that the last summation ($\sum_{j=1}^n A_{ij}$) represents the total cropland of cell i .

Next, crops are allocated proportionally to NS , RAF , and the available cropland.

$$AA_{ij} \propto NS_{ij} \times RAF_j \times \sum_{j=1}^m A_{ij} \quad (\text{Eq. 3})$$

Where AA_{ij} is the allocated area of crop j in cell i . Other possible associations between cropland suitability and crop-allocated areas are discussed below. Note that the above equation is not an equality because $\sum_j (NS_{ij} * RAF_j * \sum_{j=1}^m A_{ij}) \neq \sum_j A_{ij}$ and $\sum_i (NS_{ij} * RAF_j * \sum_{j=1}^m A_{ij}) \neq \sum_i A_{ij}$. In other words, the sum of the right side of Eq. 3 for cell i across all crops does not equal the total cropland of cell i , and adding this product across all cells for crop j does not equal the total area of crop j . Thus, the allocation is done by, first, over or under-allocating crop areas using the right side of Eq. 3 and proportionally removing any extra cropland per cell and total crop area per crop. Then, the remaining crop areas are iteratively allocated to the remaining cropland until convergence. Each iteration starts with the crops with greater area to be allocated, prioritizing the most suitable cropland for each crop, but only using a fraction of the remaining cropland at a time until all the cropland is covered. Sometimes there is no convergence because there is no remaining suitable cropland for a given crop where it can be allocated. In that case, the algorithm frees suitable area for that under-allocated crop by removing other crops from its suitable cropland and starts a new for-loop. After this step, all crop areas are fully allocated, and

all cropland is covered, but this is not necessarily the result that best honors the priors (cropland suitability).

Therefore, in the final step, the algorithm reallocates crops to minimize the cross-entropy (CE) between allocated areas and crop-specific cropland suitability indices.

$$\min_{\{AA_{ij}\}} CE(AA_{ij}, S_{ij}) = \sum_i \sum_j AA_{ij} * \ln(AA_{ij}) - \sum_i \sum_j AA_{ij} * \ln(S_{ij}) \quad (\text{Eq. 4})$$

Crops are reallocated by considering all crop pairs and identifying cells where allocated crop areas are higher than expected for one crop and lower for the other. The expected allocated area ratio for a pair of crops is their suitability ratio times their RAF ratio. Note that it is not simply the ratio of their suitability indices because, at equal suitability indices, major crops are expected to occupy a higher proportion of the available cropland. Then, the pair of crops are reallocated, switching crop areas between cells until the expected ratio is met. The algorithm repeats the reallocation process considering all possible pairs of crops until the cross-entropy is not reduced in more than 0.01% of the initial cross-entropy with any further crop reallocation.

S.3.4.2. Crop distribution assumptions and considerations

We assumed that cropland suitability and crop area are directly proportional. Thus, for example, in a given piece of cropland that is twice as suitable for crop A as for crop B, the expected crop area ratio is (for potential diversity, pD) – or would tend to be (for aD) – 2:1. However, other assumptions are possible and would lead to different results. For instance, one could allocate the most suitable crop to each piece of cropland (independently of market demand) or allocate crops to their most suitable cropland until the demand for each crop is fulfilled. In these scenarios, both local aD and pD equal one everywhere at the scale to which crops are allocated (but not at higher levels of spatial aggregation). Thus, the suitability of the croplands where the crops are grown is maximized (max cropland suitability score) at the expense of local crop diversity. In contrast, a very flat response of relative crop areas to differences in cropland suitability would make pD approach the maximum diversity (mD) at the expense of land productivity. Assuming that suitability and area are directly proportional takes into account this trade-off and is a reasonable intermediate point that would tend to maximize both D and the cropland suitability score.

Nevertheless, it would be interesting to test other functions and their effect on pD , aD , and average cropland suitability score.

Moreover, we defined demand at the global level, but it could also be constrained at the national and regional levels. In addition, we assumed that crop-specific current demands could be fulfilled if crops are distributed to their most suitable cropland without changing their current global area. In other words, planting crops based on their attainable rather than in their current distribution does not reduce the total production of any crop as long as the total area of each crop is unchanged. Yet, this assumption cannot be tested because yield data are only available for regions where the crops are currently planted.

S.3.5. R packages used in the analysis

We used the following R packages: raster (Hijmans 2021b) and terra (Hijmans 2021c) for spatial data analysis, data.table (Dowle and Srinivasan 2020) for data manipulation and allocation algorithm, ranger (Wright and Ziegler 2017), maxnet (Phillips 2017), and xgboost (Chen *et al* 2021) for relative suitability modeling, and Recocrop (Hijmans 2021a) for absolute suitability modeling.

S.4. Supplementary Results

S.4.1. Differences in potential and attainable diversity between suitability estimation methods

Potential diversity (pD) estimates are very sensitive to the suitability estimation method. The highest relative-suitability-derived potential diversity ($rs-pD$) values are observed in temperate regions, particularly the Mediterranean and coastal regions. In contrast, pD derived from absolute suitability ($as-pD$) tends to be higher in tropical regions with high rainfall or access to irrigation and no soil acidity problems (figure 4 & 5 and supplementary figure S6). $as-pD$ spans from 1 (the lowest possible value) to 169 (very close to the 171 crops considered, which is the highest possible value) while $rs-pD$ values range from 50 to 125. The maximum $rs-pD$ value is lower than the maximum $as-pD$ value because, at equal absolute suitability, minor crops (small total crop area) tend to have lower relative suitability values than major crops. Thus, in places that are highly suitable for most crops in absolute terms (i.e., they have a high sum of absolute suitability values), relative suitability is considerably lower for minor crops than for major crops, resulting in a lower pD (supplementary figure S7). Moreover, $as-pD$ reaches very low diversity values because the crop model used for absolute suitability defines clear environmental limits to each species, particularly for very cold or dry environments that are unsuitable for most crops in absolute terms (figure 5 and supplementary figure S7).

Attainable diversity (aD) estimates, in contrast, are more stable upon changes in the suitability estimation method (figure 6 and supplementary figure S8 & S9). However, some notable differences exist between the two estimates of aD . First, the absolute-suitability-derived attainable diversity ($as-aD$) has more extreme low values, particularly in areas that are very dry, cold, or have acidic soils. In contrast, aD values derived from relative suitability indices ($rs-aD$) are never lower than 7 (supplementary figure S10). Second, $rs-aD$ tends to be lower in very productive croplands currently dominated by a few major crops, such as the US Midwest, north India, and the Pampas of South America, which might be a result of relative suitability indices' dependency on observed crop distributions. Third, the crop model (absolute suitability) better accounts for sharp environmental gradients (e.g., in the Sahel and the Andes), whereas the SDM

might be affected by the low resolution of some of the crop distribution data, hiding strong environmental gradients (figure 6 and supplementary figure S8).

S.4.2. Crop diversity as the inverse of the Simpson index (2D)

We calculated crop diversity by computing their *true* diversity because a true diversity has the doubling property (e.g., a diversity of 4 is twice as diverse as a diversity of 2, which in turn is twice as diverse as a diversity of 1), which is a *sine qua non* to compute diversity gaps. However, *true* diversity values can be calculated in different ways, depending on the weight given to the proportional abundances in the computation of their mean. Thus, we first computed diversity using nominal weights, in which each crop affects the mean based on their relative proportion, and diversity equals the exponent of the Shannon entropy (${}^1D = \exp(H)$). Then, we repeat our analysis by giving more weight to more abundant crops, such that the weight of a crop equals the squared of its proportion and diversity equals the inverse of the Simpson index (Eq. 5).

$${}^2D = 1 / \sum_{j=1}^n p_j^2 \quad (\text{Eq. 5})$$

When all crops are in equal proportion (complete evenness), 1D equals 2D , but 2D tends to be lower than 1D as the unevenness in crop proportions increases because of the greater weight given to the most dominant crops.

Current diversity (cD) and attainable diversity (aD) values are consistently lower when computing diversity as the inverse of the Simpson index (2D , supplementary figures S1 & S8) than when using the exponent of the Shannon entropy (1D , figures 2 & 6). This is because current and attainable crop proportions are highly uneven in most croplands due to our heavy reliance on a few major crops for global food supply while many crop species are planted and consumed in relatively small quantities. In contrast, potential diversity (pD) values are pretty similar for 1D (figure 5) and 2D (figure S6), as potential diversity is not constraint by current crop-specific demand and, thus, potential crop proportions are more even.

Noteworthy, spatial patterns for all diversity levels and gaps are very similar, and the environmental gradients are even sharper when computing 2D . However, diversity gaps tend to

be lower with 2D (supplementary figure S11) than 1D (figure 7) and the difference is higher in Europe (${}^2Dg = 36\%$ vs. ${}^1Dg = 56\%$) and lower in Africa, Asia, Oceania (${}^2Dg \approx 60\%$ vs. ${}^1Dg \approx 70\%$), and the Americas (${}^2Dg = 72\%$ vs. ${}^1Dg = 82\%$). Because of these lower diversity gaps, the extent to which crop diversity could double without changing the aggregate amount of global food produced is relatively lower when using 2D , though still pervasive (67% of the world's cropland with 2D vs. 84% with 1D).

S.5. Supplementary references

Chen T, He T, Benesty M, Khotilovich V, Tang Y, Cho H, Chen K, Mitchell R, Cano I, Zhou T, Li M, Xie J, Lin M, Geng Y and Li Y 2021 *xgboost: Extreme Gradient Boosting* Online: <https://CRAN.R-project.org/package=xgboost>

Dowle M and Srinivasan A 2020 *data.table: Extension of `data.frame`* Online: <https://CRAN.R-project.org/package=data.table>

Guillera-Arroita G, Lahoz-Monfort J J and Elith J 2014 Maxent is not a presence–absence method: a comment on Thibaud et al. *Methods Ecol. Evol.* **5** 1192–7

Hijmans R 2021a *Recocrop: Implementation of the ecocrop model for estimating adaptation of plants to environments* Online: <https://github.com/cropmodels/Recocrop/>

Hijmans R J 2012 Cross-validation of species distribution models: removing spatial sorting bias and calibration with a null model *Ecology* **93** 679–88

Hijmans R J 2021b *raster: Geographic Data Analysis and Modeling* Online: <https://CRAN.R-project.org/package=raster>

Hijmans R J 2021c *terra: Spatial Data Analysis* Online: <https://rspatial.org/terra>

IFPRI 2019 Global Spatially-Disaggregated Crop Production Statistics Data for 2010 Version 2.0 Online: <https://dataverse.harvard.edu/dataset.xhtml?persistentId=doi:10.7910/DVN/PRFF8V>

Metzger M J, Bunce R G H, Jongman R H G, Sayre R, Trabucco A and Zomer R 2013 A high-resolution bioclimate map of the world: a unifying framework for global biodiversity research and monitoring *Glob. Ecol. Biogeogr.* **22** 630–8

Monfreda C, Ramankutty N and Foley J A 2008 Farming the planet: 2. Geographic distribution of crop areas, yields, physiological types, and net primary production in the year 2000 *Glob. Biogeochem. Cycles* **22**

- Phillips S 2017 *maxnet: Fitting "Maxent" Species Distribution Models with "glmnet"* Online:
<https://CRAN.R-project.org/package=maxnet>
- Phillips S J, Anderson R P, Dudik M, Schapire R E and Blair M E 2017 Opening the black box:
An open-source release of Maxent *Ecography* **40** 887–93
- Wright M N and Ziegler A 2017 ranger: A Fast Implementation of Random Forests for High
Dimensional Data in C++ and R *J. Stat. Softw.* **77** 1–17

CHAPTER 3

Estimating lime requirements for tropical soils: model comparison and development

To be submitted for publication

Estimating lime requirements for tropical soils: Model comparison and development

Fernando Aramburu Merlos^{* a,b}, João Vasco Silva^c, and Robert J. Hijmans^a

^a Department of Environmental Science and Policy, University of California Davis, Davis, California, United States of America.

^b Instituto Nacional de Tecnología Agropecuaria (INTA), Unidad Integrada Balcarce, Balcarce, Buenos Aires, Argentina.

^c International Maize and Wheat Improvement Center (CIMMYT), Harare, Zimbabwe

*Corresponding author. Email: faramburumerlos@ucdavis.edu

Fernando Aramburu Merlos, ORCID = 0000-0003-0957-7482

João Vasco Silva, ORCID = 0000-0002-3019-5895

Robert J. Hijmans, ORCID = 0000-0001-5872-2872

Keywords: exchangeable acidity, aluminum saturation, base saturation, pH, calcium carbonate equivalent

Abstract

Acid soils can become highly productive when treated with agricultural lime, but optimal lime rates are unknown in many tropical regions. Lime requirement models can be used to estimate lime rates in these regions. Here, we provide a comprehensive review of models for lime requirement estimation in acid tropical soils and introduce a new model based on a target acidity saturation (a proxy for aluminum toxicity). These models were tested on their ability to predict the lime rate needed to reach the target change in soil chemical properties with data from four soil incubation studies covering 31 soil types. We show that two foundational models, one targeting acidity saturation, and the other targeting base saturation, performed accurately ($r \geq 0.9$) in predicting lime requirements. However, later attempts to modify and improve the acidity saturation model were unsuccessful. In contrast, a new acidity saturation model proposed here was the most accurate in predicting lime requirements. This new model and the foundational base saturation model were used to estimate lime requirements in 303 African soil profiles. Important differences in the estimated lime rates were found, depending on the target soil chemical property of the model. Therefore, a necessary step for formulating liming recommendations is identifying the most important soil acidity problem affecting crop yield. While the model introduced here can be useful for strategic research on potential lime use, more information on other acidity problems than aluminum toxicity is needed to develop a fully comprehensive assessment of potential liming benefits.

1. Introduction

Low soil pH is associated with a high concentration of toxic elements in the soil solution, such as aluminum and manganese, and with low availability of phosphorus, calcium, and other plant nutrients (Kamprath, 1984). Soil acidity problems can be addressed with liming, the application of calcium or magnesium-rich materials that react as a base (Coleman et al., 1959). Liming has been practiced for centuries (Johnson, 2010), and its use is still expanding, particularly in tropical areas with acid soils. For example, it played a key role in the recent expansion of agriculture in the Brazilian Cerrado region (Goedert, 1983; Yamada, 2005).

The amount of lime required to adjust soil acidity depends on the soil, the target crop(s), and the liming material used. In temperate regions, lime requirements are commonly estimated with locally calibrated quick tests using buffer solutions (Goulding, 2016; Metzger et al., 2020; Rossel and McBratney, 2001; Sims, 1996). These tests can be developed by comparing the buffer's response to the soil with the soil response to lime in field or incubation studies or by slow titrations. Both the soil testing and the lime application may be a relatively small expense in intensively managed commercial farms, partly because lime is cheap and partly because the use of lime, when needed, increases the use efficiency of other inputs (de Wit, 1992). Moreover, applying a bit more lime than needed means its benefits will last longer (Li et al., 2009). Thus, blanket applications that err on the higher side are not very risky (overliming problems exist, but only at extremely high doses), so there is no need for a highly accurate determination of the amount of lime to apply.

This situation is different for smallholder farmers in sub-Saharan Africa (Crawford et al., 2008) and other tropical regions (Sanchez and Salinas, 1981). Lime may be relatively expensive, and its benefit may be relatively small if fertilizer use is low. Under these circumstances, it would be helpful to have accurate estimates of lime requirements. However, empirical (experimental) evidence from these tropical regions is limited, and laboratory-based soil testing is often inaccessible. Furthermore, methods that depend on direct measurements of soil acidity in each field with buffer solutions cannot be assumed to work elsewhere and would have to be re-developed.

Models to estimate lime requirements from generally available soil data are needed for strategic research of potential lime use across tropical regions. They can be particularly useful for sub-Saharan Africa, where the impact of soil acidity on crop productivity and nutrient-use efficiency is poorly understood (Crawford et al., 2008). Lime requirement models could serve as a starting point to develop locally optimal liming recommendations for farmers and development practitioners and provide strategic information to national governments and the private sector on potential market sizes for lime for a region of interest. The latter is now possible thanks to the availability of high-resolution spatial products for most soil properties across the continent (Hengl et al., 2017; Miller et al., 2021).

Here we provide a comprehensive review of general lime requirement models for tropical acid soils that can be used with readily available soil data. We first introduce key concepts related to estimating lime requirements that have been a source of confusion and inconsistency. We then describe and discuss published lime requirement models for tropical soils and introduce a new model to estimate lime requirements. Finally, we show substantial differences in the estimated lime requirement for acid tropical soils when using these models and discuss their implications.

2. Key concepts and definitions

Soils can be naturally acidic or become acidic because of agricultural practices such as the use of acidifying fertilizer and the removal of elements with harvested products. In the tropics, many soils in humid (and some subhumid) areas are inherently acidic because intense weathering processes have resulted in the displacement and leaching of basic (i.e., non-acidic) exchangeable cations (Ca^{2+} , Mg^{2+} , K^+ , and Na^+) and the accumulation of exchangeable acidity (Al^{3+} and H^+). The main problem with soil acidity in the tropics is not the low pH as such, but rather the associated aluminum (Al) toxicity that constrains crop growth (Sanchez, 2019). The purpose of liming should be, therefore, to remove Al toxicity, considering the sensitivity of the target crops, together with other possible constraints such as Ca and Mg deficiencies (Kamprath, 1984; Sanchez, 2019), but not to increase pH for its own sake (Fageria and Baligar, 2008; Harter, 2007).

2.1. Target soil chemical properties

2.1.1. Exchangeable acidity or aluminum?

Acidity saturation is the fraction of the effective cation exchange capacity (*ECEC*) of the soil occupied by exchangeable acid cations (Al^{3+} and H^+ , extracted with a neutral unbuffered salt such as 1N KCl). In tropical soils, nearly all exchangeable acidity comprises exchangeable Al^{3+}

(except in histosols) and, thus, Al saturation approximates acidity saturation (Deressa et al., 2020; Farina and Channon, 1991; Salinas, 1978). For that reason, acidity saturation is often used as a proxy for Al toxicity (Evans and Kamprath, 1970; Farina and Channon, 1991; Kamprath, 1980; Salinas, 1978; Smyth and Cravo, 1992). Many lime requirement models estimate the lime rate required to lower the acidity saturation to a target level that does not affect crop yield (Cochrane et al., 1980; Osmond et al., 2002; Yost et al., 1988).

The terms exchangeable acidity and exchangeable Al^{3+} have been used interchangeably in tropical soil literature, with the term exchangeable Al^{3+} more commonly used in older literature (Sanchez, 2019). Indeed, several authors of the lime requirement models reviewed here measured acidity saturation but referred to it as Al saturation (Cochrane et al., 1980; Kamprath, 1970). Consequently, some models were originally formulated for exchangeable Al^{3+} (and Al saturation) but derived from exchangeable acidity measurements.

2.1.2. Exchangeable calcium and magnesium

Some highly weathered acid soils can have very low *ECEC* and, thus, low exchangeable Ca^{2+} and Mg^{2+} but low acidity saturation, resulting in Ca and Mg deficiencies without Al toxicity problems (Kamprath, 1984). Therefore, some lime requirement models based on acidity saturation also estimate the lime rate needed to cover such deficiencies (Sanchez, 2019; Teixeira et al., 2020b; van Raij, 1996). Such mineral deficiencies can also be addressed with compost or inorganic fertilizers such as calcium nitrate, which might be more convenient in soils with no Al toxicity problems.

2.1.3. Base saturation

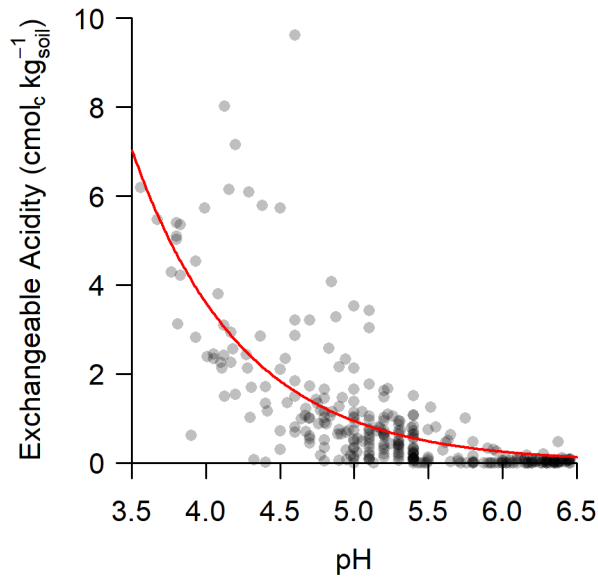
An alternative approach to alleviating soil acidity problems aims to raise the “base saturation” to a certain level rather than focusing on acidity saturation (Quaggio, 1983; van Raij, 1996). Base saturation (V) is the sum of all exchangeable bases (Ca^{2+} , Mg^{2+} , K^+ , and Na^+) divided by the Cation Exchange Capacity at pH 7 (CEC_7). CEC_7 is different from ECEC , especially in acid soils, where $\text{CEC}_7 \gg \text{ECEC}$. For ECEC , exchangeable acid cations (Al^{3+} and H^+) are extracted with a neutral unbuffered salt. In contrast, a pH 7 buffer solution is used for CEC_7 , which extracts both exchangeable and non-exchangeable acidity (for example, from hydroxy-Al organic matter complexes), comprising the potential acidity. The magnitude of the potential acidity of the soil depends on the type and amount of clay and organic matter. Although there is some inverse parallelism between acidity saturation and base saturation, these terms are not complementary because they have different denominators (ECEC and CEC_7 , respectively).

Contrary to Al toxicity and acidity saturation, there is no direct association between base saturation and crop yields. Instead, a minimum base saturation threshold is defined such that, above it, no soil acidity problems are detected (Fageria and Baligar, 2008). Therefore, recommended target base saturation levels must be defined locally for each crop type (van Raij, 1996).

2.1.4. pH in water

Most lime requirement methods used in temperate regions target soil pH (as measured in water), estimating with locally-calibrated models the lime rate required to raise the soil pH to a specific level (6 to 6.5 for most crops and soils) (Goulding, 2016; Sims, 1996). In acid tropical soils, maximum yields can be obtained with a pH as low as 5, depending on other soil chemical properties (Abruña et al., 1969; Bell, 1996; Pearson et al., 1977), and raising the pH to higher values can result in a loss of soil structure and other problems (Harter, 2007). Therefore, a target pH level is seldomly used, and when used, it must be defined locally (Fageria and Baligar, 2008; Teixeira et al., 2020a).

There is a negative exponential relationship between exchangeable acidity and soil pH (Supplementary Figure 1). Very high exchangeable acidity values are only found in soils with a low pH, but not all soils with a low pH have high exchangeable acidity. Exchangeable acidity approaches 0 at a pH above 5.5, and there is virtually no exchangeable acidity at a pH above 6 (Farina and Channon, 1991; Lollato et al., 2013; Sanchez, 2019). Therefore, a target pH between 5.5 and 6 should be high enough to address Al toxicity problems.



Supplementary Figure 1. Soil pH measured in water as a function of the exchangeable acidity extracted with 1 M KCl unbuffered salt. Data extracted from the Africa Soil Profile Database (Leenaars et al., 2014) for the 0 – 20 cm soil layer. The red line is a negative exponential regression line $Exchangeable\ acidity\ (cmol_c kg_{soil}^{-1}) = 765 e^{-1.34 pH}$

2.1.5. Phosphorus availability

Acid tropical soils have very low plant-available phosphorus because of the high P fixation capacity of Fe and Al oxides often present in weathered tropical soils. Liming has the associated benefit of increasing P availability, which might result in significant yield responses, particularly when P fertilization is low (Salinas, 1978). However, liming can only provide short-term relief to P deficiencies in soils with low P reserves (Smithson and Giller, 2002). Therefore, phosphorus availability is not considered a direct target of liming, and lime requirement models do not consider it. However, the increase in P availability can be an important reason for observing a yield response to lime.

2.2. Lime rate units

Lime rates (LR) are commonly expressed in charges per soil mass (e.g., meq per 100g of soil or cmol_c per kg of soil, which are equivalent) or in the equivalent mass of pure calcium carbonate lime per unit area (CaCO_3 tons per ha). To transform lime rates between charges per soil mass and calcium carbonate mass per ha, soil bulk density (sbd) and liming depth (ld) are needed. Lime rates in t ha^{-1} and $\text{cmol}_c \text{ kg}^{-1}$ are the same when $sbd = 1 \text{ g cm}^{-3}$ and $ld = 20 \text{ cm}$. Thus, LR can be converted from charges per soil mass to calcium carbonate mass per area with Eq. 1, where sbd is expressed in g cm^{-3} and ld in cm.

$$LR (t_{\text{CaCO}_3} \text{ ha}^{-1}) = LR(\text{cmol}_c \text{ kg}_{\text{soil}}^{-1}) \times sbd \times ld / 20 \quad (\text{Eq. 1})$$

Many lime requirement models reviewed here provide lime rates in $\text{cmol}_c \text{ kg}^{-1}$. Therefore, when using these models to estimate lime rates in tons of liming material per hectare, these must be transformed by considering the soil bulk density, lime incorporation depth, and the calcium carbonate equivalents (CCE) of the liming material to be applied. In addition, a few other models (Osmond et al., 2002; Yost et al., 1988) assume certain incorporation depth and soil bulk density and provide lime rates in t ha^{-1} . However, these lime rates should be adjusted to account for potential differences between the assumed ld and sbd and the actual ld and sbd .

3. Materials and methods

We searched for general use lime requirement models that only require measured soil properties often available in soil databases. The terms “acid*” AND “soil*” AND (“lim* requirement” OR “lim* recommendation” OR “lim* rate”) were used in the Web of Science and Google Scholar databases to screen and retrieve relevant literature and references therein. Methods that required additional soil tests to measure the “buffer capacity” of the soil (e.g., Shoemaker et al., 1961) and methods developed for use in specific regions in temperate climates (e.g., Heckman et al., 2002, and Rossel and McBratney, 2001) were not considered and excluded from further analysis. The search yielded seven models that can, in principle, be applied to a wide range of tropical soils. The selected models include five acidity saturation models, one base saturation model, and one pH model. These seven lime requirement models were reviewed and used to derive a new model based on acidity saturation. The tested models were implemented in an R package called “limer” (Aramburu Merlos, 2022) to facilitate the evaluation, comparison, and use of these models against empirical data. The R package, data, and scripts used for analysis in this paper are available on GitHub (<https://github.com/gaiafrica/limer>).

The lime recommendation models were evaluated using data from four soil incubation studies that measured the effect of liming on exchangeable acidity and *ECEC* or acidity saturation (Ananthacumaraswamy and Baker, 1991; Cochrane et al., 1980; Kamprath, 1970; Teixeira et al., 2020a). Studies only measuring the effect of liming on pH were not considered. Soil incubation studies are experiments in which soil samples are mixed with different lime treatments and incubated under controlled conditions (~ 30 °C and soil moisture at field capacity) for about a month to ensure that all lime reacts with the soil. The liming effect is assessed by measuring

chemical soil properties before and after each treatment. The data from Kamprath (1970), Cochrane et al. (1980), and Ananthacumaraswamy and Baker (1991) were readily available, but Teixeira et al. (2020a) soil data were not. The Teixeira et al. (2020a) data was reconstructed in two steps: (i) the initial soil properties were back solved from lime requirement formulas and lime rates, and (ii) the final soil properties were estimated using the regression formulas provided in the supplementary information ($R^2 \approx 0.9$). Table 1 describes the main features of these four data sets.

Table 1. Description of the lime incubation studies data used to assess the lime requirement models. Data were extracted from Kamprath (1970) (Kamp.), Cochrane et al. (1980) (Coch.), Ananthacumaraswamy and Baker (1991) (Anan.), and Teixeira et al. (2020a) (Teix). The range of values (minimum – maximum) is presented for lime rates (*LR*) and chemical soil properties. *ECEC*: effective cation exchange capacity; *AS* (%): acidity or aluminum saturation (exchangeable acidity divided by *ECEC*). *CEC₇*: cation exchange capacity at pH 7. *OM*: organic matter. “-” indicates that this was not measured, while “m-” means it was measured but not available for each treatment (in which case we report the range of values reported in the original paper). Soil properties measured at the end of the experiments are in square brackets.

	<i>Kamp.</i>	<i>Coch.</i>	<i>Anan.</i>	<i>Teix.</i>
<i>Year of study</i>	1970	1980	1991	2020
<i>Number of soil types</i>	4	2	3	22
<i>LR treatments per soil</i>	5	5	4 or 5	8
<i>Soils region</i>	North Carolina, USA	Colombia	Sri Lanka and Kenya	Minas Gerais, Brazil
<i>LR (cmol_c kg⁻¹)</i>	0.5 – 8.4	0.4 – 4	1 – 21.5	0.2 – 23.9
<i>pH</i>	4.5 – 4.7 [4.9 – 6]	-	-	4.1 – 5.3 [5.1 – 7.3]
<i>AS (%)</i>	53 – 82 [2 – 52]	68 – 86 [27 – 79]	49 – 81 [0 – 30]	9 – 96 [0 – 18]
<i>ECEC (cmol_c kg⁻¹)</i>	1.1 – 7.8 [1.2 – 10.4]	3.4 – 4.4	6.3 – 9.1 [7 – 22.5]	0.5 – 3 [0.7 – 11.3]
<i>CEC₇ (cmol_c kg⁻¹)</i>	-	-	12 – 21	1.7 – 14
<i>Clay content (%)</i>	10 – 17	37 – 71	-	5 – 88 (m-)
<i>OM (%)</i>	2 – 7	-	-	0.4 – 8

We used all models to predict the lime rate required to reach the observed soil responses, which were then compared with the actual amount used in the experiment. The response variables evaluated varied by the model's target soil chemical property. For instance, the actual lime rate was compared with the predicted lime rate needed to reach the observed acidity saturation for models that use a target acidity saturation. The (dis)agreement between observed (y) and predicted (\hat{y}) values was expressed with the root mean squared error ($RMSE = \sqrt{\frac{1}{n} \sum_1^n (y - \hat{y})^2}$) and its components: bias ($Bias = \bar{y} - \bar{\hat{y}}$), the difference between population standard deviations ($\Delta_{SD} = SD_y - SD_{\hat{y}}$), and Pearson's correlation coefficient (r) (Kobayashi and Salam, 2000). All the available data were used to test each model, including the originally used to calibrate the model (when possible) and other independent datasets. Six-fold cross-validation was used when only the same data used to develop a model was available for testing it. Model coefficients were recalibrated on five folds and tested on the remaining fold, repeating the process for each fold (James et al., 2013).

Lastly, we compared lime rates required for different target soil chemical properties and acidity levels using soil data from the Africa Soil Profile Database (Leenaars et al., 2014). Soil samples tested for at least exchangeable acidity, $ECEC$, and CEC_7 , in which exchangeable acidity was extracted with 1 M KCl, and CEC_7 measured in 1 M NH_4OAc buffered at pH 7 were selected for analysis. Lime requirements were estimated with the models described below for a lime incorporation depth of 20 cm.

4. Acidity saturation models

This section describes five published lime requirement estimation models based on acidity saturation (Kamprath, Cochrane, ACID4, NuMASS, and MG5) that were evaluated against data from four soil incubation studies (Ananthacumaraswamy and Baker, 1991; Cochrane et al., 1980; Kamprath, 1970; Teixeira et al., 2020a).

4.1. Kamprath

In a soil incubation study, Kamprath (1970) tested soil responses to different lime rates in four very acidic soils ($\text{pH} < 5$, acidity saturation $> 50\%$). This study illustrated that acidity saturation does not decrease linearly with the amount of lime applied. When lime application rates are lower than the initial exchangeable acidity, acidity saturation is sharply reduced. However, for lime rates much greater than the initial exchangeable acidity, the fraction of lime charges that neutralizes exchangeable acidity is much lower because it reacts with other forms of Al (e.g., organic-Al complex). Consequently, acidity saturation decay can be modeled as a decreasing exponential relation with the lime rate that approaches zero at high lime rates (Figure 1).

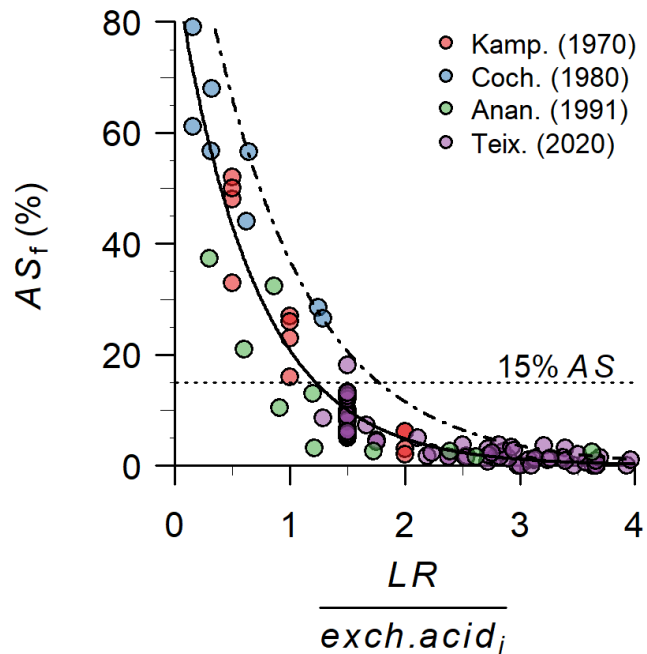


Figure 1. Acidity saturation after liming (AS_f , %) as a function of the lime rate (LR , $\text{cmol}_c \text{ kg}^{-1}$) divided by the initial exchangeable acidity of the soil (exch. acid_i , $\text{cmol}_c \text{ kg}^{-1}$) for soils with an initial acidity saturation $> 30\%$. Data were extracted from Kamprath (1970) (Kamp.), Cochrane et al. (1980) (Coch.), Ananthacumaraswamy and Baker (1991) (Anan.), and Teixeira et al. (2020a) (Teix). The solid line is a negative exponential regression line AS_f (%) = $95.7 e^{-1.4 LR / \text{exch. acid}_i}$ and the dot-dash line is a 95% negative exponential quantile regression line fitted with all the observations. Soil samples with $LR > 4 \times \text{exch. acid}_i$ had AS_f values ranging from 0 to 3.1%, with quartiles equal to 0, 0.2%, and 0.4% (these extreme values are not shown).

Kamprath (1970) concluded that a lime rate ($\text{cmol}_c \text{ kg}^{-1}$) of 1.5 times the initial exchangeable acidity ($\text{cmol}_c \text{ kg}^{-1}$) was enough to reduce the acidity saturation to 15% (or less), which was considered to be a threshold below which most crops are not affected by acidity (Figure 1). For sensitive crops needing less than 15% of acidity saturation, such as beans (Abruña et al., 1969; Fageria et al., 2011; Kamprath, 1980), the required lime rate suggested was twice the exchangeable acidity. Thus, Kamprath's (1970) lime requirement model can be written as follows:

$$LR(\text{cmol}_c \text{ kg}_{\text{soil}}^{-1}) = lf \times \text{exch. acid}_i (\text{cmol}_c \text{ kg}_{\text{soil}}^{-1}) \quad (\text{Eq. 2})$$

Where *exch. acid_i* is the initial exchangeable acidity of the soil, and *lf* is the lime factor, which equals 1.5 for most staple crops (e.g., cereals) and 2 for beans and other sensitive crops, including many vegetable and fruit crops (Alvarez and Ribeiro, 1999).

This simple model worked well for almost all the experimental data available from the four studies (Figure 1). Out of 21 very acidic soils (acidity saturation, *AS*, between 30% and 97%) that received a lime rate of exactly 1.5 of the initial exchangeable acidity, only one ended with an acidity saturation greater than 15%, but it was very close to that value (18%). Furthermore, all soil samples with a lime rate of at least twice the initial exchangeable acidity had a final acidity saturation of 6% or less. Hence, when liming to reduce the acidity saturation to a level that does not affect crop yield, liming is only needed when the acidity saturation is above 15% (or 5% for sensitive crops). In such cases, lime rates of 1.5 times (or two times for sensitive crops) the initial exchangeable acidity would suffice for most tropical crops.

Modifications of the Kamprath (1970) model were used in different regions of Brazil (Lopes et al., 1991) and Ethiopia (Alemu et al., 2022). For instance, in Minas Gerais, Brazil, a *lf* of 2 was recommended for most soil types, except for sandy soils (*lf* = 1) and clay soils (*lf* = 3; Lopes et al., 1991). This distinction might have accounted for differences in soil bulk density, as the modified formulas gave lime requirements in tons per hectare. Furthermore, all modifications added a second term that accounted for possible Ca and Mg deficiencies, also used in Minas Gerais (MG5, Section 0).

4.2. Cochrane

Cochrane et al. (1980) introduced the concept of *target acidity saturation (TAS)* to estimate lime rates (originally called *required percentage Al saturation*, see Section 2.1.1). Considering the great genetic variability in acidity saturation tolerance among and within crops (Kamprath, 1980; Lollato et al., 2019), Cochrane et al. (1980) developed a model that allowed estimating the lime rate needed to reduce the acidity saturation to a crop's (or variety) specific target.

To derive their formula, Cochrane et al. (1980) started with a hypothetical situation where all lime reacts with the exchangeable acidity; thus, the *ECEC* itself does not change (the decrease in exchangeable acidity equals the increase in exchangeable bases). In this scenario, the required lime rate to reach a given acidity saturation would be $LR = \text{exch. acid}_i - \text{exch. acid}_f = \text{exch. acid}_i - (TAS/100) \times ECEC$. The target acidity saturation (*TAS*, %) is divided by 100 to change it to a fraction, and the subscript *i* indicates the initial and *f* the final values. The unit of *LR*, *exch. acid*, and *ECEC* is $\text{cmol}_c \text{ kg}^{-1}$.

The original formula uses the sum of exchangeable acidity (H^+ and Al^{3+}), Ca^{2+} , and Mg^{2+} instead of *ECEC* because these were the cations measured by Kamprath (1970). The concentration of other bases, such as K^+ and Na^+ , was considered negligible, as these are normally very low in acid soils. Thus, the sum of exchangeable acidity, Ca^{2+} , and Mg^{2+} was considered equivalent to

the *ECEC*. We present the formula using *ECEC*, noting that *ECEC* might not always include all cations but should always include at least exchangeable Al^{3+} , Ca^{2+} , and Mg^{2+} , as these are the most abundant cations in acid soils. If data on exchangeable K^+ and Na^+ are available, they might be included depending on which exchangeable cations were considered for the derivation of the crop *TAS*.

Since not all the applied lime is expected to react with the exchangeable acidity, the formula is multiplied by a lime factor (*lf*) that equals 1.5 or 2 depending on the relation between initial exchangeable acidity, *TAS*, and *ECEC*. The authors defined the following rule: “*factor 1.5 is replaced by 2 when the estimated liming requirement using the factor 1.5 is greater than the chemical lime equivalent of the exchangeable Al (acidity).*” Thus:

$$LR(cmol_c kg_{soil}^{-1}) = lf \times [exch. acid_i - (TAS/100) \times ECEC_i]$$

$$lf = \begin{cases} 1.5, & \text{if } 1.5 \times [exch. acid_i - (TAS/100) \times ECEC_i] \leq exch. acid_i \\ 2, & \text{if } 1.5 \times [exch. acid_i - (TAS/100) \times ECEC_i] > exch. acid_i \end{cases} \quad (\text{Eq. 3})$$

Which can be simplified as

$$lf = \begin{cases} 1.5, & \text{if } TAS \geq AS_i/3 \\ 2, & \text{if } TAS < AS_i/3 \end{cases}$$

Where AS_i is the initial acidity saturation. In other words, when the target acidity saturation is less than one-third of the initial saturation, the lime factor is 2; otherwise, it is 1.5. For example, for soils with an initial acidity saturation of 60%, $lf = 1.5$ when $TAS \geq 20\%$ and $lf = 2$ when $TAS < 20\%$.

Notably, when $TAS = 0\%$, the Cochrane et al. (1980) model equals the Kamprath (1970) model for sensitive crops, and the required lime rate is twice the initial exchangeable acidity. For that reason, Cochrane et al. (1980) suggested that their formula should not be evaluated for lime rates greater than twice the initial exchangeable acidity. Such lime rates result in about 5% acidity saturation or less (Figure 1). Therefore, we recommend restricting the use of the Cochrane et al. (1980) model (and any other acidity saturation model) to a $TAS \geq 5\%$. Accordingly, we only evaluated models based on TAS for cases in which liming led to a final $AS \geq 5\%$, as lower AS values should not be the target of these models (Figure 2). A model with a target pH of 6 might be more appropriate for extremely sensitive crops requiring an acidity saturation of $< 5\%$.

We found several instances in the literature where the rule of changing the lime factor at low TAS in (Eq. 3) was misused or ignored. First, Cochrane et al. (1980) themselves inconsistently applied this rule when testing the performance of their model, perhaps to improve the accuracy of their model (Figure 2). Second, no description or modification of the model included their rule (Alvarez and Ribeiro, 1999; Osmond et al., 2002; Yost et al., 1988). For instance, Sanchez (2019) and Fageria and Baligar (2008) described the formula with a unique $lf = 1.8$, which results from multiplying the original lf of 1.5 by 1.2 to express the LR in tons per hectare by assuming a soil bulk density (sbd) of 1.2 g cm^{-3} and a lime incorporation depth (ld) of 20 cm (Eq. 1). Despite these inconsistencies, the model of Cochrane et al. (1980) has very good accuracy ($RMSE = 0.61$, $r = 0.97$), even when tested with the independent data from Ananthacumaraswamy and Baker (1991) and Teixeira et al. (2020a) ($RMSE = 0.63$, $r = 0.97$), and represented a breakthrough in lime requirement models. All models based on TAS derive from it.

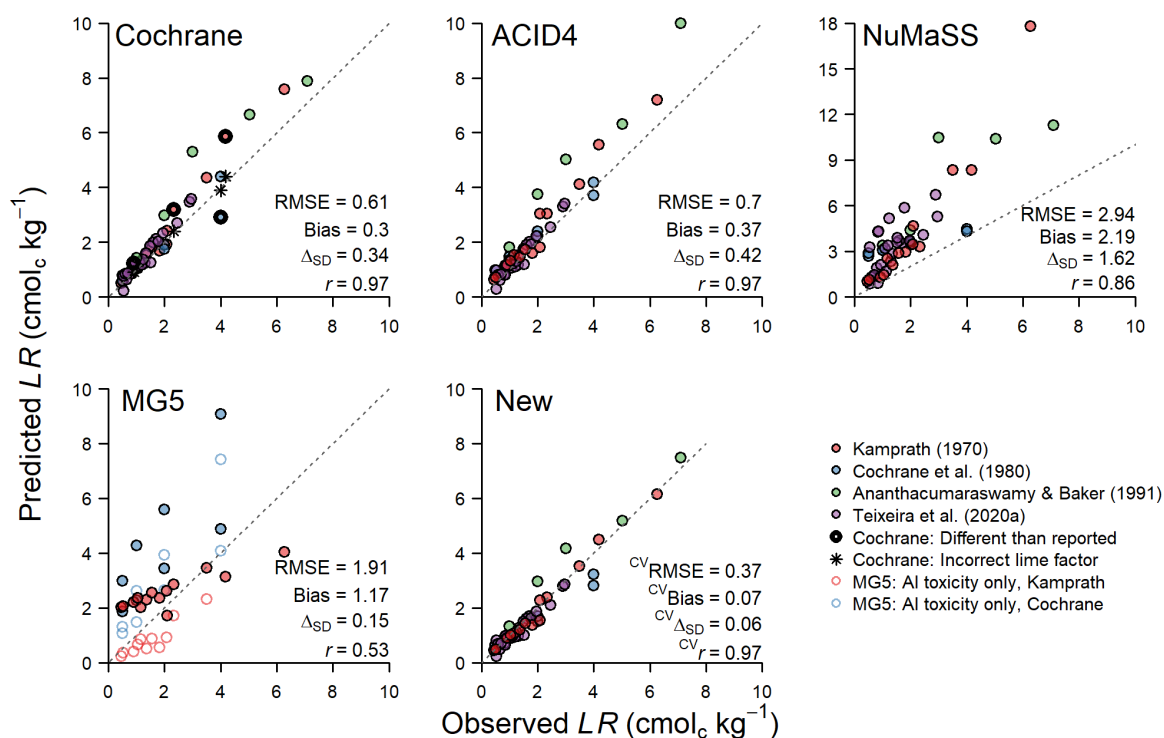


Figure 2. Observed and predicted lime rates (LR , $\text{cmol}_c \text{kg}^{-1}$) to reach the exchangeable acidity saturation obtained with the observed lime rates for five lime requirement estimation models based on a target acidity saturation (TAS). Observed data were extracted from Kamprath (1970) (red), Cochrane et al. (1980) (blue), Ananthacumaraswamy and Baker (1991) (green), and Teixeira et al. (2020) (purple). Samples with a final acidity saturation of $< 5\%$ were excluded. In the Cochrane et al. (1980) model, thick points are values computed with Eq. 3 that are different from the values reported in Cochrane et al. (1980), and asterisks are values reported by Cochrane et al. (1980) that did not follow their own model (incorrect lf). In the Minas Gerais 5th approximation model (MG5), filled circles were predicted using the complete formula, and empty circles by only considering its first term (acidity saturation requirements). Teixeira et al. (2020a) and Ananthacumaraswamy and Baker (1991) data are not included in MG5 due to the lack of the original soil texture data. The gray dashed line is the identity function ($\text{Predicted } LR = \text{Observed } LR$). RMSE is the root mean square error, Δ_{SD} the difference in standard deviation, and r the Pearson's correlation coefficient between observed and predicted LR . Accuracy statistics with the superscript ^{CV} were obtained with 6-fold cross-validation.

4.3. ACID4

Yost et al. (1988) developed the ACID4 expert system to make lime requirement predictions in the humid tropics. They used the Cochrane et al. (1980) formula with a fixed lime factor (lf) and a unit conversion from $\text{cmol}_c \text{ kg}^{-1}$ to t ha^{-1} . Based on preliminary data from Sitiung, Indonesia, Yost et al. (1988) estimated that 0.53 cmol_c of exchangeable acidity are neutralized per cmol_c of CaCO_3 and computed the lf as the inverse of that fraction ($1/0.53 = 1.9$). Their model yielded a slightly lower accuracy ($RMSE = 0.7$, $r = 0.97$, Figure 2) than Cochrane et al. (1980) model.

To convert the results from $\text{cmol}_c \text{ kg}^{-1}$ to tons of CaCO_3 per ha, Yost et al. (1988) changed the lf to 1.4, assuming $sbd = 1 \text{ g cm}^{-3}$ and $ld = 15 \text{ cm}$ (Eq. 1). Several authors have used such arbitrary sbd and a fixed ld to estimate the lime requirement in tons per hectare (Osmond et al., 2002; Sanchez, 2019; Yost et al., 1988). However, this practice should be avoided because it greatly affects the results. For example, a soil with $sbd = 1.2 \text{ g cm}^{-3}$ requires 20% more lime than one with the same chemical properties and $sbd = 1 \text{ g cm}^{-3}$, while an $ld = 15 \text{ cm}$ needs 25% less lime than $ld = 20 \text{ cm}$.

4.4. NuMaSS

The Integrated Soil Nutrient Management Decision Support System (NuMaSS) was developed to provide fertilizer (N and P) and liming recommendations for acid soils with nutrient problems (Osmond et al., 2002; Walker et al., 2009). In NuMaSS, soil N, P, and acidity constraints are computed individually. Then, the final management recommendation is computed considering the costs and benefits of different nutrient management strategies. The acidity module considers Al toxicity and deficiencies of Ca and Mg, although the main focus was on Al toxicity. Al toxicity is computed based on crop critical acidity saturation, exchangeable acidity, and *ECEC*.

Default crop critical acidity saturation values for many crops and varieties were included. The lime rate was calculated with another modified Cochrane et al. (1980) formula (Eq. 4).

$$LR(t\ ha^{-1}) = lf \times \left(\text{exch. acid} - \frac{TAS}{100} \times ECEC \right) + \left[10 \times ECEC \times \frac{\max(19 - TAS, 0)}{100} \right]$$

$$lf = \begin{cases} 2.5, & \text{if } ECEC/clay < 4.5 \\ 1.3, & \text{if } ECEC/clay \geq 4.5 \end{cases} \quad (\text{Eq. 4})$$

Where *clay* is the clay content in the soil.

This model uses different lime factors depending on the soil's clay activity (effective cation exchange capacity of the soil's clay fraction). According to its authors, soils with low clay activity ($ECEC/clay < 4.5$) require almost twice the lime rate of soils with high clay activity per unit of exchangeable acidity to be neutralized. In addition, they considered that reducing the acidity saturation below 19% requires an additional amount of lime equivalent to 10% of the *ECEC* per percentage point. The NuMaSS model predicts lime rates in tons per hectare by assuming $ld = 15\ \text{cm}$ and $sbd = 1\ \text{g cm}^{-3}$.

To test the NuMaSS model with the soil incubation studies data, the predicted LR was transformed from t ha^{-1} to cmolc kg^{-1} with Eq. 1. Moreover, to take advantage of all the data while being conservative in the lime requirement prediction, high clay activity (lowest *lf* and lower *LR*) was assumed when clay data were unavailable (Table 1, Figure 2).

The NuMaSS formula adds much complexity to the formula of Cochrane et al. (1980). It considers that the acidity saturation response to increasing lime rates is not linear and that the response depends on a soil's clay activity. However, our analysis shows that NuMaSS consistently overpredicted the lime rates required to reach a certain acidity saturation (Figure 2), particularly for low *TAS* (< 10%), indicating that the second term of the formula for *TAS* < 19% should be revised or omitted. Unfortunately, the software is no longer available, and the data used to derive the formula are unavailable, so the model cannot be further scrutinized.

4.5. Minas Gerais 5th approximation

This Minas Gerais 5th approximation (MG5) model developed for the state of Minas Gerais, Brazil (Alvarez and Ribeiro, 1999) also has two terms, one of them deriving from the model of Cochrane et al. (1980). It considers the lime rate needed to lower the acidity saturation of the soil to a target level as well as possible Ca and Mg deficiencies for the crop. The formula can be written as follows:

$$LR(t \text{ ha}^{-1}) = lf \times \left[\text{exch. acid}_i - \left(\frac{TAS}{100} \right) \times ECEC_i \right] + \max(X - (\text{exch. Ca} + \text{Mg}), 0) \quad (\text{Eq. 5})$$

$$lf = 0.0302 + 0.06532 \%clay - 0.000257 \%clay^2$$

Where *X* is the sum of the minimum quantity of exchangeable Ca and Mg required by the crop (estimated as 2 cmol_c kg⁻¹ for most cereals and legumes and 3 cmol_c kg⁻¹ for most fruits and vegetables, Alvarez and Ribeiro, 1999). Note that the second term of the formula becomes zero when the initial exchangeable Ca²⁺ and Mg²⁺ meet crop demands, while the first term is equal to

the model of Cochrane et al. (1980) but with a different lime factor that depends on soil texture. The lf can take any value between 0 and 4, with higher values in clay soils.

The Kamprath (1970) and Cochrane et al. (1980) soil incubation studies data show very little support for such a drastic change in lf (Figure 2). Furthermore, the addition of the second term in (Eq. 5) has no theoretical justification, as the Ca^{2+} from the $CaCO_3$ used to neutralize exchangeable acidity stays in the cation exchange complex and becomes available for the crop (Sanchez, 2019). Therefore, it would be more appropriate to adjust for possible Ca and Mg deficiencies when the sum of the initial exchangeable Ca^{2+} and Mg^{2+} and the Ca supplied by the lime (to neutralize the exchangeable acidity) does not meet crop demand.

5. A new model to estimate lime requirements

Defining a target acidity saturation and estimating lime rates as a function of that target is a useful concept. There has been a proliferation of *TAS* models, presumably because of perceived shortcomings in the Cochrane et al. (1980) model (e.g., fixed lf of 1.5 or 2). However, while more complicated, the derived models did not appear to improve the prediction quality. Below we introduce a new lime requirement model based on *TAS* obtained from a formal mathematical derivation of the concept of acidity saturation. Our goal is to provide a model based on strong empirical relations that can be easily updated as more data become available.

First, let us decompose the numerator and denominator of final acidity saturation ($AS_f(\%) = \frac{exch.acid_f}{ECEC_f} \times 100\%$) into their initial values and degree of change (Eq. 6).

$$AS_f(\%) = \frac{exch.acid_i - \Delta exch.acid}{ECEC_i + \Delta ECEC} \times 100\% \quad (\text{Eq. 6})$$

$\Delta exch.acid$ is the exchangeable acidity equivalents neutralized by liming, and $\Delta ECEC$ is the change in the effective cation exchange capacity, which equals the difference between the increase in exchangeable bases ($\Delta exch.bases$) minus the neutralized exchangeable acidity ($\Delta exch.acid$). $\Delta ECEC$ would be 0 if there were a perfect substitution between basic (Ca^{2+} and Mg^{2+}) and acid (Al^{3+} and H^+) cations in the cation exchange complex, but it is usually positive because normally $\Delta exch.bases > \Delta exch.acid$. Thus:

$$AS_f(\%) = \frac{exch.acid_i - \Delta exch.acid}{ECEC_i + \Delta exch.bases - \Delta exch.acid} \times 100\% \quad (\text{Eq. 7})$$

Considering that our goal is to equalize the final acidity saturation to the target acidity saturation ($AS_f = TAS$), AS_f can be replaced with TAS in Eq. 7 (Eq. 6). Then, TAS becomes a function of the initial soil properties ($ECEC_i$ and $exch.acid_i$), the increase in exchangeable bases ($\Delta exch.bases$), and the exchangeable acidity equivalents neutralized ($\Delta exch.acid$). Therefore, to estimate the required LR to reach a given TAS , we need to find the association of $\Delta exch.acid$ and $\Delta exch.bases$ with LR so that the two former variables can be replaced for some function of LR in Eq. 7. For soils with $AS_f \geq 5\%$, these two associations can be modeled with a linear regression without intercept (Figure 3), despite slight differences between studies. In Figure 3B, most Teixeira et al. (2020a) observations are above the regression line, and most Kamprath (1970) observations are below.

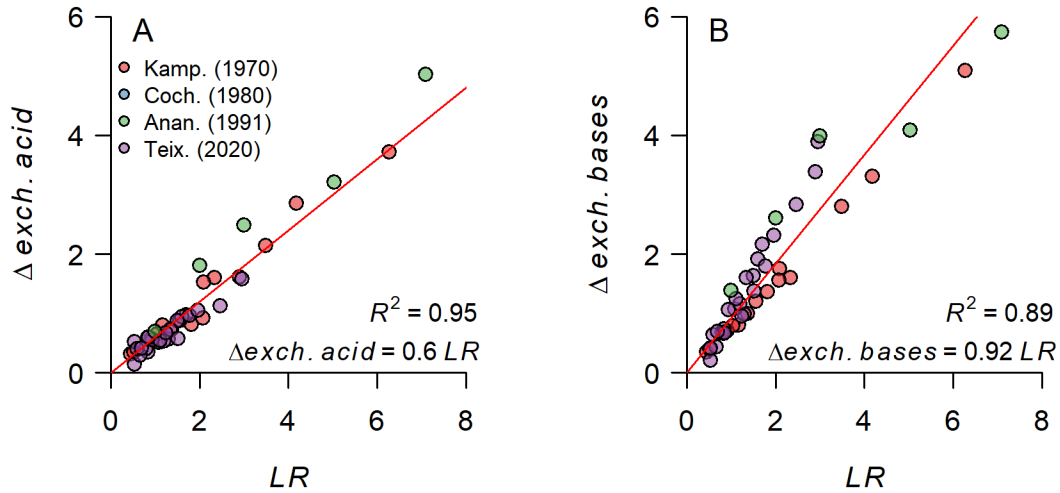


Figure 3. (A) Exchangeable acidity neutralized ($\Delta exch. acid$, $cmol_c kg^{-1}$) and (B) exchangeable bases increase ($\Delta exch. bases$, $cmol_c kg^{-1}$) as a function of the lime rate (LR , $cmol_c kg^{-1}$), for soil samples with a final acidity saturation $\geq 5\%$. The red lines are regression lines forced through the origin (equations shown in the plot). To avoid the high leverage of soil samples with the highest LR , LR and Δs were transformed with the square root before linear regression fitting, and then the coefficients estimates were back-transformed. The coefficient of determination was computed as the square of Pearson's correlation coefficient between observed and linear-regression-predicted values. Data extracted from Kamprath (1970) (Kamp.), Cochran et al. (1980) (Coch.), Ananthacumaraswamy and Baker (1991) (Anan.), and Teixeira et al. (2020) (Teix.).

Based on this assumption, we have:

$$\Delta exch. acid = a \times LR \quad (\text{Eq. 8})$$

$$\Delta exch. bases = b \times LR \quad (\text{Eq. 9})$$

We replace the deltas in (Eq. 7) with (Eq. 8 and (Eq. 9) to obtain:

$$TAS(\%) = \frac{exch. acid_i - a \times LR}{ECEC_i + b \times LR - a \times LR} \times 100 \quad (\text{Eq. 10})$$

And we solve for LR to get

$$LR(\text{cmol}_c \text{ kg}^{-1}) = \frac{\text{exch. acid}_i - \text{TAS}/100 \times \text{ECEC}_i}{a + \text{TAS}/100 \times (b - a)} \quad (\text{Eq. 11})$$

Based on the soil incubation studies data and the regression lines shown in Figure 3, the parameter estimates for a and b were 0.60 and 0.92, respectively. These parameters were estimated using the square root of the values to reduce the leverage of very high LR values and then back-transformed. Note that a , which is the cmol_c of exchangeable acidity neutralized per cmol_c of CaCO_3 , is similar to the value reported by Yost et al. (1988), which was 0.53. These values can be updated or calibrated for a particular region. Moreover, if new evidence refutes the assumption of a linear association between LR and the change in exchangeable bases and acidity, all formulas from Eq. 7 onwards would need to be updated. Still, the steps to take would remain the same.

Notably, the numerator in (Eq. 11) is the same subtraction term found in the model of Cochrane et al. (1980) and all other models derived from it. Hence, if (Eq. 11) is rewritten by splitting the numerator and denominator, the inverse of the denominator can be interpreted as a new lime factor (lf), which is an inverse function of TAS (Eq. 12). Although the lf derived in Eq. 12 is very different conceptually from the lf introduced by Cochrane et al. (1980; Eq. 3), its possible values are similar to those used by previous models. Given our a and b parameter estimates, the value of the lf would be between 1.5 and 1.6 for most crops.

$$LR(\text{cmol}_c \text{ kg}^{-1}) = lf \times [\text{exch. acid}_i - (\text{TAS}/100) \times \text{ECEC}_i] \quad (\text{Eq. 12})$$

$$lf = \frac{1}{a + \text{TAS}/100 \times (b - a)} \quad ; \quad \hat{lf} = \frac{1}{0.6 + \text{TAS}/100 \times (0.92 - 0.6)}$$

In addition to the 6-fold cross-validation (accuracy statistics in Figure 2), the model in Eq. 12 was cross-validated by fitting parameters a and b with three of the four datasets and testing the lime rate predictions with the remaining dataset, repeating the process for each dataset. This “dataset-based” cross-validation resulted in even higher accuracy statistics ($RMSE = 0.32$, $r = 0.98$). Therefore, the new model has improved accuracy and general validity because its extrapolation to different tropical regions did not result in a precision loss.

6. Base saturation model

A “*base saturation*” model originally proposed by Quaggio (1983) is widely used in São Paulo state, Brazil (Sanchez, 2019; van Raij, 1996). Base saturation (V) is the sum of exchangeable bases over CEC_7 , expressed as a percentage (see section 0). The model’s formula is

$$LR (cmol_c kg_{soil}^{-1}) = CEC_7 \times (V_t - V_i)/100 \quad (\text{Eq. 13})$$

V_t is the target, and V_i is the initial base saturation. Like TAS , V_t is crop-specific and expresses a crop’s sensitivity to soil acidity. In São Paulo, Brazil, V_t is 50% for most cereals and legumes, including maize, wheat, rice, sorghum, soybeans, and beans, while it is between 60% to 80% for most fruits and vegetables (Alvarez and Ribeiro, 1999; Sanchez, 2019).

Since CEC_7 is, in principle, not affected by liming (contrary to $ECEC$), CEC_7 can be distributed to V_t and V_i in (Eq. 13) and canceled out. Thus, the lime requirement estimated by this model is equal to the difference between the target and the initial sum of exchangeable bases:

$$LR (cmol_c kg_{soil}^{-1}) = exch. bases_t - exch. bases_i = \Delta exch. bases \quad (Eq. 14)$$

The base saturation model implicitly assumes that all Ca^{2+} (and Mg^{2+}) equivalents from the lime become part of the exchangeable complex (Quaggio, 1983). Figure 3B shows the association between observed LR and $\Delta exch. bases$ for soil samples with $AS_f \geq 5\%$. Figure 4 expands that association to all soil samples with LR equal to or lower than the initial potential acidity ($pot. acid_i = CEC_7 - exch. bases_i$). It excludes soil samples with $LR > pot. acid_i$ because the increase in exchangeable bases cannot be greater than what the cation exchange complex can take. When $LR \leq 50\% pot. acid_i$, there is almost a one-to-one association between the lime rate and the increase in exchangeable bases ($\Delta exch. bases = LR \times 0.95(\pm 0.05) \forall LR < 0.5 \times pot. acid_i$, Figure 4), supporting the base saturation model assumption. However, as the lime rate approaches the potential acidity, that association becomes weaker ($\Delta exch. bases = LR \times 0.8(\pm 0.03) \forall 0.5 \times pot. acid_i < LR < pot. acid_i$, Figure 4). Thus, this model yields a final base saturation close to the target when $V_t \leq 50\%$, but it does not perform well at higher base saturation targets.

Consequently, in the future, a liming correction factor (lf) that depends on V_t could be considered for the model. For example, the lf could be 1.05 when $V_t \leq 50\%$ (i.e., $1/0.95$), and then slightly increase as V_t approaches 100%, with a maximum V_t of 1.25 (i.e., $1/0.8$).

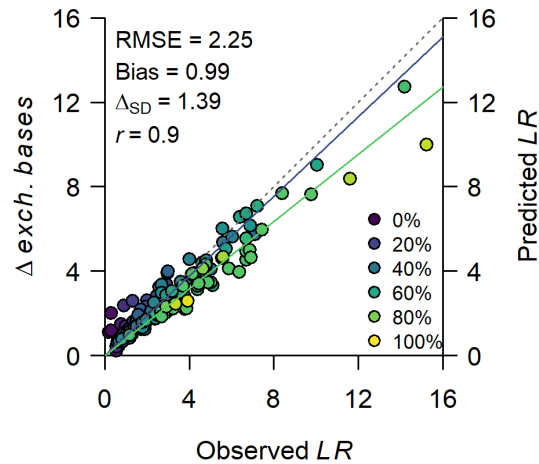


Figure 4. Difference in exchangeable bases before and after liming ($\Delta\text{exch. bases} = \text{exch. bases}_i - \text{exch. bases}_f$, $\text{cmol}_c \text{ kg}^{-1}$) as a function of the observed lime rate (LR , $\text{cmol}_c \text{ kg}^{-1}$). $\Delta\text{exch. bases}$ equals the predicted lime rate by the base saturation model. The color of the points represents the ratio between LR ($\text{cmol}_c \text{ kg}^{-1}$) and the potential acidity of the soil ($\text{pot. acid} = \text{CEC}_7 - \text{exch. bases}_i$). The gray dashed line is the identity function ($\Delta\text{exch. bases} = LR$). The solid lines are regression lines forced through the origin. The blue line is for soil samples with $LR \leq 50\%$ pot. acid ($\Delta\text{exch. bases} = LR \times 0.95(\pm 0.05)$). The green line is for $LR > 50\%$ pot. acid ($\Delta\text{exch. bases} = LR \times 0.8(\pm 0.03)$). Data extracted from Kamprath (1970), Teixeira et al. (2020), and Ananthacumaraswamy and Baker (1991). Soil samples with lime rates higher than the potential acidity were omitted.

7. Target pH model

Teixeira et al. (2020b) developed a lime requirement model that targets raising the soil pH to a level considered optimal for crop production. The model is based on four nonlinear models that relate the difference between the initial pH and two target pHs (5.8 and 6) with either organic matter content (OM , g kg^{-1}) or potential acidity (Eq. 15). It also considers that the lime rate must be greater than the Ca and Mg requirement of the crop (X) and lower than the potential acidity of the soil (pot. acid_i). Thus, the estimated lime requirement results from a series of rules such that it selects the lowest LR from the four nonlinear models that is higher than X and lower than pot.

$acid_i$. When no model returns a lime rate higher than X , the estimated LR is X . If the selected LR (either from the models or X) is greater than the initial potential acidity of the soil, the estimated LR equals $pot. acid_i$. This model always recommends liming because the Ca and Mg available in the soil are not considered available to the crop, and it thus assumes that all Ca and Mg must be provided by liming. Therefore, the minimum lime rate is X (Ca and Mg crop requirements), except when X is higher than $pot. acid$, in which case $LR = pot. acid$.

$$\begin{aligned}
 LR_{5.8OM} &= 0.0699 \times [(5.8 - pH)OM]^{0.9255} \\
 LR_{5.8PA} &= 0.375 \times [(5.8 - pH)pot. acid]^{0.9127} \\
 LR_{6OM} &= 0.1059 \times [(6 - pH)OM]^{0.8729} \\
 LR_{6PA} &= 0.4558 \times [(6 - pH)pot. acid]^{0.9162}
 \end{aligned}
 \tag{Eq. 15}$$

The model parameters were calibrated with the same soil incubation study data from Teixeira et al. (2020a). However, data from five soils were excluded from the calibration because the authors considered that they deviated too much from the nonlinear regression models compared to the data from other soils. We tested the model with 6-fold cross-validation using data from Teixeira et al. (2020a), including the five excluded soils (Figure 5). The target pH model has much lower accuracy than all other models above. Furthermore, as the model selects the minimum LR from the nonlinear models instead of the average, it often underpredicts LR .

The Teixeira et al. (2020b) model is the most recent of a large list of regression models based on a target pH developed for acid soils in Brazil (see, for example, Combatt Caballero et al., 2019). These models use linear or nonlinear regressions and predictors such as ΔpH , organic matter, potential acidity, and base saturation to predict lime rates for a particular region. However, when tested with an independent dataset, these models have low accuracy (Teixeira et al., 2020a),

which might be related to the many factors affecting soil pH. Most likely, no simple model can predict soil pH responses to liming for different soil types with regular soil testing data. Future incorporations of additional soil properties measuring the soil acid-base buffering capacity to routine soil tests could help develop better predictive liming-soil pH models (Yang et al., 2020).

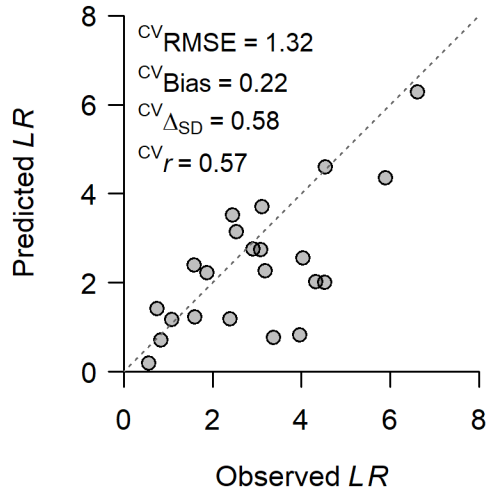
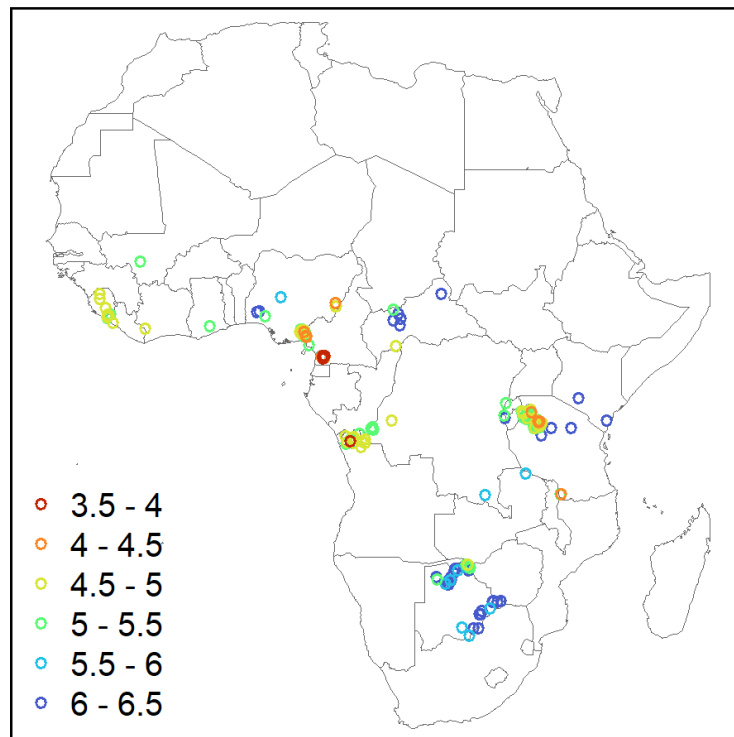


Figure 5. Predicted lime rate (LR) to reach a pH of 5.8 by Teixeira et al. (2020b) as a function of the observed LR that resulted in such a pH. The gray dashed line is the identity function ($\Delta_{exch. bases} = LR$). The 6-fold cross-validation accuracy statistics shown are the root mean square error (RMSE), bias, the difference in standard deviation (Δ_{SD}), and Pearson’s correlation coefficient (r).

8. Case study

We used two models with different target soil chemical properties (acidity saturation and base saturation) to compute lime requirements for 303 African soils with pH between 3.5 and 6.5 (Supplementary Figure 2) and two representative crops with different acidity tolerance. A target acidity saturation (TAS) of 15% and a target base saturation (V_t) of 50% were defined for the

more tolerant crop (i.e., common critical values for cereals, such as maize and wheat), and a TAS of 5% and a V_t of 70% were defined for the more sensitive crop (i.e., common critical values for many vegetables, such as tomato, onion, and cabbage; Alvarez and Ribeiro, 1999). The best available model was used for each target soil chemical property. No pH model was included because these models are location-specific and have low accuracy when extrapolated to other regions. The new model presented here (Eq. 12) was used to predict lime requirements for the two acidity saturation targets and Quaggio's (1983) model to predict lime requirements for the two base saturation targets (Eq. 14). Lime rates were computed in $\text{cmol}_c \text{kg}^{-1}$ because only 27% of these soil profiles had soil bulk density data available.



Supplementary Figure 2. Location of the 303 soil samples used for the case study. Data extracted from the Africa Soil Profile Database (Leenaars et al., 2014). The color of the points indicates the pH of the soil measured in water for a 0 – 20 cm depth.

The most striking difference between the new model presented here (Eq. 12) and Quaggio's (1983) model is that the latter predicts liming for many soils in which the former predicts none (Figure 6). For instance, for a tolerant crop, 18.5% of the soils do not require liming according to the two models, while 31% require liming for the base saturation model but not for the acidity saturation model. The latter fraction goes down to 25% for a more sensitive crop. In contrast, only 1.7% of the soils require liming based on acidity saturation but not according to the base saturation. Moreover, the base saturation model predicts lime rates as high as $12 \text{ cmol}_c \text{ kg}^{-1}$ for soils with a pH higher than 6, while virtually no soil with such a pH requires liming based on acidity saturation (Supplementary Figure 3). Furthermore, 87% of the soils that do not require liming based on acidity saturation but do for base saturation have an exchangeable $\text{Ca}^{2+} > 1 \text{ cmol}_c \text{ kg}^{-1}$, enough to meet most cereal crop demands. Thus, neither Al toxicity nor calcium deficiencies justify liming application in these soils.

Lime rates of soils requiring liming for the two models are weakly correlated ($r = 0.43$) but comparable in magnitude (mean difference = $0.47 \text{ cmol}_c \text{ kg}^{-1}$). The acidity saturation model predicts higher lime rates in soils with very low pH for the more tolerant crop but similar values for the more sensitive crop. Conversely, the base saturation model predicts higher lime rates for most soils with a pH above 5, particularly for the more sensitive crop.

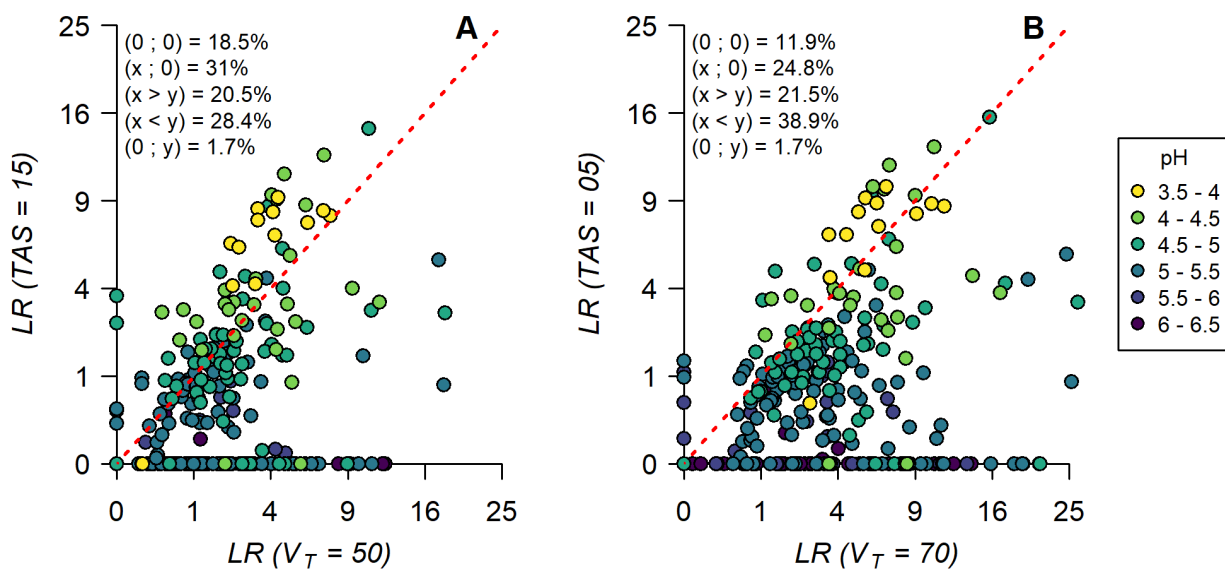
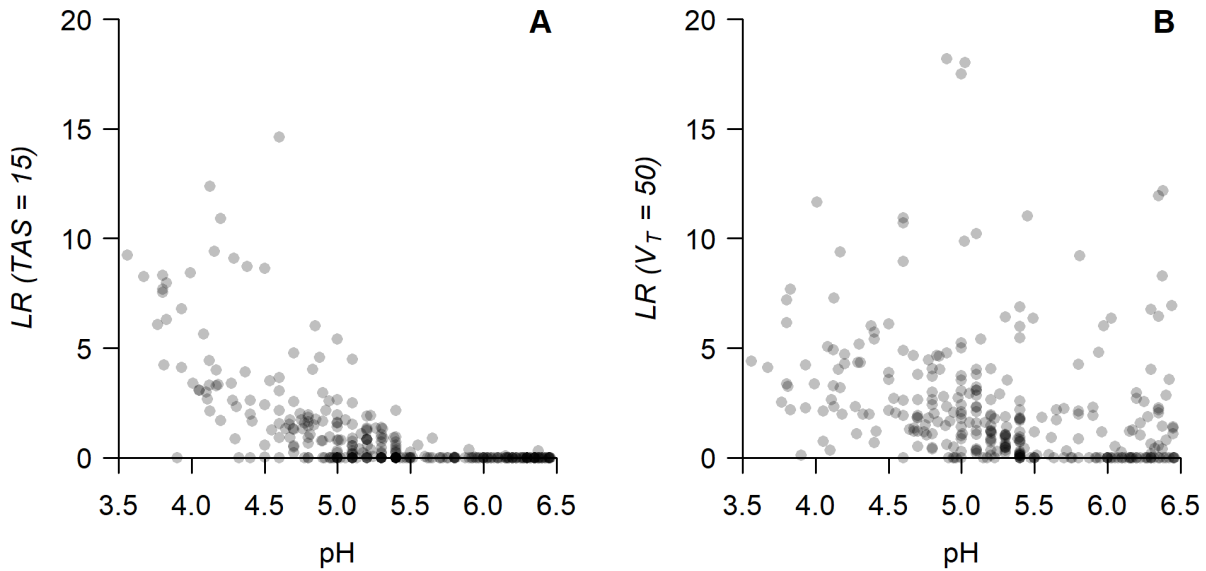


Figure 6. Predicted lime rates (LR , $\text{cmol}_c \text{ kg}^{-1}$) for 303 African soils with pH between 3.5 and 6.5, two target soil chemical properties: a target base saturation (V_t , x-axis) and a target acidity saturation (TAS , y-axis), and two representative crops: (A) a cereal ($TAS = 15\%$ and $V_t = 50\%$) and (B) a vegetable ($TAS = 5\%$ and $V_t = 70\%$). The red dashed line is the identity function ($LR(TAS) = LR(V_t)$). The values inside the plot indicate the fraction of soils in a specific scatter plot position: the origin (0;0), the x-axis (x;0), between the x-axis and the identity function ($x > y$, lower triangle), between the identity function and the y-axis ($x < y$, upper triangle), and the y-axis (0;y). Lime rates based on TAS were predicted with the acidity saturation model presented in Eq. 12, and LR based on V_t with Quaggio (1983).



Supplementary Figure 3. Predicted lime rates (LR , $\text{cmol}_c \text{ kg}^{-1}$) as a function of soil pH (measured in water) for 303 African soils with pH between 3.5 and 6.5 and two target soil chemical properties: a target acidity saturation (TAS) of 15% and a target base saturation (V_t) of 50%. Lime rates for $TAS = 15\%$ were predicted with the acidity saturation model presented in Eq. 12, and LR for $V_t = 50\%$ with Quaggio (1983).

9. Discussion

9.1. Model comparison

We have shown important differences in lime rates and prediction accuracy depending on the target soil property and model (Figures 2, 4, and 5). When the target is to ameliorate the Al toxicity of the soil by neutralizing its acidity saturation to a certain level, both Kamprath (1970) and Cochrane et al. (1980) models provided reasonable accuracy (Figures 1 and 2). Nevertheless, the new model formulated in Eq. 12 offers improved accuracy and the advantage of being sustained by a formal mathematical derivation that can be expanded (Figures 2 and 3). Similarly,

the base saturation model also has great prediction accuracy, particularly for target base saturation levels of around 50% (Figure 4). In contrast, no model based on a target pH can deliver accurate results without additional soil tests, and they need to be developed locally (Figure 5).

The model presented here is the only model based on a target acidity saturation (*TAS*) with greater accuracy than the original Cochrane et al. (1980) model (Figure 2). The authors of the ACID4, NuMaSS, and MG5 models claimed that they modified the Cochrane et al. (1980) model to improve the accuracy for their target region. However, there are no available data supporting those statements. The decreased accuracy that we found may partly be because we did not have access to these data. However, we believe that these more complex models suffer from overfitting to the datasets used to build them. In other words, they may perform better in particular regions, but this has come at the expense of general validity. Conversely, the new model is more robust than previous models because it is based on mathematical foundations and strong empirical relations. These relations are consistent through a wide range of soils from different regions (Figure 3).

However, we observed a small incubation study effect in the relations shown in Figure 3, which might be a consequence of the soil region (parental material) or, more likely, because of the incubation study per se (differences in the liming material or soil incubation method).

Experimental results have an error component, including systematic errors that are consistent within one experiment but differ between experiments, introducing statistical bias. This bias can

be reduced with standardized procedures. However, lime incubation studies are not fully standardized, and they differ in the incubation time and temperature, liming materials, and water additions, among other variables. For instance, we excluded data from an incubation study that used tap water rather than distilled water to keep the soil samples moist during the incubation (Deressa et al., 2020) because control treatments had significantly more exchangeable Ca^{2+} and less exchangeable acidity than the initial conditions. A more thorough standardization of experimental procedures for measuring liming effects would help the development of general models for lime requirement estimation.

A novel feature of the model formulated in Eq. 12 is that the lime factor (lf) is a continuous function of TAS . The Cochrane et al. (1980) model modifies the lf depending on TAS and the initial acidity saturation, using a discontinuous rule with two fixed lf (Eq. 3). However, the proposed rule does not always improve accuracy, not even in their data, as shown by the points with incorrect lf (Figure 2). In the MG5 and NuMaSS methods, the lf depends on clay content or activity. Our review does not show evidence for a need to adjust the lf as a function of clay, despite the wide range of clay content and soils included in the four soil incubation studies used here. Adjusting the lf and lime rates by clay content might be a work-around to account for differences in soil bulk density when the method returns lime rates in tons per hectare without directly including the soil bulk density in the formulas. Nevertheless, clay type and content could be considered in future corrections of the TAS method, particularly if there are high deviations in the association between lime rate and $\Delta_{exch. acid}$ and $\Delta_{exch. bases}$.

It seems counterintuitive that, while both the acidity saturation and base saturation models are highly accurate on their target, the lime requirement they predict can be so sharply different (Figure 6). These differences highlight the importance of identifying the soil chemical property most associated with the crop yield response to liming. Tropical soils can have several acidity problems affecting crop growth (Kamprath, 1984; Sanchez, 2019). It might be that reaching a given level for some property, such as a base saturation of 70% or a pH of 6, guarantees that all soil acidity problems are solved without leading to overliming problems. However, this approach can also result in lime requirement estimates that are much too high (Farina and Channon, 1991; Smyth and Cravo, 1992), which might be particularly problematic when lime is expensive, and its manipulation cumbersome. The alternative is to target the most limiting factor for crop yield, which is frequently Al toxicity in acid tropical soils (Sanchez, 2019). However, this approach can underpredict lime requirements when Al toxicity is the only target but not the acidity problem most limiting crop yields. A comprehensive approach would predict the lime rate needed to tackle every potential acidity problem while considering other management alternatives. However, crop responses to other acidity problems, such as calcium and magnesium deficiencies, are unclear, and their liming requirements have not been defined. Thus, more research on crop responses to lime in soils with these specific acidity problems is needed to develop a lime requirement method that tackles them all.

9.2. Model applications

Lime requirement models can be useful for strategic research on potential lime use in tropical regions where liming is still a rare practice and the experimental evidence is scarce (Crawford et al., 2008). These models estimate the lime rate needed to reach a target soil condition based on readily available standard soil data (Hengl et al., 2017; Miller et al., 2021). Such information could be used together with the crop response to that soil condition to estimate the effect of liming on crop yield. For instance, there is ample evidence of the association between acidity saturation and crop yields (Abruña et al., 1969; Farina and Channon, 1991; Lollato et al., 2019; Smyth and Cravo, 1992). Therefore, the expected yield response to lime can be predicted by estimating what fraction of the maximum yield is observed at the current acidity saturation level while assuming that the final yield after liming is the inverse of that fraction. If data on lime and grain prices is available, such functions can be used to get a first approximation of the potential profitability of liming. Such analysis can help identify regions where liming investments might be more successful, pinpointing national governments and private sector efforts.

However, this does not mean that the readily available soil data used by the models reviewed here has sufficient quality for farm-level recommendations (Vanlauwe et al., 2019). Therefore, farm-level lime requirements would be more accurate when based on soil properties measurements or additional local soil-quality indicators, such as soil color, soil texture, or presence of specific plant species (Mairura et al., 2007). The soil properties used by the lime requirement models reviewed here are wet-lab measurements, which are costly and may be inaccessible for farmers in the tropics. Therefore, farmers in the tropics could benefit from cost-effective, quick tests for lime requirement prediction, but these need to be developed locally.

10. Conclusions

Liming can boost the productivity of acid soils, but the lime rate required to achieve this is unknown for many tropical regions where food production increases are urgently needed. While lime requirement models could be very useful in these places, the variety of models available in the literature introduces much uncertainty. We showed important differences in the results obtained from these models, particularly depending on their target soil chemical property. For instance, many more African soils require liming based on base saturation rather than acidity saturation. The new acidity saturation model introduced here has more precision than all earlier models across a wide range of acid tropical soils from different regions and can effectively estimate the lime rate required to address aluminum toxicity. This model could be incorporated into more comprehensive models once lime rates needed for other acidity problems are well established.

References

Abruña, F., Rodríguez García, J.A., Badillo Feliciano, J., 1969. Crop Response to Soil Acidity Factors in Ultisols and Oxisols in Puerto Rico. VII. Dry Beans. *J. Agric. Univ. P. R.* 67, 429–437. <https://doi.org/10.46429/jaupr.v67i4.7737>

Alemu, E., Selassie, Y.G., Yitaferu, B., 2022. Effect of lime on selected soil chemical properties, maize (*Zea mays* L.) yield and determination of rate and method of its application in Northwestern Ethiopia. *Heliyon* 8, e08657. <https://doi.org/10.1016/j.heliyon.2021.e08657>

Alvarez, V., Ribeiro, A., 1999. Calagem, in: *Recomendação Para o Uso de Corretivos e Fertilizantes Em Minas Gerais*. Viçosa: Comissão de Fertilidade Do Solo Do Estado de Minas Gerais. pp. 43–60.

Ananthacumaraswamy, S., Baker, R.M., 1991. Effect of increasing level of lime (CaCO_3) on soil chemical properties of acid soils 60, 4–15.

Bell, P.F., 1996. Predicting Liming Needs of Soybean Using Soil pH, Aluminum, and Manganese Soil Tests. *Commun. Soil Sci. Plant Anal.* 27, 2749–2764. <https://doi.org/10.1080/00103629609369737>

Cochrane, T.T., Salinas, J.G., Sanchez, P.A., 1980. An equation for liming acid mineral soils to compensate crop aluminium tolerance. *Trop. Agric. Trinidad Tobago* 57, 133–140.

Coleman, N.T., Kamprath, E.J., Weed, S.B., 1959. Liming, in: Normax, A.G. (Ed.), *Advances in Agronomy*. Academic Press, pp. 475–522. [https://doi.org/10.1016/S0065-2113\(08\)60073-5](https://doi.org/10.1016/S0065-2113(08)60073-5)

Combatt Caballero, E., Jarma Orozco, A., Palencia Luna, M., 2019. Modeling the Requirements of Agricultural Limestone in Acid Sulfate Soils of Brazil and Colombia. *Commun. Soil Sci. Plant Anal.* 50, 935–947. <https://doi.org/10.1080/00103624.2019.1594877>

Crawford, T.W., Singh, U., Breman, H., 2008. Solving Agricultural Problems Related to Soil Acidity in Central Africa's Great Lakes Region CATALIST Project Report. International Center for Soil Fertility and Agricultural Development (IFDC), Kigali, Rwanda.

de Wit, C.T., 1992. Resource use efficiency in agriculture. *Agric. Syst., Systems approaches for agricultural* 40, 125–151.

Deressa, A., Yli-Halla, M., Mohamed, M., Wogi, L., 2020. Exchangeable aluminum as a measure of lime requirement of Ultisols and Alfisols in humid tropical Western Ethiopia.

Evans, C.E., Kamprath, E.J., 1970. Lime Response as Related to Percent Al Saturation, Solution Al, and Organic Matter Content. *Soil Sci. Soc. Am. J.* 34, 893–896. <https://doi.org/10.2136/sssaj1970.03615995003400060023x>

Fageria, N.K., Baligar, V.C., 2008. Chapter 7 Ameliorating Soil Acidity of Tropical Oxisols by Liming For Sustainable Crop Production, in: *Advances in Agronomy*. Academic Press, pp. 345–399. [https://doi.org/10.1016/S0065-2113\(08\)00407-0](https://doi.org/10.1016/S0065-2113(08)00407-0)

Fageria, N.K., Baligar, V.C., Jones, C.A., 2011. Growth and Mineral Nutrition of Field Crops 574.

Farina, M.P.W., Channon, P., 1991. A field comparison of lime requirement indices for maize. *Plant Soil* 134, 127–135. <https://doi.org/10.1007/BF00010725>

Goedert, W.J., 1983. Management of the Cerrado soils of Brazil: a review. *J. Soil Sci.* 34, 405–428. <https://doi.org/10.1111/j.1365-2389.1983.tb01045.x>

Goulding, K.W.T., 2016. Soil acidification and the importance of liming agricultural soils with particular reference to the United Kingdom. *Soil Use Manag.* 32, 390–399. <https://doi.org/10.1111/sum.12270>

Harter, R.D., 2007. Acid soils of the tropics. ECHO Tech. Note ECHO 11.

Heckman, J.R., Pavlis, G.C., Anastasia, W.L., 2002. Lime Requirement for New Jersey Blueberry-producing Soils. *HortTechnology* 12, 220–222. <https://doi.org/10.21273/HORTTECH.12.2.220>

Hengl, T., Jesus, J.M. de, Heuvelink, G.B.M., Gonzalez, M.R., Kilibarda, M., Blagotić, A., Shangquan, W., Wright, M.N., Geng, X., Bauer-Marschallinger, B., Guevara, M.A., Vargas, R., MacMillan, R.A., Batjes, N.H., Leenaars, J.G.B., Ribeiro, E., Wheeler, I., Mantel, S., Kempen, B., 2017. SoilGrids250m: Global gridded soil information based on machine learning. *PLoS One* 12, e0169748. <https://doi.org/10.1371/journal.pone.0169748>

James, G., Witten, D., Hastie, T., Tibshirani, R., 2013. *An introduction to statistical learning*. Springer.

Johnson, D.S., 2010. *Liming and agriculture in the Central Pennines: the use of lime in land improvement from the late thirteenth century to c. 1900*. BAR Publishing.

Kamprath, E., 1980. Soil acidity in well-drained soils of the tropics as a constraint to food production. *Priorities Alleviating Soil-Relat. Constraints Food Prod. Trop.* 171–187.

Kamprath, E.J., 1984. Crop Response to Lime on Soils in the Tropics, in: Adams, F. (Ed.), *Agronomy Monographs*. American Society of Agronomy, Crop Science Society of America, Soil Science Society of America, Madison, WI, USA, pp. 349–368. <https://doi.org/10.2134/agronmonogr12.2ed.c9>

Kamprath, E.J., 1970. Exchangeable Aluminum As a Criterion for Liming Leached Mineral Soils. *Soil Sci. Soc. Am. J.* 34, 252–254.

<https://doi.org/10.2136/sssaj1970.03615995003400020022x>

Kobayashi, K., Salam, M.U., 2000. Comparing simulated and measured values using mean squared deviation and its components. *Agron. J.* 92, 345–352.

Leenaars, J.G.B., Van Oostrum, A.J.M., Ruiperez Gonzalez, M., 2014. Africa Soil Profiles Database, Version 1.2. *Compil. Geo-Ref. Stand. Leg. Soil Profile Data Sub Sahar. Afr. Dataset Wagening. Neth. Afr. Soil Inf. Serv. AfSIS Proj. ISRIC—World Soil Inf.*

Li, G.D., Singh, R.P., Brennan, J.P., Helyar, K.R., Li, G.D., Singh, R.P., Brennan, J.P., Helyar, K.R., 2009. A financial analysis of lime application in a long-term agronomic experiment on the south-western slopes of New South Wales. *Crop Pasture Sci.* 61, 12–23.

<https://doi.org/10.1071/CP09103>

Lollato, R.P., Edwards, J.T., Zhang, H., 2013. Effect of Alternative Soil Acidity Amelioration Strategies on Soil pH Distribution and Wheat Agronomic Response. *Soil Sci. Soc. Am. J.* 77, 1831–1841. <https://doi.org/10.2136/sssaj2013.04.0129>

Lollato, R.P., Ochsner, T.E., Arnall, D.B., Griffin, T.W., Edwards, J.T., 2019. From Field Experiments to Regional Forecasts: Upscaling Wheat Grain and Forage Yield Response to Acidic Soils. *Agron. J.* 111, 287–302. <https://doi.org/10.2134/agronj2018.03.0206>

Lopes, M., de Carvalho Silva, M., Guilherme, L.R.G., 1991. Acidez do solo e calagem. (Boletim Técnico No. 1). Associação Nacional para Difusão de Adubos, São Paulo, Brazil.

Mairura, F.S., Mugendi, D.N., Mwanje, J.I., Ramisch, J.J., Mbugua, P.K., Chianu, J.N., 2007. Integrating scientific and farmers' evaluation of soil quality indicators in Central Kenya.

Geoderma 139, 134–143. <https://doi.org/10.1016/j.geoderma.2007.01.019>

Metzger, K., Zhang, C., Ward, M., Daly, K., 2020. Mid-infrared spectroscopy as an alternative to laboratory extraction for the determination of lime requirement in tillage soils.

Geoderma 364, 114171. <https://doi.org/10.1016/j.geoderma.2020.114171>

Miller, M.A.E., Shepherd, K.D., Kisitu, B., Collinson, J., 2021. iSDAsoil: The first continent-scale soil property map at 30 m resolution provides a soil information revolution for Africa.

PLOS Biol. 19, e3001441. <https://doi.org/10.1371/journal.pbio.3001441>

Osmond, D.L., Smyth, T.J., Yost, R.S., Reid, W.S., Hoag, D.L., Branch, W., Li, H., 2002. Nutrient Management Support System (NuMaSS) v. 2. *Soil Manag. Collab. Res. Support*

Program USA U. S. Agency Int. Dev. Soil Manag. Collab. Res. Support Program Obtenido
Httppdf Usaid Govpdfdocspnada473 Pdf.

Pearson, R.W., Pérez-Escolar, R., Abruña, F., Lund, Z.F., Brenes, E.J., 1977. Comparative Response of Three Crop Species to Liming Several Soils of the Southeastern United States and of Puerto Rico. *J. Agric. Univ. P. R.* 61, 361–382. <https://doi.org/10.46429/jaupr.v61i3.10436>

Quaggio, J.A., 1983. Critérios para calagem em solos do estado de São Paulo (PhD Thesis). Universidade de São Paulo.

Rossel, R.A.V., McBratney, A.B., 2001. A response-surface calibration model for rapid and versatile site-specific lime-requirement predictions in south-eastern Australia. *Soil Res.* 39, 185–201. <https://doi.org/10.1071/sr99131>

Salinas, J.G., 1978. Differential response of some cereal and bean cultivars to Al and P stress in an Oxisol of Central Brazil. Thesis (Ph. D.).

Sanchez, P.A., 2019. Properties and Management of Soils in the Tropics. Cambridge University Press.

Sanchez, P.A., Salinas, J.G., 1981. Low-Input Technology for Managing Oxisols and Ultisols in Tropical America, in: Brady, N.C. (Ed.), *Advances in Agronomy*. Academic Press, pp. 279–406. [https://doi.org/10.1016/S0065-2113\(08\)60889-5](https://doi.org/10.1016/S0065-2113(08)60889-5)

Shoemaker, H.E., McLean, E.O., Pratt, P.F., 1961. Buffer Methods for Determining Lime Requirement of Soils With Appreciable Amounts of Extractable Aluminum. *Soil Sci. Soc. Am. J.* 25, 274–277. <https://doi.org/10.2136/sssaj1961.03615995002500040014x>

Sims, J.T., 1996. Lime requirement. *Methods Soil Anal. Part 3 Chem. Methods* 5, 491–515.

Smithson, P.C., Giller, K.E., 2002. Appropriate farm management practices for alleviating N and P deficiencies in low-nutrient soils of the tropics. *Plant Soil* 245, 169–180. <https://doi.org/10.1023/A:1020685728547>

Smyth, T.J., Cravo, M.S., 1992. Aluminum and Calcium Constraints to Continuous Crop Production in a Brazilian Amazon Oxisol. *Agron. J.* 84, 843–850. <https://doi.org/10.2134/agronj1992.00021962008400050016x>

Teixeira, W.G., Alvarez V, V.H., Neves, J.C.L., Paulucio, R.B., 2020a. Evaluation of traditional methods for estimating lime requirement in Brazilian soils. *Rev. Bras. Ciênc. Solo* 44.

Teixeira, W.G., Víctor Hugo Alvarez, V., Neves, J.C.L., 2020b. New methods for estimating lime requirement to attain desirable pH values in Brazilian soils. *Rev. Bras. Ciênc. Solo* 44. <https://doi.org/10.36783/18069657rbc20200008>

van Raij, B., 1996. *Recomendações de adubação e calagem para o Estado de São Paulo*. IAC Campinas.

Vanlauwe, B., Coe, R., Giller, K.E., 2019. Beyond averages: new approaches to understand heterogeneity and risk of technology success or failure in smallholder farming. *Exp. Agric.* 55, 84–106. <https://doi.org/10.1017/S0014479716000193>

Walker, T., Friday, J., Casimero, M., Dollentas, R., Mataia, A., Acda, R., Yost, R., 2009. The early economic impact of a nutrient management decision support system (NuMaSS) on small farm households cultivating maize on acidic, upland soils in the Philippines. *Agric. Syst.* 101, 162–172. <https://doi.org/10.1016/j.agsy.2009.05.004>

Yamada, T., 2005. The *Cerrado* of Brazil: A Success Story of Production on Acid Soils. *Soil Sci. Plant Nutr.* 51, 617–620. <https://doi.org/10.1111/j.1747-0765.2005.tb00076.x>

Yang, Y., Wang, Y., Peng, Y., Cheng, P., Li, F., Liu, T., 2020. Acid-base buffering characteristics of non-calcareous soils: Correlation with physicochemical properties and surface complexation constants. *Geoderma* 360, 114005. <https://doi.org/10.1016/j.geoderma.2019.114005>

Yost, R., Uehara, G., Wade, M., Sudjadi, M., Widjaja-adhi, G., Li, Z.-C., 1988. *Expert Systems in Agriculture: Determining Lime Recommendations for Soils of the Humid Tropics* 12.

SUMMARY

This dissertation analyzed patterns and processes in crop species diversity in the US and the world. It also introduced a new lime requirement model for acid tropical soils, which was evaluated and compared with previous models. Spatial and temporal diversity patterns, their relation, and how the spatial scale conditions them were investigated for the US. Current spatial diversity patterns were also assessed globally and compared with attainable diversity to compute diversity gaps. Attainable diversity was defined as the diversity obtained when all crops are planted to maximize diversity while considering crop-specific environmental suitability and demand (i.e., environmental and demand-side constraints). Attainable diversity patterns reflect environmental processes shaping diversity, while diversity gap patterns result from specialization processes. The new lime requirement model was built on strong empirical relations and a formal mathematical derivation of acidity saturation. Lime requirement models were evaluated using data from incubation studies of soils from different countries, and their estimates were compared using a large dataset of African soils.

S.1. Pattern and Process in Crop Species Diversity

The average temporal diversity in the United States is 2.1 effective crop species, and 6 out of 10 hectares of cropland have two or fewer crops in rotation. In addition, temporal diversity is lower in croplands planted with major crops, which results in a negative correlation between the total area planted with a crop and the temporal diversity of the cropland where it is grown. Therefore, a possible approach to increasing temporal (and, thus, farm-scale) diversity in the US and

elsewhere is to incentivize the production of and demand for “middle class” crops while lowering the incentives for wheat, maize, soybean, and rice. Another approach that does not require changes in consumption patterns would be to increase the area of the most under-utilized crop, that is, crops with the highest difference between the attainable and actual crop proportion. Such a crop is usually a major crop adapted to but not widely planted in a region. For instance, in most US Corn Belt, that crop is wheat.

Crop species diversity in space strongly increases with the size of the area in which it is measured. For instance, 75% of US croplands have less than two effective crop species when diversity is measured in units of 44 ha, but a diversity greater than 2 when measured at 1,500 ha. This spatial crop diversity scale dependency can be described with a double sigmoid curve. At the lower end, spatial diversity increases exponentially as the size of the observational unit increases from a point (an infinitesimally small area) to beyond single fields (with usually one crop) and captures the farm-level diversity. When the size of the observational unit reaches typical farm sizes, the increase in diversity slows down as neighboring farms are usually similar to each other. Then, spatial diversity increases exponentially in very large areas because of regional cropping system differences. Thus, the shape of this relation can inform different features of the study area, such as farm size and diversity (first exponential growth) and regionalization level (second exponential growth). This regional differentiation can also be observed in the difference between the diversity gap of total national diversity and local diversity averages. Diversity gaps are usually greater for the average local diversity than for the total national diversity because different farms and regions might specialize in particular cropping systems. Countries might take advantage of that specialization while ensuring that the demand

for agricultural products is covered as much as possible with the production from different regions.

Spatial diversity is most strongly associated with temporal diversity at the farm level, as farmers typically plant all components of their crop rotation in different fields. At intermediate aggregation levels (e.g., county level), the total spatial diversity is always greater than the farm-level diversity, yet, farm-level diversity is its biggest component. Thus, it is possible to estimate the farm-level (and, hence, temporal) diversity from county-level spatial diversity if the regional-to-local diversity ratio is considered. At higher levels of aggregation (e.g., countries), the lack of correlation between the temporal and spatial diversity increases exponentially because the diversity among farms is normally much greater than the diversity within them.

The largest tracts of high crop species diversity are found in East Asia, humid and sub-humid regions of sub-Saharan Africa, and the Mediterranean. In the US, crop diversity is higher in North Dakota, the West Coast, and the Southern Seaboard. Crop diversity is very low in most of the non-mountainous regions of the Americas (where croplands are dominated by maize and soybean) and central Asia (wheat), as well as in parts of Southeast Asia (rice and oil palm). Moreover, crop diversity patterns partially follow general latitudinal biodiversity gradients. Crop diversity is the highest around the Equator and the Tropic of Cancer, from where it linearly decreases when going northwards. However, southern hemisphere patterns are somehow different. South of the Equator, crop diversity decreases rapidly with latitude between the Equator and the Tropic of Capricorn, which might be a consequence of the southern hemisphere's lower amount of cropland, most of which is in South America.

Attainable diversity is also higher in the tropics than in temperate regions. Outside the tropics, it is higher in coastal than continental regions. The lowest attainable diversity values are observed in Kazakhstan, Mongolia, Russia, the Baltic States, Scandinavia, Canada, and the northern US. Temperature strongly affects the attainable diversity: it increases linearly with the annual average temperature until it plateaus at 20 to 25 °C, and it slightly decreases at a higher temperature.

Nearly five-sixths of the world's croplands have a diversity gap of 50% or more. In other words, they have less than half of the crop diversity they would have if crops were planted to maximize suitability and diversity while considering the current demand for crops. Diversity gaps are particularly high in most plain regions of the Americas, intermediate in Africa, Asia, and Oceania, but with great spatial variability, and relatively small in Europe, especially in the Mediterranean, Eastern Europe, and the Netherlands. Cropland with low diversity tends to have large diversity gaps. Therefore, regions with low diversity values are seldomly the result of large environmental constraints, except maybe for some regions in Eastern Europe and Central Asia.

S.2. Lime Requirement Models

The lime rate required to reduce soil acidity problems in the tropics and the accuracy with which it is predicted largely depends on the target soil chemical property. When the target is to neutralize the aluminum toxicity of the soil, the foundational acidity saturation models provided reasonable accuracy. Nevertheless, the new acidity saturation model introduced in this dissertation provides improved accuracy over many acid soils from different countries and the

benefit of being founded on a formal mathematical derivation that can be expanded. In contrast, previous attempts to improve these models showed less accuracy, maybe because they were developed to perform better in a particular region at the expense of general validity. The lime rate required to raise the base saturation level of the soil can also be accurately estimated with the available models. However, no general model can accurately predict the lime required to raise the soil pH to a target, probably because of the many factors affecting soil pH. Consequently, lime requirement models based on soil pH are usually developed locally and involve testing the acid-base buffer capacity of the soil with buffer solutions.

The great differences in the estimated lime rates between target soil chemical properties highlight the importance of identifying the acidity problems affecting crop yields. Some targets, such as base saturation and pH, are not directly associated with crop yields. They are used to ensure that no acidity problems affect the crop when these are raised above a certain threshold, but lower values do not necessarily imply lower yields. Such a strategy could be effective where lime is cheap, but not for most smallholder farmers in the tropics. In contrast, acidity saturation is tightly associated with aluminum toxicity and crop yields. Therefore, overprediction is less likely for models based on acidity saturation, but these models do not estimate the required lime rate to deal with other soil acidity problems. Acidity saturation models could hence be improved by integrating them with lime requirement models for other acidity problems, but such models are not well established yet.